Studies on the Synthesis and Structural Characterization of Magnesium Carboxylates with Flexible and Rigid Organic Acid Linkers

By

Tausif Siddiqui

Submitted in Partial Fulfillment of the Requirements

for the Degree of

Master of Science

in the

Chemistry

Program

YOUNGSTOWN STATE UNIVERSITY

December, 2013

ETD Program

Digitally signed by ETD Program
DN: cn=ETD Program, o=Youngtown State University, ou=School of Graduate Studies and Research, email=etdadmin@cc.ysu.edu, c=US
Date: 2014.01.15 14:06:45 -05'00'

Studies on the Synthesis and Structural Characterization of Magnesium Carboxylates with Flexible and Rigid Organic Acid Linkers

Tausif Siddiqui

I hereby release this thesis to the public. I understand that this thesis will be made available from the OhioLINK ETD Center and the Maag Library Circulation Desk for public access. I also authorize the University or other individuals to make copies of this thesis as needed for scholarly research.

Signature:

_____

Tausif Siddiqui, Student Date

Approvals:

_____

Dr. Sherri Lovelace-Cameron, Thesis Advisor Date

_____

Dr. Ruigang Wang, Committee Member Date

_____

Dr. Timothy R. Wagner, Committee Member Date

_____

Dr. Salvatore A. Sanders, Associate Dean of Graduate Studies Date

Thesis Abstract

Metal organic framework structures are an important research area in materials chemistry due to their many potential applications in the areas of gas-adsorption, ion-exchange, selective gas separation, potential drug delivery application and catalysis. The inorganic compounds that possess open channels and cavities in their structures are classified as framework materials. This thesis presents various studies conducted on the synthesis and structural characterization of magnesium carboxylates with flexible and rigid organic acid linkers. These syntheses were conducted in order to synthesize magnesium based novel framework compounds with desired porosities and structural attributes.

Acknowledgments

I would like to thank Youngstown State University and the School of Graduate Studies for giving me the opportunity to pursue the master's degree in Chemistry. I would like to take this opportunity to express my sincere gratitude and appreciation to the entire YSU Chemistry Department.

Special thanks to Dr. Sherri Lovelace-Cameron, my research advisor; she has been an inspiration and mentor throughout the duration of my course here at YSU. I thank her for the confidence she has had in me, the training she has given me in research and teaching, and for giving me the opportunity to participate in various conferences and encouraging me to write research publications. Without her support and guidance, it would not have been easy.

Very warm thanks to Dr. Koteswara Rao Vandavasi for his continuous guidance and support on the project research and production of thesis. His direction was instrumental in shaping my research and the overall success of the project.

My sincere gratitude goes to my thesis committee comprising Dr. Tim Wagner and Dr. Ruigang Wang. Dr. Wang has also been very helpful with the TEM and TGA data production and analysis. I would also like to thank Dr. Zeller for collecting and processing my X-ray crystallography data and providing regular insights on the research; Ray Hoff for help with PXRD data and maintenance.

Further, I would like to thank Kaitlyn Lucas, Samuel Mutinda, Seon Young Ka and other lab partners and friends who were a regular encouragement and inspiration towards

the common goal of research. Without their friendly contribution and feedback, it would not have been the same awesome experience.

Finally, I would like to thank my family, for supporting me in my decisions and endeavors and believing in me that I can do it.

Table of contents

List of Figures

List of Abbreviations

S.No.	Abbreviation	Full form
	Compounds	
1	1,4-CHDA or 1,4-CHDC	1,4-cyclohexanedicarboxylic acid
2	1,3-BDC or IPA	1,3-benzene dicarboxylic acid or isophthalic acid
3	4,4'-TMDiPy	4,4'-trimethylene dipyridine
4	Bipy or bipy	4,4'-bipyridine
5	DHTA	2,5-dihydroxyterephthalicacid
6	DMF	N,N-dimethylformamide
7	EtOH	Ethanol
8	Me-	Methyl group
9	PIP	Piperazine
10	TEA	Triethylamine
	General Abbreviations	
1	BET	Brunauer–Emmett–Teller
2	MOF	Metal–Organic Framework
3	NETL	National Energy Technology Laboratory
4	PXRD	Powder X-Ray Diffraction
5	Q_{st}	Adsorption Enthalpy
6	SXRD	Single Crystal X-Ray Diffraction
7	TEM	Transmission Electron Microscope
8	TGA	Thermal Gravimetric Analysis

	Units	
1	Å	Angstrom
2	cc	Cubic Centimeter
3	°C	° Celsius
4	g	Grams
5	K	Kelvin
6	m	Meter
7	M	Molar
8	mL	Milliliter
9	mmol	Milli Moles
10	nm	Nano Meter
11	P/P_0	Gas's Relative Pressure
12	Vol.	Volume

Introduction:

Metal organic frameworks (MOFs) have become a rapidly progressing new category of functional materials over the last decade. This study provides details about metal organic framework materials and in particular the synthesis, novel structures and characteristic properties of Magnesium frameworks. MOFs are highly crystalline inorganic–organic hybrid compounds constructed by assembling metal ions or small metal-containing clusters [also called Secondary Building Units (SBUs)] with multi-dentate organic ligands (such as carboxylates, tetrazolates, and sulfonates) by coordination bonding. MOFs are also known as coordination polymers. They can form one-, two-, or three-dimensional infinite networks. Out of these, those three-dimensional MOFs which possess permanent porosity, as porous MOFs, are the focus of research because the voids inside the frameworks can hold guest molecules (e.g. gas molecules) for a number of applications. A careful selection of the metal ions or SBUs and organic linkers, can be utilized to develop a variety of topologies and structures and can also be helpful in controlling the pore sizes systematically and the pore walls can be functionalized for specific applications in catalysis, sensor, gas storage/separation, etc. Current research focuses more on the current status of gas adsorption applications of porous MOFs, including hydrogen storage, methane storage, and selective gas adsorption.[1]

Background Research:

A careful study of the different work on the MOFs indicates magnesium[2] can serve as a choice metal center in the building block of a coordination complex. The dimensionality of the networks produced by the coordination environment of magnesium, coupled by the

role played by the coordinating strength of the solvent molecules is a critical in understanding the crystal structure. In one study, a total of four different coordination networks were synthesized on the basis of selection of reaction solvents, while the other synthetic parameters were kept constant. The reactions in pure solvents like N,N-dimethylformamide (DMF), ethanol and water resulted in the formation of different framework structures. At times these framework networks incorporate either water or DMF as a part of the framework and further processing with other solvents promised formation of required porosity and dimensionality. Since water from the metal salts is present in sufficient quantities to hydrate and at a relatively lower concentration than other solvents like ethanol, it was observed that solvation by water is more favorable in case of magnesium (Fig. 1).[1, 2]

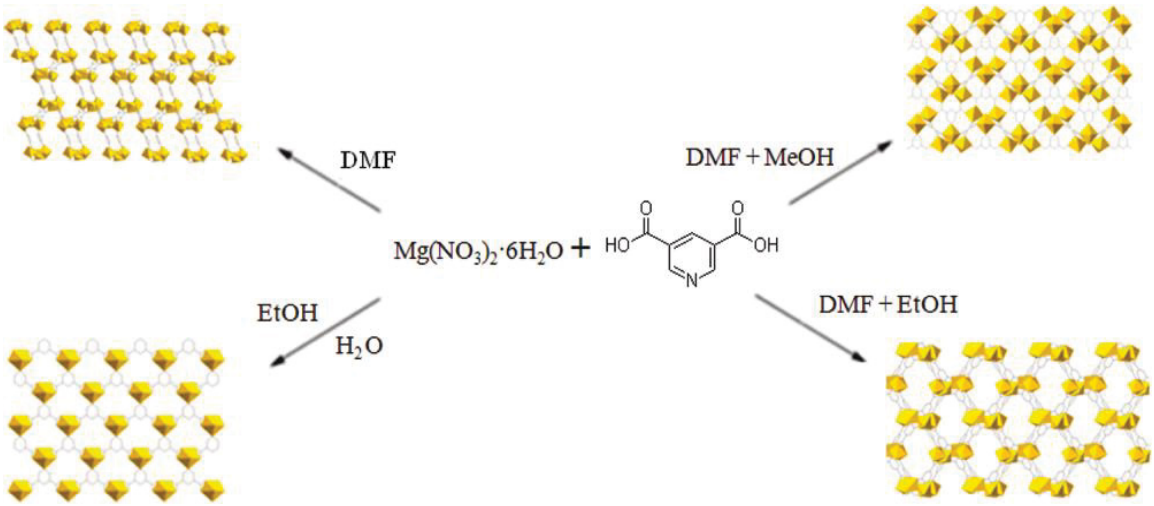

Figure 1: Different structures derived from Mg nitrate and DMF reaction displaying the role of different solvents[1]

Different magnesium based coordination networks were synthesized using different solvents under solvothermal conditions. The relative coordination ability of the solvents with the metal center plays a vital role in determining the topologies of the networks. It has been established that water has the highest affinity to coordinate with the magnesium metal centers, followed by DMF, while solvents such as methanol and ethanol tend not to coordinate with the metal center in the presence of the water and DMF. Such studies encourages continued efforts to explore the chemistry of magnesium based coordination networks using different organic linkers and synthetic conditions.[1]

Another major area of study under the development of metal organic frameworks is related to their capacity to selectively retain certain gases by either chemi-sorption or physi-sorption. They can even play an important role in separation of a specific gas like CO_2 from a mixture of gases and such property can be effectively utilized to prevent toxic and pollutant gases from their release into the atmosphere. Also for natural gas utilization, separation of carbon dioxide from methane is an important issue in the processing of low-quality natural gas such as biogas, coal-seam, and landfill gases. The co-occurrence of CO_2 with CH_4 lowers the energy content of natural gas and also causes pipeline corrosion. CO_2 must be removed usually to below 2–3% in the pipeline-grade methane before it can be used for low-temperature processing. Biogas is another very important source of renewable methane produced by the decomposition of organic matter under anaerobic conditions. CO_2, a major noncombustible component (25–45%), is required to be separated from the biogas.[2] The coal-seam gas mainly contains CH_4 and higher hydrocarbons along with CO_2 and N_2. Landfill gas consists of primarily CH_4 and CO_2 as well as a small amount of N_2 and sulfur compounds.[2] To promote the utilization

of low-quality natural gases for energy and transport applications, the effectiveness of CO_2 removal is a very crucial step in the separation of CO_2/CH_4 mixture. Previously, various techniques were employed for the mass separation of CO_2 from CH_4. The conventional absorption and stripping technology employed in the natural gas industry used amines and glycol derivatives for the selective removal of CO_2 but this approach is applicable to huge volumes of gases. These processes are heavily energy consuming as they need relatively high regeneration temperatures and requires recycling a large amount of water consequently. Additionally, the volatile solvents could undergo degradation and loss during the operation, forming toxic compounds and polluting the environmental further. The adsorptive separation of CO_2 is considered a more energy-efficient and economical alternative for smaller volume applications. There has been a continuous effort towards the development of adsorption processes such as pressure swing adsorption $(PSA)^2$, which are based on differences in adsorption equilibrium and kinetics. In this technique, the selection of a proper adsorbent with adequate selectivity, capacity, and diffusivity is critical step in designing the practical adsorption processes. Earlier studies of CO_2/CH_4 separation were focused mainly on zeolites, functionalized mesoporous silica adsorbents, active carbons, and basic resin.[7, 8]

Non-porous and microporous metal-organic framework compounds can be synthesized by reacting a metal salt, an organic linker in the presence of a base and selected solvents for e.g. a commonly studied Mg-MOF is produced by reacting magnesium nitrate and 2,5-dihydroxyterephthalic acid (subject to the degree of deprotonation of the organic linker and determined by the quantity of base added in the synthesis). The microporous compound formed was found to be isostructural with the other compounds containing

zinc, cobalt, or nickel in place of magnesium. This group of materials was consequently used to study how their properties are dependent on the metal component too. The magnesium compound has been of special interest as an adsorbent owing to the combination of large pore volume and light weight of the structure. The bulk of the water in the structure consists of non-coordinating water molecules that can be removed easily and reversibly without disturbing the framework structural integrity. The final metal-coordinating water is more strongly bound than in the analogous nickel compound for which the complete removal of the water is easily attainable. Still, the metal sites in particular Mg based MOFs are observed to be possibly available for various guest molecules.[11]

The activated compounds of the Mg based MOFs contain large open metal sites which offers a high affinity towards adsorption of guest molecules onto the porous three dimensional structure of an MOF. Large amounts of methane and carbon dioxide have been demonstrated to be adsorbed in nickel and magnesium based MOFs. Adsorption uptakes of more than 50 wt% were observed at 298 K at high pressure. Considerable quantities of 25–30 wt% CO_2 were adsorbed at elevated temperatures such as 473 K, indicating possible use of the material's porosity in processes requiring higher temperatures. Both magnesium and nickel based MOFs demonstrate methane storage capacities close to 180 cm^3 per cm^3 at 298 K and 3500 kPa.[3] At 179 K and 100 kPa, the density of methane was found to be in the range of 40–45% of the density of liquid methane at the boiling point. The relative amounts of molecules adsorbed were compared for CO_2, CH_4, and N_2. These indicated a strong preference of the MOF compounds toward the adsorption of CO_2. This has been conclusively demonstrated in experiments

using nickel based MOF for a precise 40% CO_2 and 60% CH_4 or N_2 mixture.[3] It was observed that quantitative separation of CO_2 from N_2 and significant retention of CO_2 in mixtures with CH_4 is taking place, thereby establishing the utility of MOFs (in this case Mg and Ni) as the material of choice for application in separation processes.[3]

As a relatively new class of materials, porous MOFs are expected to continue to attract research interests and various studies by both industry as well as academia. Apart from gas separation and purification in industrial applications, these compounds have potential for hydrogen and methane storage in energy applications. The synthesis process can be modified to adjust the pore size and alter the pore wall functionality. This flexibility allows researchers to focus on those factors which hold more promise, increasing both the volume available for storage and the affinity of the framework for the stored gas. In particular, as clean and alternative fuels such as hydrogen and methane continue to be developed in automotive and other applications, the need for effective storage technologies will continue to increase therefore the porous MOFs compounds are going to remain as the center of the research.[9, 10]

A good number of new Mg-containing metal–organic framework materials have been synthesized and structurally characterized. A particular MOF (Mg-MOF-1, synthesized from 3,5-pyridine dicarboxylic acid) adopts a chiral hexagonal topology. It has one-dimensional hexagonal channels and shows reversible hydrogen and CO_2 up-take (at 298 K, 760 torr). Such works may guide potential ways of using achiral pyridine carboxylic acid based ligands in constructing chiral MOFs.[4]

Certain studies also established that the MOF-74 series of materials provide a viable means of adsorbing ammonia at capacities and retentions not available in traditional adsorbent media. Octane adsorbs on all the MOF-74 analogs at loadings consistent with the surface area of the materials. These studies are helpful in ascertaining the important steps in quantifying the capability of these framework materials to perform separations in realistic environments, particularly in the presence of humidity.[5]

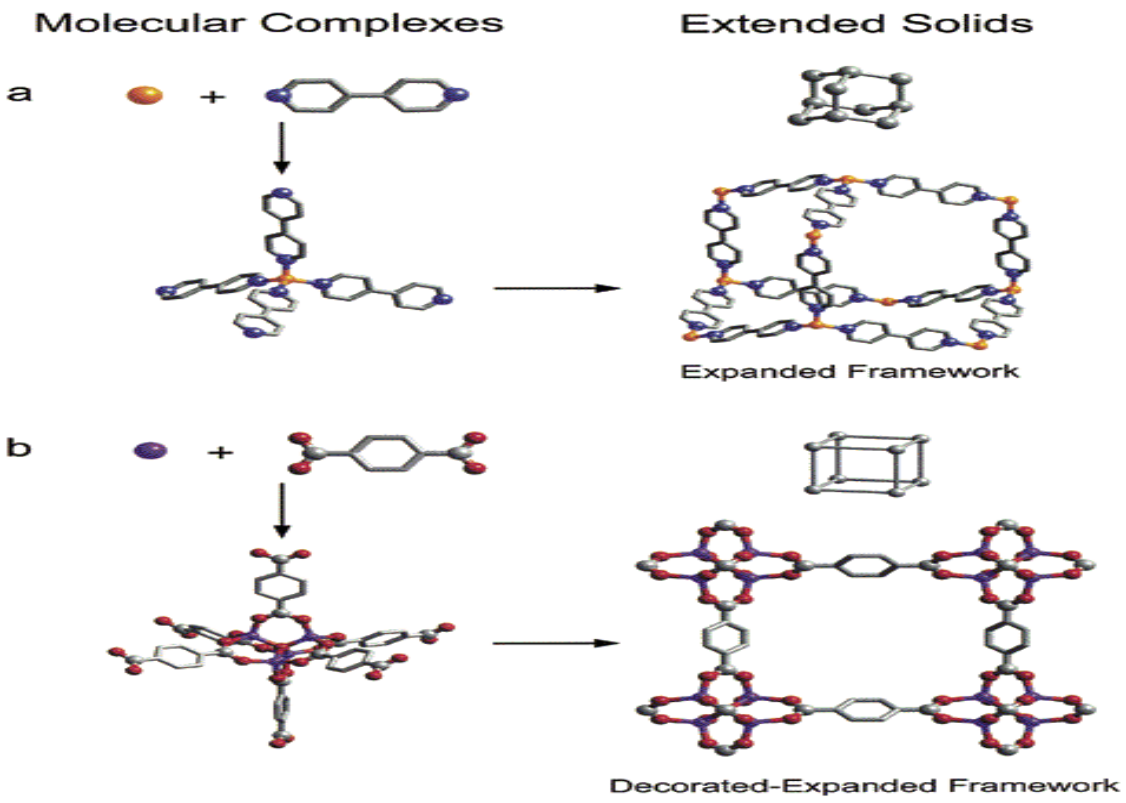

Figure 2: Assembly of metal−organic frameworks (MOFs) by the copolymerization of metal ions with organic linkers to give (a) flexible metal−bipyridine structures with expanded diamond topology and (b) rigid metal−carboxylate clusters that can be linked by benzene “struts” to form rigid extended frameworks in which the M−O−C core of each cluster acts as a large octahedron decorating a 6-connected vertex in a cube[16]

Recent concepts and ideas:

The organic linker units are either ditopic or polytopic organic carboxylates along with other similar negatively charged structures, which can be linked to metal-containing units, leading to the formation of architecturally robust crystalline MOF structures sometimes possessing typical porosities of more than 50% of the MOF crystal volume. The surface area values of MOFs typically range from 1000 to 10,000 m^2/g, which far exceeds the surface area values of traditional porous materials, such as zeolites, silicates and activated carbons. To date, MOFs with permanent porosity are far more extensively developed in their variety and multiplicity than any other class of porous materials. Such characteristics have made MOFs perfect candidates for the storage of fuels (hydrogen and methane), capture of carbon dioxide, and catalysis applications, among others.[17]

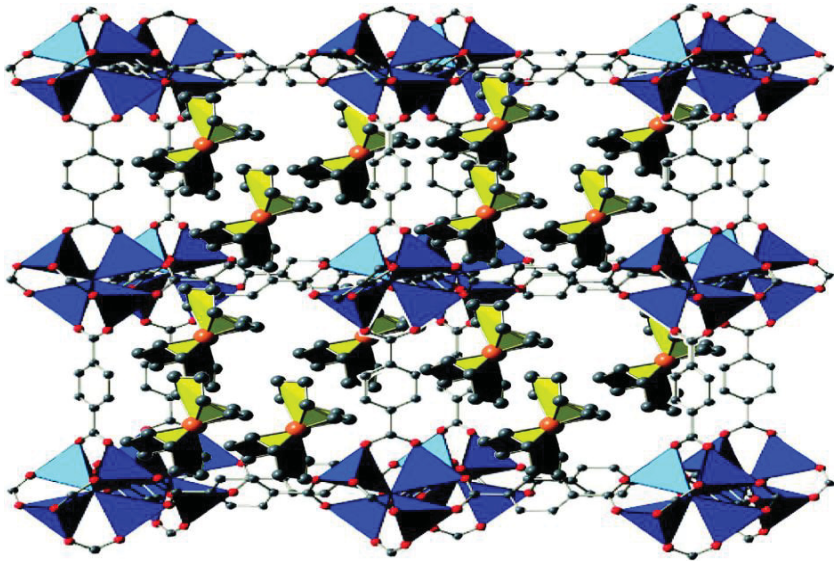

Figure 3: Model of the inclusion compound $[Ru(cod)(cot)]_{3.5}$@MOF-5[17]

A highly useful alternative high-density fuel source as compared to hydrogen and gasoline is natural gas (methane, CH_4). As is the case for hydrogen adsorption, the total

gravimetric methane uptake capacity was observed to be proportional to the pore volume of MOFs. The calculated total uptake values for MOF-177, MOF-200, and MOF-210 are 345 mg/g, 446 mg/g, and 476 mg/g, respectively, at 80 bar and 298 K (25 °C).[18] These values are much greater than those of any other MOF. The quantity of methane stored in a container supported with one of these MOFs is almost double the amount that could be stored in an empty container at room temperature and pressures up to 80 bar.[18]

An important property of MOFs is that they offer reversible carbon dioxide adsorption and are favorable materials for the selective capture of carbon from the atmosphere and flue gases. Carbon dioxide adsorption in MOFs was first reported in 1998 for MOF-2 [Zn(BDC)]. A study of carbon dioxide adsorption in a series of MOFs at room temperature showed MOF-177 to have an uptake capacity of 1470 mg/g at 35 bar. This uptake of carbon dioxide surpassed that of any known porous material under similar conditions. The large quadrupole moment of carbon dioxide molecules causes them to interact with the framework more strongly than hydrogen and methane. The best excess carbon dioxide uptake reported around 2005 was observed in a MOF with ultrahigh porosity, MOF-200 (2437 mg/g at 50 bar and 298 K). For example, a gas tank filled with MOF-177 or MOF-200 would store 9 times or 17 times as much carbon dioxide at 35 bar, respectively, as the same pressurized tank without MOF. Also, many carbon dioxide capture applications operate at low pressure so that the Henry's law constant (i.e., initial slope of the isotherm) can be employed as an indicator of the carbon dioxide selectivity. MOFs with open metal sites were found to have appropriate high initial Q_{st} values of 62 kJ/mol and 47 kJ/mol for MIL-101(Cr) and Mg-MOF-74, respectively, thus offering enhanced carbon dioxide uptake and selectivity at low pressures. Since suitable materials

for carbon dioxide capture from flue and combustion gases require higher selectivity in the presence of water, it seems quite beneficial to target MOFs in which the competition between carbon dioxide and water for adsorption is minimized. Therefore, chemical binding of carbon dioxide in a recent MOFs to make organic carbonates reversibly appears to be a promising approach.[18] These days the gas storage experiments on MOFs have also been performed to test the separation of hydrocarbons, toxic molecules such as ammonia and chlorine, from water. For example, $Cu_2(PZDC)_2(Pyz)$ (PZDC = pyrazine-2,3-dicarboxylate; Pyz = pyrazine) selectively takes up acetylene over carbon dioxide through hydrogen bonding between acetylene and oxygen atoms on the MOF pores and cavities. Even though certain compounds like ammonia, which were previously considered to be too reactive for MOFs, are now being observed to be ineffective in certain MOFs like Zr-MOFs, (e.g., UiO-66-NH_2 $[Zr_6O_4(OH)_4(BDC\text{-}NH_2)_6]$ and other derivatives. They are found to be chemically stable and easily maintain their structures after the process of ammonia adsorption and desorption .[18]

Selective/non-selective gas separation processes in MOFs are normally dependent on both the size of the pores and the affinity of MOFs for the targeted gases. But as the permanent porosity of MOFs was discovered, equilibrium adsorption isotherms for various gases were collected to estimate probable gas selectivity. High selectivity calculated from equilibrium data does not ensure high selectivity under dynamic gas separation conditions. Due to the various important industrial processes, the latter is more required, as the diffusion rate and Q_{st} (adsorption enthalpy) value of gas binding in the adsorbent are sensitive to the operating conditions. One of the initial illustrations of a dynamic separation was performed using a gas chromatographic column filled with

MOF-508 [$Zn_2(BDC)_2(BPy)$] to separate alkanes such as n-pentane, n-hexane, 2,2-dimethylbutane, and 2-methylpentane. It has also been reported that Mg and Fe-MOF-74, packed in a column, exhibit enhanced carbon dioxide separation from methane and C1 to C3 hydrocarbon, respectively.[17]

The capability to vary the size and nature of MOF structures without changing their fundamental topology gave rise to the isoreticular principle (the isoreticular principle is one way to tune the size of the pores by acting on the length of the rigid linker, keeping constant the inorganic part) and its application in making MOFs with the biggest pore aperture (98 Å) and lowest density (0.13 g/cm^3).[15] This has permitted the preferred inclusion of large molecules (e.g., vitamins) and proteins (e.g., green fluorescent protein) and the utilization of the pores as reaction vessels and platforms. Owing to these properties, the thermal and chemical stability of a majority of MOFs has rendered them open to post-synthetic covalent organic and metal-complex functionalization. These competencies enable substantial augmentation of gas storage in MOFs and have led to their extensive study in the catalysis of organic reactions, selective/non-selective gas separation, activation of small molecules (hydrogen, methane, and water), biomedical imaging, targeted nano drug-delivery and proton, electron, and ion conduction using porous rods created using MOFs. At present, methods are being developed for making nanocrystals and supercrystals of MOFs for their incorporation into devices.[15]

The defined control over the assembly of MOFs is expected to propel this research advance into new areas of synthetic chemistry in which far more sophisticated materials may be evaluated. Such materials can be expected to have compartments linked together to operate separately, yet act coherently; functionality to carry out numerous operations;

ability to translate sorting, and ability of dynamics with high conformity.[18] Efforts to achieve such usefulness are already being undertaken through the application of these MOFs on multiple substrates and introduction of a large number of different functional groups within the pores of MOFs. The multivariate frameworks can be produced in which the changing arrangement of functionalities gives rise to materials that promises a synergistic blend of properties.

Importance of magnesium and Mg-MOF-74

The importance of carefully picking the starting material for MOF synthesis is paramount. For an MOF to be synthesized with desired properties, a hydroxyl group on an organic linker has to be deprotonated by a base, and then the deprotonated oxygen of the hydroxide group has to donate its electrons to a possible metal cation. For a linking bond to occur in a reaction it is suggested that the organic linkers be planer with good symmetry. It is observed that most metals in MOFs are originally an ionic salt having an ionic bond between the cation and the anion and they are easily dissociated in the solvent. Once the metal salt is dissociated, the metal cation is able to accept electrons from the solvent or deprotonated oxygen.[21]

Magnesium is a relatively reactive metal and connects with many organic ligands and can form stable MOFs. Magnesium can be used in reactions because of its reactivity to exchange ligands. Magnesium is able to bond to water molecules, and can be easily removed from the bonded water molecules with a weak base. Another property of magnesium is its ability to form good crystals. Being an alkaline earth metal, it has certain advantages for applications in materials science; it is relatively non-toxic, cheap

and generally soluble in aqueous preparation. Due to these properties in general the alkaline earth salts are the preferred formulations for a range of commercial materials, including many common pharmaceuticals, dyes and pigments. It is observed that the MOFs formed by light main-group metals such as Mg^{2+} and Al^{3+} may are slated to play an important role in exhibiting a promising hydrogen storage capacity, due to their low framework density, high specific surface area and adjustable surface structures on which hydrogen molecules can be adsorbed.[22] In this project, Mg-MOF-74 was the first material to be studied due to its high BET surface area, high CO_2 adsorption capacity, high regeneration capacity and relatively simpler synthesis conditions.[20]

Future work will involve the assembly of chemical structures from many different types of elemental structure units, such that the structures' function is guided by the heterogeneity of the explicit preparation of their components.

Statement of Problem:

The following materials shall be used to synthesize novel porous coordination frameworks, containing a metal and an organic linker. The different magnesium salts that will be studied are magnesium nitrate hexahydrate $[Mg(NO_3)_2].6H_2O$ and magnesium chloride hexahydrate ($MgCl_2.6H_2O$). Also, a careful selection of flexible organic linkers like 1,4-cyclohexanedicarboxylic acid (1,4-CHDA), 4,4'-trimethylene dipyridine (4,4'-TMDiPy), piperazine (an N-donor ligand), and rigid organic linkers like isophtahlic acid (1,3-BDC or IPA), trimesic acid (1,3,5-benzene tricarboxylic acid), 4,4'-bipyridine (bipy, an N-donor ligand), and adenine will be explored to synthesize different structures. A mix of non-polar and polar solvents like N,N-dimethylformamide (DMF), methanol, ethanol, acetonitrile and distilled water will be used to understand their role in the synthesis of different frameworks. A variety of instrumentation will be utilized to characterize the products of several reactions to determine their chemical and physical properties.

Experimental Details

Materials

1,4-cyclohexanedicarboxylic acid (1,4-CHDA), isophtahlic acid (1,3-BDC or IPA), trimesic Acid (1,3,5-benzene tricarboxylic Acid), piperazine and 4,4'-bipyridine (bipy), 4,4'-trimethylene dipyridine (4,4'-TMDiPy) and dimethylformamide (DMF) were purchased from Sigma-Aldrich. Magnesium nitrate hexahydrate $[Mg(NO_3)_2].6H_2O$, magnesium chloride hexahydrate ($MgCl_2.6H_2O$), acetonitrile (CH_3CN) were purchased

from Fischer Scientific. Ethanol and methanol were purchased from Pharmo-AAPER. Triethylamine $(C_2H_5)_3N$ was purchased from Mallinckrodt. All materials were used without further purification.

Autoclave Preparation

Autoclave vessels were cleaned with diluted nitric acid (HNO_3) in a 1:1 ratio of HNO_3 and distilled water. 2.0-3.0 mL of 8M HNO_3 was added into each Teflon-lined stainless steel vessel; the vessels were sealed and put into the oven for 4-6 hours with the oven temperature at 140 °C. The vessels were taken out and washed with soap and deionized water.

Preparing for the Reaction

In each of the synthesis or reactions, generally the reactants or the starting materials were added in the following order. The solvent was pipetted, to the exact milliliter, into the Teflon liners or the glass vial. Then the organic linkers were added and the mixture was stirred until the reagents were fully dissolved. If required, the base was then added to the solution while being stirred. The magnesium salts were added (magnesium nitrate, $Mg(NO_3)_2.6H_2O$ or magnesium chloride, $MgCl_2.6H_2O$) separately in the required solvent. Both the mixtures were then mixed at desired temperatures. The base was then added and the solution was stirred for at least 10 minutes or until the reactants were fully dissolved. The vessels were capped and sealed. The internal temperature of the oven was calibrated to the required temperature and the samples were placed in the oven for the time specified for each experiment.

The products obtained were dried by being placed into a Schlenk tube. The valve was connected to a Schlenk line with a high vacuum pump. A dewar filled with liquid nitrogen was placed over the glass tube to keep the products cool under vacuum for 24 hours. The crystals retained their shape through the drying process, and lightened in color going from a darker bluish to a lighter purple.[23]

Characterization Techniques

Powder X-Ray Diffraction

Powder X-ray diffraction patterns were collected at room temperature using a Bruker D8 Advance or a Rigaku Miniflex diffractometer with Cu-Kα radiation in reflective mode, with open sample cups, or open aluminum disc cups, respectively. The data were analyzed using the EVA Application 7.001 software of SOCABIM (1996-2001), distributed by Bruker AXS, Madison, WI. Also, Rietveld refinements were performed using Topas.[23]

Single Crystal X-Ray Diffraction

A single crystal selected by size and shape, was mounted onto a thin fiber from a pool of Flurolube® oil and immediately placed on a Bruker AXS SMART APEX CCD diffractometer with a fine-focus sealed X-ray tube and a graphite monochromator. The experiments were carried out with Mo Kα radiation at 100K. The lattice parameters were optimized from a least-squares calculation on carefully centered reflections. Apex2 v.2012.4-3 was data collection, SAINT V8.18C was used for integration of data,

SHELXS97 and SHELXL2012 were used for solving structures, and SHELXLE Rev576, Shelxle and SHELXTL were used for refinement.[23]

Absorption was corrected by multi-scan methods. Each structure was solved using direct methods. This procedure yielded the heavy atoms, along with a number of C atoms. Subsequent Fourier synthesis yielded the remaining C atom positions. The reflections were merged according to the crystal class for structure refinement and the calculation of statistics. The final refinement of each compound included refinement of anisotropic thermal parameters on all non-hydrogen atoms.[23]

TGA Analysis

Thermal gravimetric analysis (TGA) profiles were recorded on a TA Instruments TGA2050 Thermogravametric Analyzer. Samples were heated at a rate of 10 °C min^{-1} from 25 to 500 °C under a flow of 60 mL min^{-1} nitrogen. Platinum pans were used and then cleaned in 16M concentrated nitric acid.

TEM Analysis

JEOL 2010 transmission electron microscope (TEM) was used for structural and chemical analysis of the particles of the Mg-MOF-74 (at atomic level) synthesized in the lab. The TEM instrument was operated at 200 kV and equipped with an EDAX detector for chemical composition analysis and annular dark–field detector. The general morphology of the samples of MOFs was studied for individual nanocrystals and was determined by energy dispersive X-ray spectroscopy (EDX) analysis in scanning transmission electron microscopy (STEM) mode with a focused electron probe. TEM samples were prepared by using dilute suspensions of the nano-powder samples. These

solutions were obtained by ultra-sonicating particles in ethanol for 10 min then dropping the suspension of the sample powders onto an ultrathin carbon film/holey carbon, 400 mesh copper grid and letting it air dry for several hours.[24]

Results and Discussion:

Synthetic Strategy

The main goal of this research was to synthesize porous inorganic frameworks using magnesium as the principle metal and a series of organic linkers along with a solvent or an added base, which helps in the deprotonation of the organic linker. The choice of metal and linker has substantial effects on the structure and properties of the MOF. The metal's coordination preference influences the size and shape of pores by dictating the number of ligands that can bind to the metal ion and in which orientation. A systematic approach was taken to select the linkers. Different multi-valent flexible organic linkers were chosen such as 1,4-cyclohexanedicarboxylic acid, piperazine, 4,4'-trimethylene dipyridine (4,4'-TMDiPy) and different rigid organic linkers like isophthalic acid (1,3-BDC or IPA), benzene-1,3,5-tricarboxylic acid (trimesic acid), 4,4'-bipyridine, and adenine etc. were selected with an objective to obtain large structures with possible porosities. The main solvent of choice was DMF, as it is frequently utilized in the synthesis of various porous MOFs.[19] Choice of DMF was made primarily due to its property of the deprotonation of the linker. In some other reaction the use of some bases helped in the deprotonation of the linkers used as the starting material. Other solvent choices included water, acetonitrile, methanol and ethanol.

Synthesis of Mg-MOF-74, using Mg with 2,5-dihydroxyterephthalicacid (DHTA)[2]

In order to synthesize Mg-MOF-74, the conventional solvo-thermal technique was employed to perform a reaction of magnesium nitrate ($Mg(NO_3)_2.6H_2O$)(Fischer Scientific) with 2,5-dihydroxyterephthalicacid (DHTA)(Aldrich), with the solvents N,N-dimethylformamide (DMF), ethanol (C_2H_5OH) and de-ionised water. In a solution of 135 mL of DMF, 9 mL ethanol and 9 mL water were dissolved 0.337 g DHTA and 1.4 g magnesium nitrate under sonication. The resulting stock solution was decanted into fifteen 20 mL glass vials, which were capped tightly and heated at 125 °C for 26 hrs. The mother liquor was then decanted, the products washed with methanol, then immersed in methanol. The product was combined and exchanged with fresh methanol for 3 days. It was then dried and heated under vacuum at 250 °C for 15 hrs. This procedure yields yellow colored crystals.[2] The samples were sent to the National Energy Technology Laboratory (NETL) for gas adsorption and BET surface area testing. The results were as follows:

	N_2 isotherm at -196 °C (77 K)	**CO_2 isotherm at 30 ^oC (303 K)**
Lab Sample	BET Area (m^2/g)	Amount adsorbed at 760 torr (cc/g)
Mg-MOF-74	15.83	18.31

Source: National Energy Technology Laboratory (NETL) labs data (July, 2011)

SAMPLE:	Mg-MOF-74
SAMPLE WEIGHT (g):	0.1709
GAS TEMP.	N_2 77 K

P/Po	P (torr)	Vol. adsorbed (cc)	Vol. adsorbed (cc/g)
0.104584	79.48384	0.602068	3.523
0.152376	115.80576	0.669512	3.918
0.203268	154.48368	0.724068	4.237
0.251073	190.81548	0.799647	4.679
0.303148	230.39248	0.852988	4.991
BET Surface Area (m^2/g):	**15.83 m^2/g**		

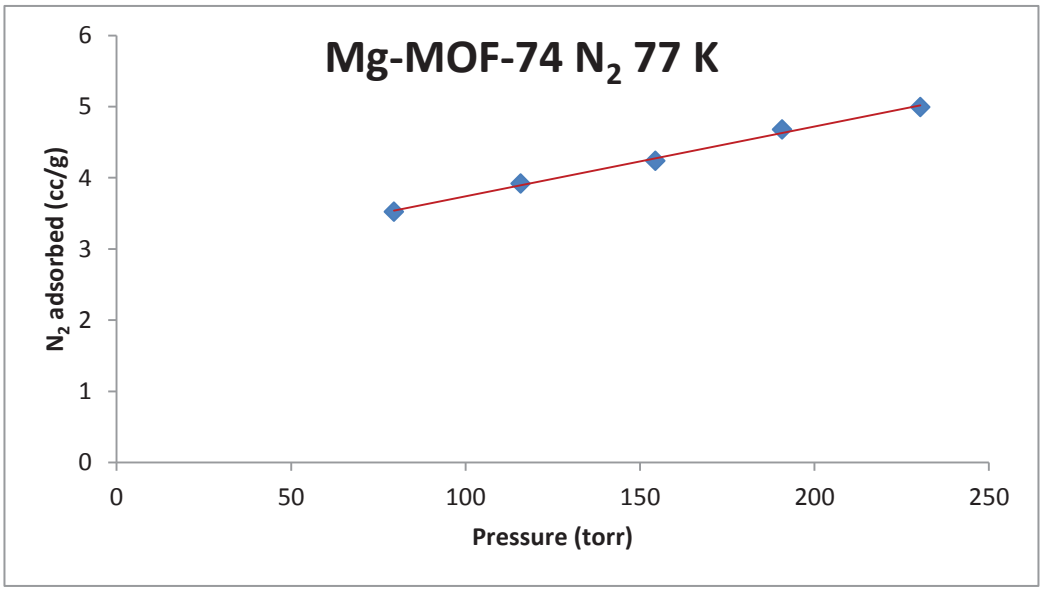

Figure 4: Nitrogen (N_2) adsorption data at 77 K form NETL (July, 2011) using the Mg-MOF-74 sample prepared in lab

SAMPLE	Mg-MOF-74
SAMPLE WEIGHT (g):	0.1709
GAS TEMP.	CO_2 303 K

P/Po	P (torr)	Vol. adsorbed (cc)	Vol. adsorbed (cc/g)	CO_2 adsorbed (wt. %)		Difference
				Experimental	Calculated	
0.000999327	0.759	0.00339981	0.020	0.004	0.004	-0.0004
0.00512641	3.896	0.0321303	0.188	0.037	0.023	0.0140
0.0100245	7.619	0.0651997	0.382	0.075	0.045	0.0296
0.0522478	39.708	0.205316	1.201	0.236	0.240	-0.0042
0.0981357	74.583	0.382695	2.239	0.440	0.449	-0.0092
0.201565	153.189	0.79309	4.641	0.912	0.902	0.0099
0.298345	226.742	1.13511	6.642	1.305	1.301	0.0035
0.398391	302.777	1.4697	8.600	1.689	1.690	-0.0012
0.498711	379.020	1.79647	10.512	2.065	2.058	0.0068
0.599374	455.524	2.11205	12.358	2.428	2.406	0.0219
0.698372	530.763	2.36139	13.817	2.714	2.728	-0.0141
0.799245	607.426	2.66732	15.607	3.066	3.039	0.0269
0.898709	683.019	2.90263	16.984	3.336	3.329	0.0077
0.994125	755.535	3.13024	18.316	3.598	3.592	0.0057

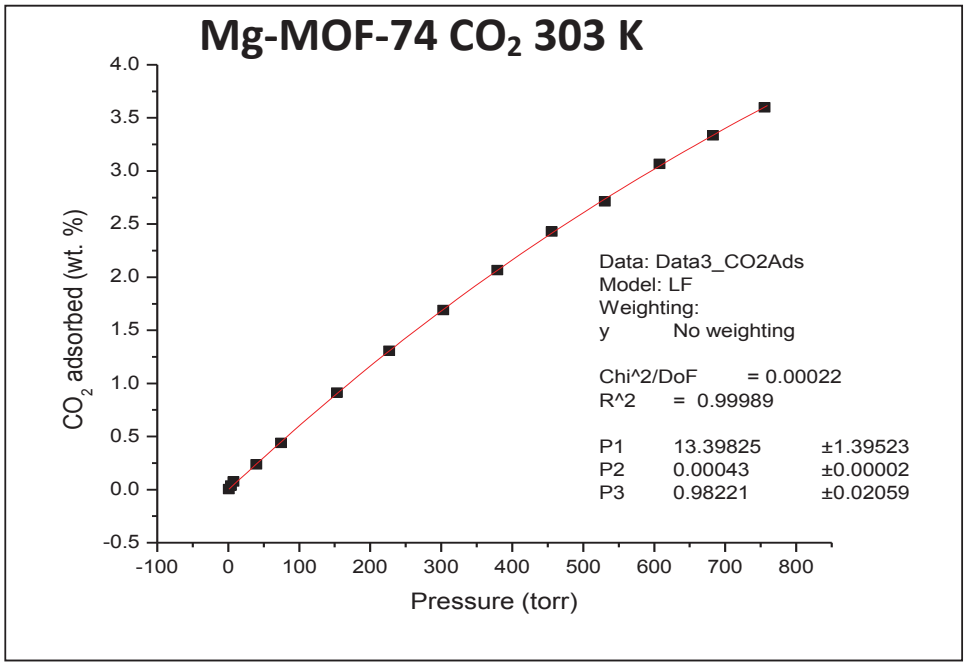

Figure 5: Carbon dioxide (CO_2) adsorption data at 303 K form NETL (July, 2011) using the Mg-MOF-74 sample prepared in lab

TEM analysis of the lab synthesized Mg-MOF-74

Following are representative TEM images observed for the Mg-MOF-74 samples produced in the lab using the above mentioned synthesis. The resulting images are taken at varying magnifications:

(a) (b)

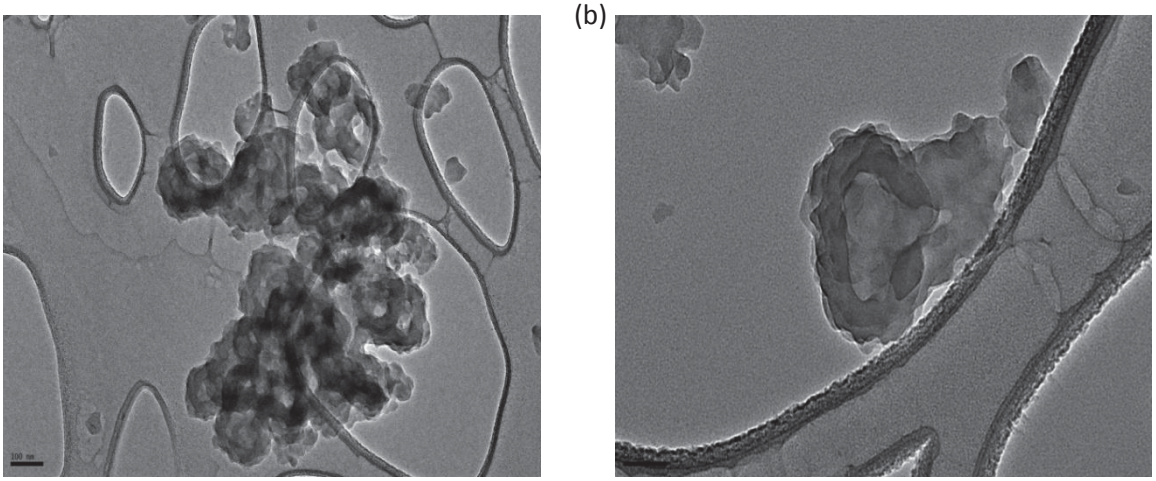

Figure 6: Mg-MOF-74 (lab sample) - Magnification for (a) 15K and (b) 40K

(a) (b)

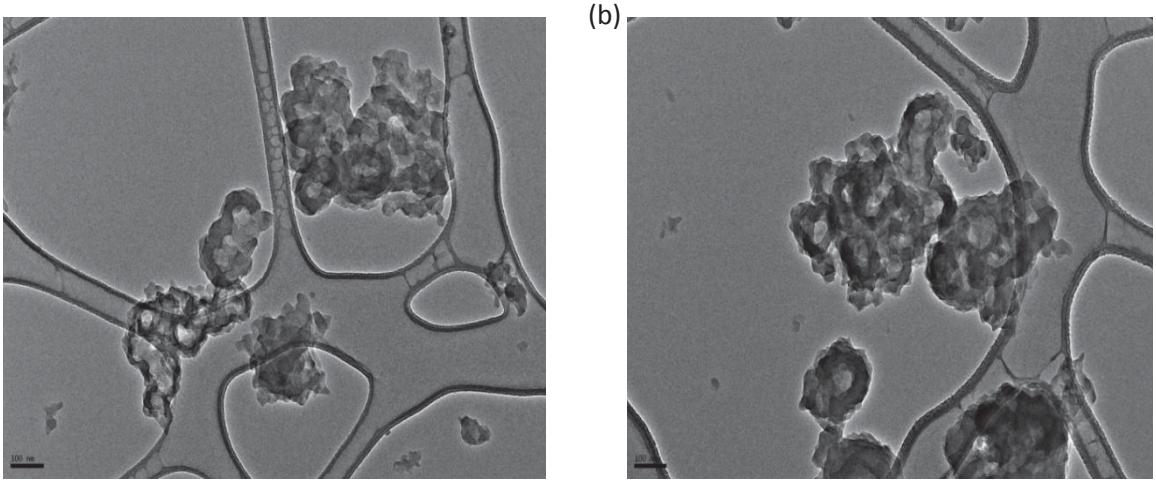

Figure 7: Mg-MOF-74 (lab sample) - Magnification for (a) 15K and (b) 40K

These images help in understanding the physical structure of the MOFs synthesized in the lab. With the help of transmission electron microscopy (TEM), a general idea of the

compound's morphology and porosity was obtained at the nanocrystal level. These images can help in building a relationship between the structures of the MOF sample with their adsorption characteristics. The particles in Figure 6(b) display certain porosity in their structure whereas the particles in Figure 6(a) looks more like solid granular structure. The particles in Figure 7(a) & 7(b) appears to have limited porosities in the structure. Using the online software "ImageJ version 1.47", the average particle size for the samples was found close to 200 nm and the average pore size in the hollow particles is around 100 nm. A list of TEM images taken for various samples of Mg-MOF-74 are provided in Appendix B.

Powder X-ray diffraction (PXRD) data for lab synthesized Mg-MOF-74 (solvothermal synthesis)

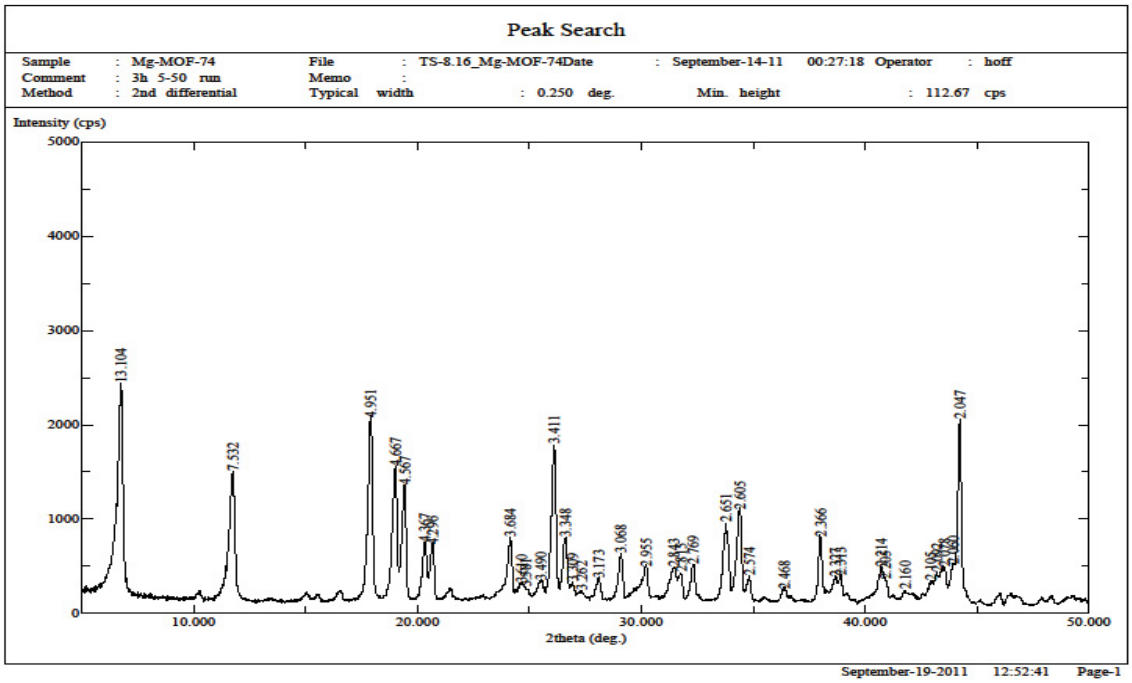

Figure 8: Powder X-ray diffraction data for Mg-MOF-74 (lab sample)

Owing to the presence of impurities and the use of aluminum spot plates, the PXRD data for lab synthesized Mg-MOF-74 deviated somewhat from the reported PXRD. Detailed powder XRD patterns for all the lab synthesized samples are provided in Appendix A.

Moving forward in the synthesis of MOFs, a set of organic linkers and magnesium salts (magnesium nitrate and magnesium chloride) were identified as potential substrates along with some solvents and bases like DMF, water, ethanol, methanol, acetonitrile, tetrehydrofuran etc. to try out some novel syntheses. Following are the some of the novel framework materials synthesized during the research along with the lab synthesis of Mg-MOF-74. Space group table number in the crystal data section is provided from International Tables for Crystallography.[28]

Synthesis using Mg with flexible linker 1,4-cyclohexanedicarboxylic acid (1,4-CHDA)

I. Zero Dimensional, $[PIP\text{-}H_2][Mg(H_2O)_6].4.0Cl$

The asymmetric unit of the title compound, $[PIP\text{-}H_2][Mg(H_2O)_6].4.0Cl$, consists of one molecule of each piperazine, two chlorine molecules, and magnesium that is crystallized in the monoclinic space group. The piperazine molecule is strongly bonded with magnesium and forms zero-dimensional chains. The piperazine molecule in the lattice acts as a bridge between two magnesium atoms, which is strongly bonded to six water molecules, through strong coordinate bonds forming linear chains. The chains are stacked one over the above and form zero-dimensional supramolecular structure through

interactions between piperazine and magnesium-H_2O forming a hexagonal plate like crystals upon synthesis. Unit cell dimensions are as follows: Unit cell dimensions: a = 13.167(5) Å, b = 10.967(4) Å, c = 12.305(5) Å, β = 112.12(0)° and Cell volume: V = 1646.07(110) Å^3. Space group: $C12/c1$ (no. 15).

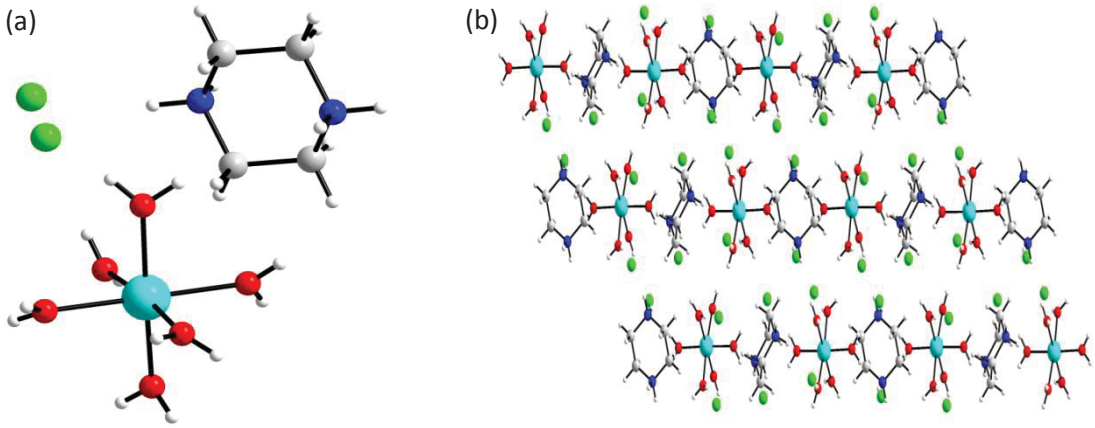

Figure 9: (a) Unit cell packing and (b) Zero-dimensional SXRD projection of the supramolecular structure of the [PIP-H_2][$Mg(H_2O)_6$].4.0Cl

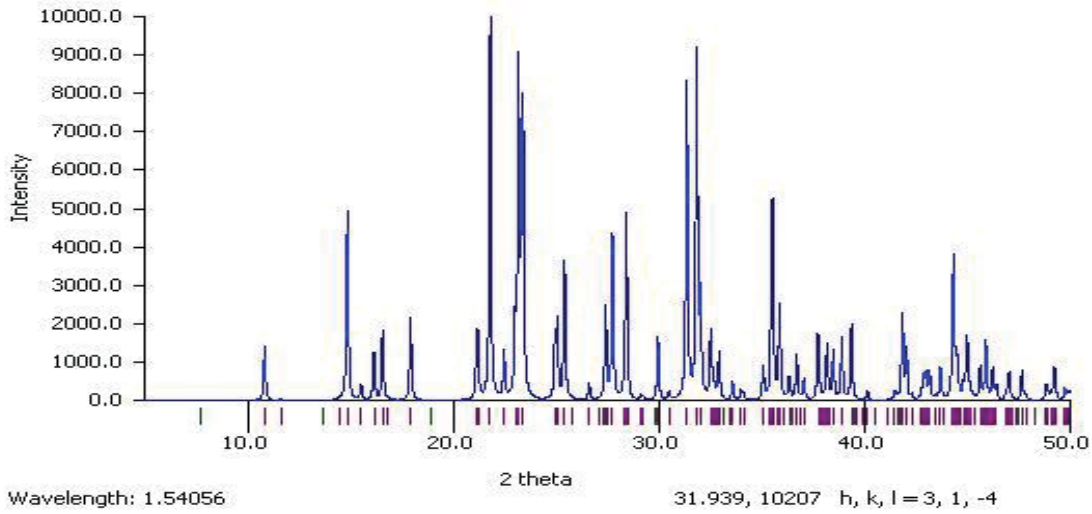

Figure 10: Simulated X-ray diffraction pattern of [PIP-H_2][$Mg(H_2O)_6$].4.0Cl

II. Zero Dimensional, $[Mg(H_2O)_6][trans\text{-}(1,4\text{-}CHDA)].3H_2O$

The asymmetric unit of the title compound, $[Mg(H_2O)_6][trans\text{-}(1,4\text{-}CHDA)].3H_2O$, consists of one molecule of trans 1,4-CHDA, three independent water molecules, and magnesium which is strongly bonded to six water molecules and is crystallized in the monoclinic space group. The 1,4-CHDA molecule is strongly bonded with magnesium and forms zero-dimensional layered structure. The 1,4-CHDA molecule in the lattice acts as a connecting bridge between two alternate magnesiums chains. The chains are stacked one over the above and form zero-dimensional supramolecular structure through interactions between 1,4-CHDA and magnesium-H_2O forming a unimolecular layer like structure. Unit cell dimensions were as follows: Unit cell dimensions: a = 12.2351(16) Å, b = 5.4163(7) Å, c = 14.0489(18) Å, β = 115.78(0)°, V = 838.33(83) Å^3. Space group: P1 2/c1 (no. 13).

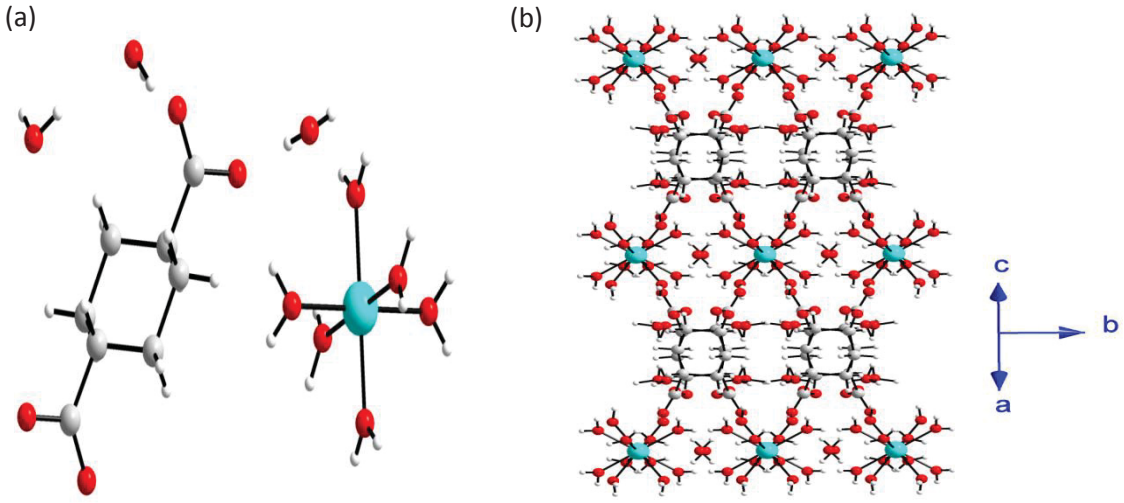

Figure 11: (a) Unit cell packing and (b) Zero-dimensional SXRD projection of the supramolecular structure of the $[Mg(H_2O)_6][trans\text{-}(1,4\text{-}CHDA)].3H_2O$

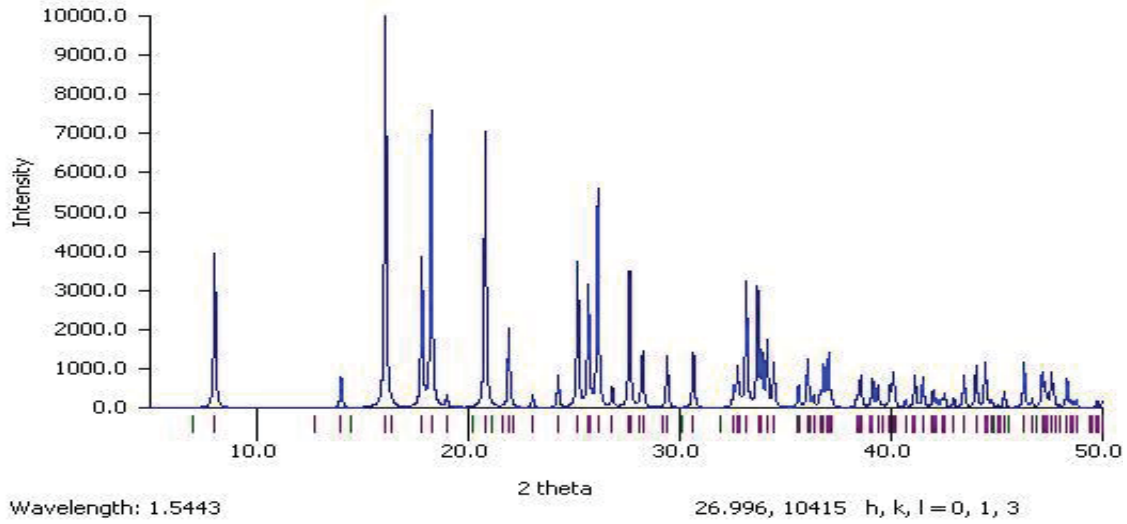

Figure 12: Simulated X-ray diffraction pattern of $[Mg(H_2O)_6][trans\text{-}(1,4\text{-}CHDA)].3H_2O$

III. Zero Dimensional, $[Mg(H_2O)_6][Mg(H_2O)_4(1,4\text{-}CHDA)_2].H_2O$

The asymmetric unit of the title metal-organic salt, $[Mg(H_2O)_6][Mg(H_2O)_4(1,4\text{-}CHDA)_2].H_2O$, consists of two molecule of 1,4-CHDA, two magnesiums strongly bonded with six and four water molecules respectively, and one independent water molecule packed in a triclinic crystal space group. The 1,4-CHDA molecule is strongly bonded with two different magnesium centers through strong C-H···O bonds and forms zero-dimensional layers. The water molecule in the lattice acts as a bridge between two alternate molecules of 1,4-CHDA and magnesium centers. The entire structure is stabilized by intramolecular interactions. The oxygen atoms possess tetrahedral geometry through H-bonding. Unit cell dimensions: a = 5.213(2) Å, b = 9.436(5) Å, c = 14.147(8) Å, α = 90.35(1)°, β = 98.34(1)°, γ = 104.89(1)°, V = 664.72(60) Å^3. Space group: P-1 (no. 2).

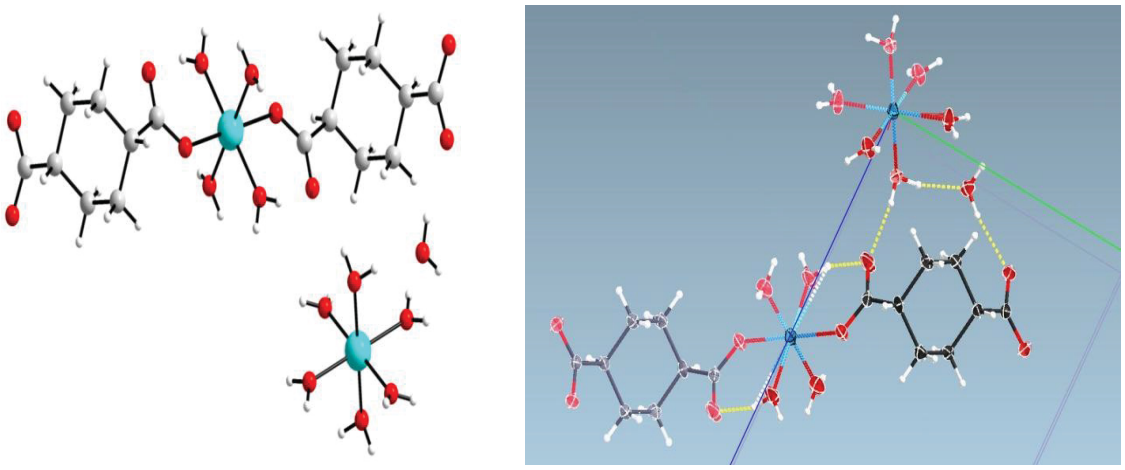

Figure 13: Unit cell packing (left) and Zero-dimensional SXRD projection of the supramolecular structure (right) of the $[Mg(H_2O)_6][Mg(H_2O)_4(1,4\text{-}CHDA)_2].H_2O$

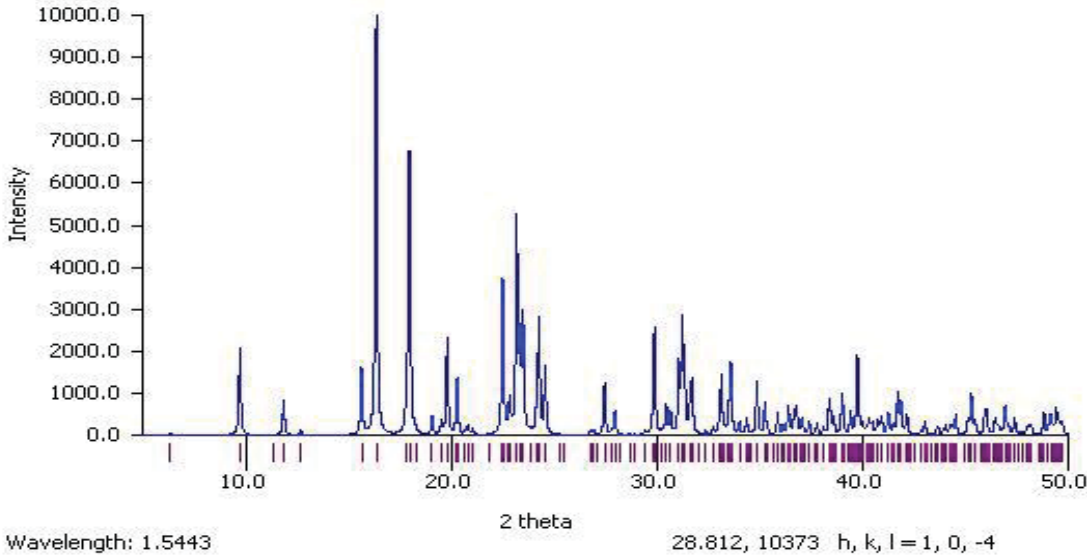

Figure 14: Simulated XRD pattern of $[Mg(H_2O)_6][Mg(H_2O)_4(1,4\text{-}CHDA)_2].H_2O$

IV. Two Dimensional magnesium carboxylate, $[Mg(1,4\text{-}CHDA\text{-}H)_2(H_2O)_2]$

The asymmetric unit of the above compound, $[Mg(1,4\text{-}CHDA\text{-}H)_2(H_2O)_2]$, consists of two molecules of each cis-1,4-CHDA and water, and magnesium that is crystallized in the triclinic crystal system. The magnesium is strongly bonded with the oxygen of two 1,4-CHDA and two water molecules forming two-dimensional layer stacked over each other. The 1,4-CHDA molecule in the lattice connects two magnesiums which is strongly bonded to two water molecules, through strong coordinate bonds forming linear chains. The chains are stacked one over the above and form two-dimensional supramolecular structure through electrostatic interactions between 1,4-CHDA and magnesium-H_2O forming a multi-layered stacked structure on synthesis. Unit cell dimensions are as follows: a = 9.7286(3) Å, b = 14.1805(5) Å, c = 14.1890(5) Å, α = 93.83(0)°, β = 106.49(0)°, γ = 106.78(0)°, Cell volume: 1773.23(10) $Å^3$. Space group: $P1$ (no. 1).

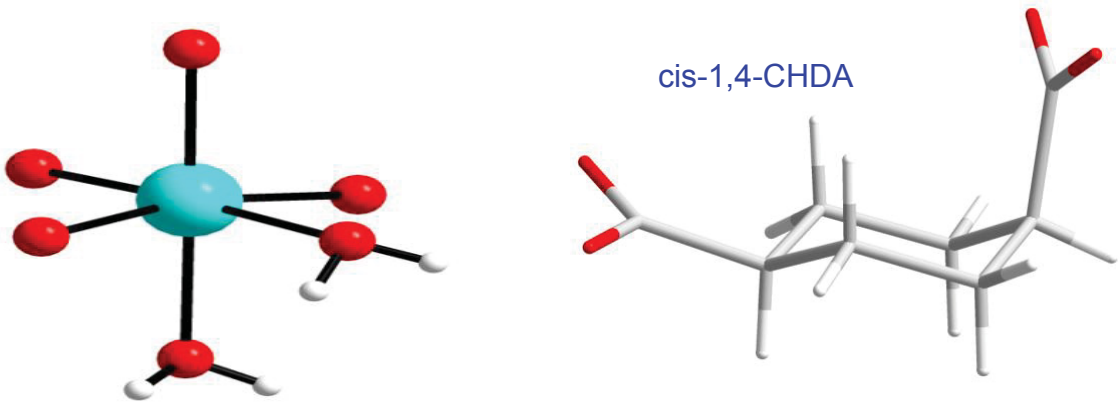

Figure 15: SXRD projection displaying the Mg coordination with water and cis-1,4-CHDA in the structure of two-dimensional $[Mg(1,4\text{-}CHDA\text{-}H)_2(H_2O)_2]$

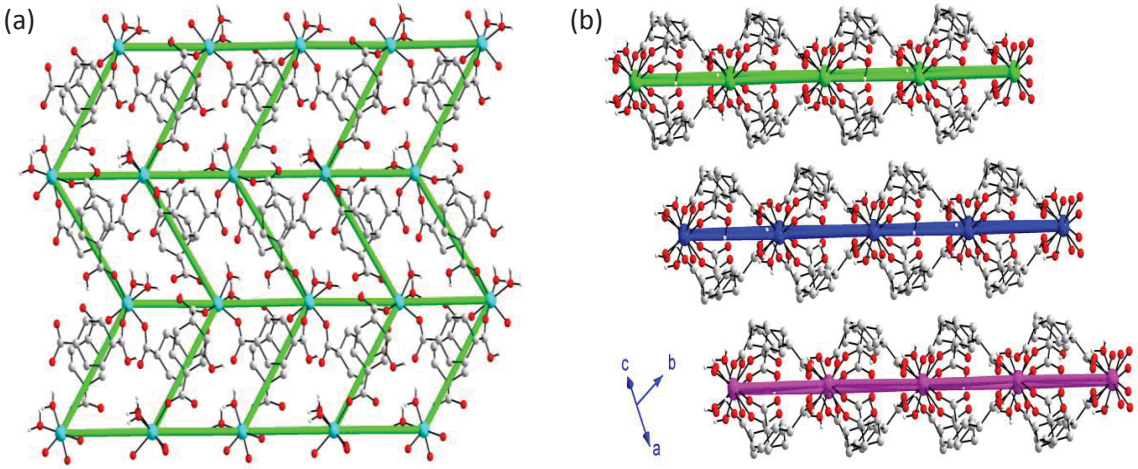

Figure 16: (a) Layer and (b) stacking arrangement of $[Mg(1,4\text{-CHDA-H})_2(H_2O)_2]$

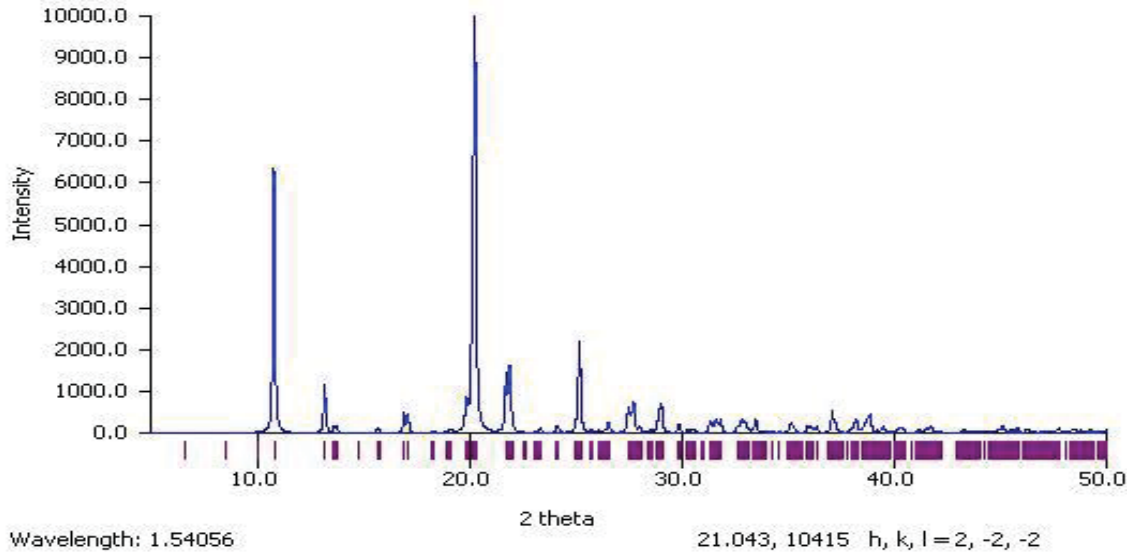

Figure 17: Simulated X-ray diffraction pattern of $[Mg(1,4\text{-CHDA-H})_2(H_2O)_2]$

Mg with rigid linker isophtahlic acid (1,3-BDC or IPA):

Six novel compounds were synthesized in glass vials by employing a variety of synthesis conditions.

I. Zero Dimensional, Dimethyl ammonium 3-carboxybenzoate, $[(CH_4)_2NH\text{-}H][IPA\text{-}H]$

The asymmetric unit of the title organic salt, $[(CH_4)_2NH\text{-}H][IPA\text{-}H]$, consists of two dimethylammonium cations and two 3-carboxybenzoate anions. The 3-carboxybenzoate anions are linked via strong intermolecular and nearly symmetrical O-H···O hydrogen bonds forming infinite chains. Adjacent chains are additionally connected by the dimethylammonium ions via N-H···O bonds, forming a double-chain-like structure. The dihedral angles of all carboxylate groups with respect to the phenylene rings are in the range 7.9 (1)-20.48 (9)°. Molecules in the chains are arranged in an ABAB···fashion, with crystallographically different mono-anions alternating with each other. The O—H···O hydrogen bonds are characterized by nearly equidistant D—H and A—H distances. The keto oxygen atoms of the carboxylate units, those which are not involved in the O—H···O H-bonds, act as acceptors for N—H···O H-bonds that originate from both of the dimethylammonium cations, which make a double bridge arising out of the carboxylic acid and carboxylate groups of the anions into a bis(dimethylammonium)—bis(COO-···H+···-OOC) cluster (Fig. 3). In such a manner parallel infinite 3-carboxybenzoate chains are connected into an inversion symmetric double chain like structure. The result has been published in Acta. Cryst. (2012). E68, o1778. Title of the paper: Dimethyl ammonium 3-carboxybenzoate.[27]

Crystal system: Triclinic, Space group: *P*-1 (no. 2), Unit cell dimensions:

a = 8.4386(52) Å, b = 10.1331(75) Å, c = 12.3044(87) Å, α = 91.86(1)°, β = 94.60(2)°, γ = 90.01(1) °, Cell volume: V = 1048.20(196) Å^3.

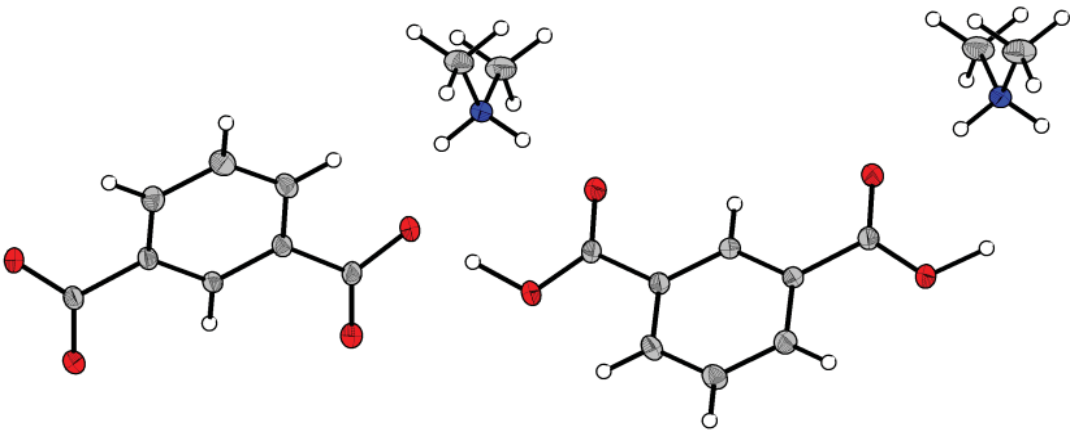

Figure 18: View of the asymmetric unit cell packing

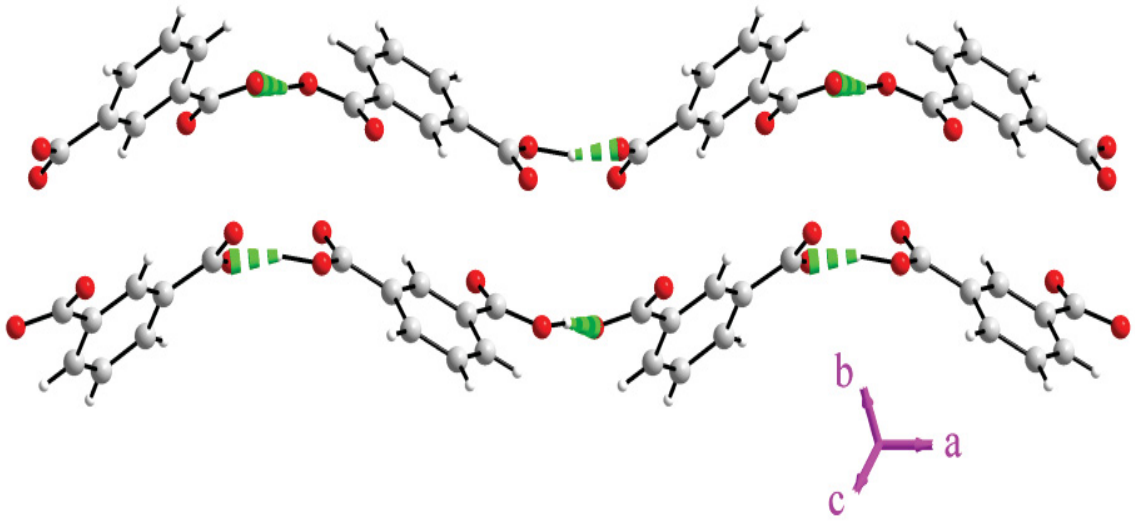

Figure 19: View of the one-dimensional 3-carboxybenzoate chains formed through intermolecular nearly symmetrical O-H···O bonds parallel to the (111) direction

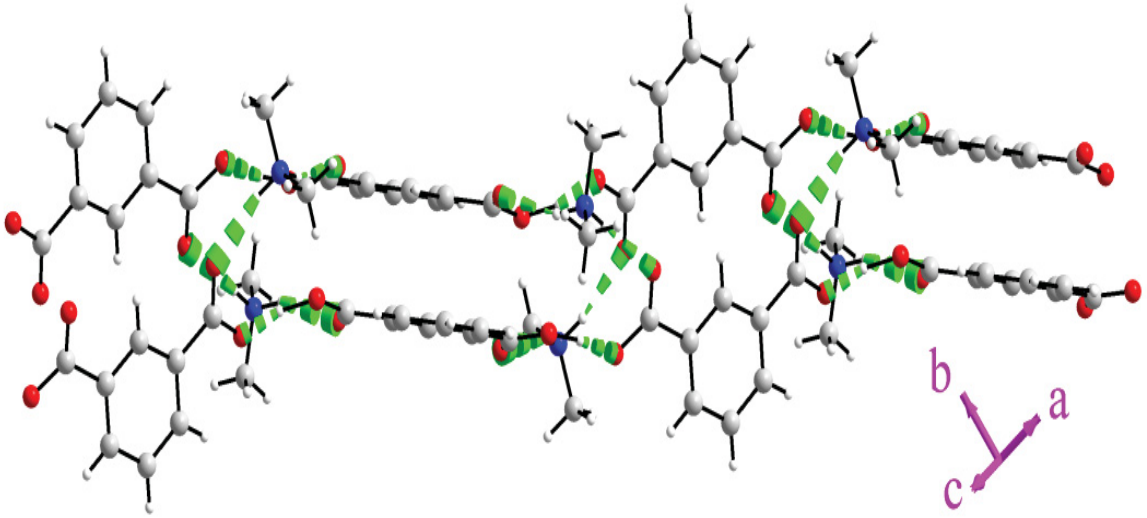

Figure 20: View of the double chain-like structure. A crystallographic inversion center between the two central phenylene rings relates the parallel chains to each other

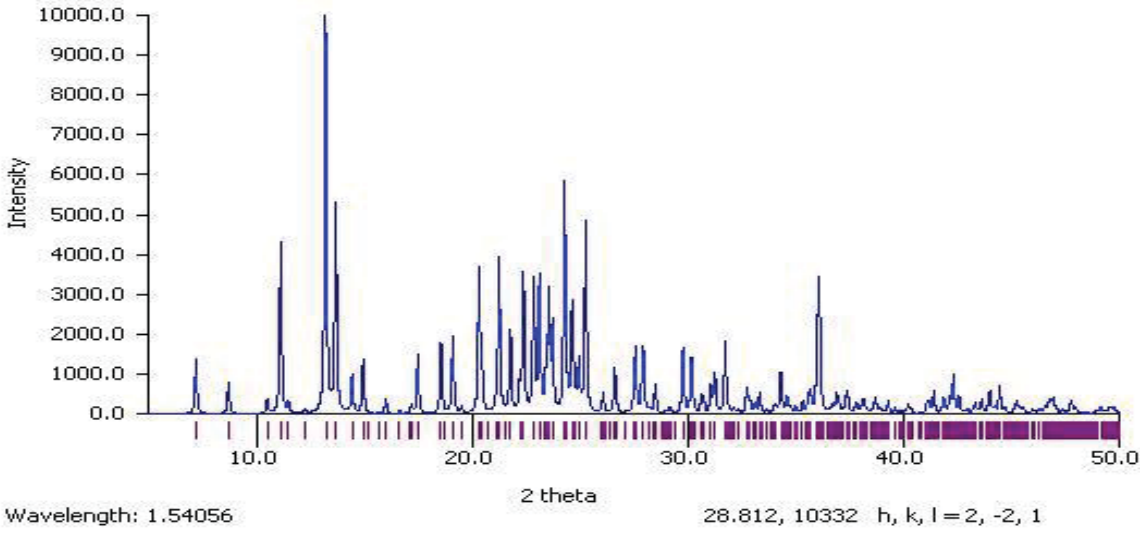

Figure 21: Simulated X-ray diffraction pattern of $[(CH_4)_2NH\text{-}H][IPA\text{-}H]$

II. Zero Dimensional, Adenin-1-ium isophthalate dimethylformamide, $[C_5H_{6.3}N_5]^+.[C_8H_{4.7}O_4]^-.C_3\ H_7\ NO$

The asymmetric unit of the title proton-transfer organic salt, $[C_5H_{6.3}N_5]^+.[C_8H_{4.7}O_4]^-.C_3H_{7N}O$, consists of one molecule of each 1,3-dicarboxy benzene (isophthalic acid or IPA), adenine, and dimethylformamide (DMF) that is crystallized in the orthorhombic space group. During the synthesis, hydrogen from the IPA moves to pyrimidine nitrogen of adenine molecule and formed proton-transferred organic salt. The adenine molecule is hydrogen bonded with IPA through strong N-H···O bonds and forms one-dimensional undulated chains. The DMF molecule in the lattice acts as a bridge between two chains, through strong N-H···O and C-H···O bonds forming criss-cross chains. The chains are stacked one over the above and form three-dimensional supramolecular structure through π-π interactions between adenine-adenine and IPA-IPA. The entire structure is stabilized by N-H···*O,* C-H···O and C-H···π interactions.

Crystal system: Orthorhombic, Unit cell dimensions: a = 3*8*.307(18) Å, b = 46.05(2) Å, c = 3.7832(18) Å, α = 90.00°, β = 90.00°, γ = 90.00°, Cell volume: V = 6673.71 Å^3, Space group: *Fdd*2 (no. 43).

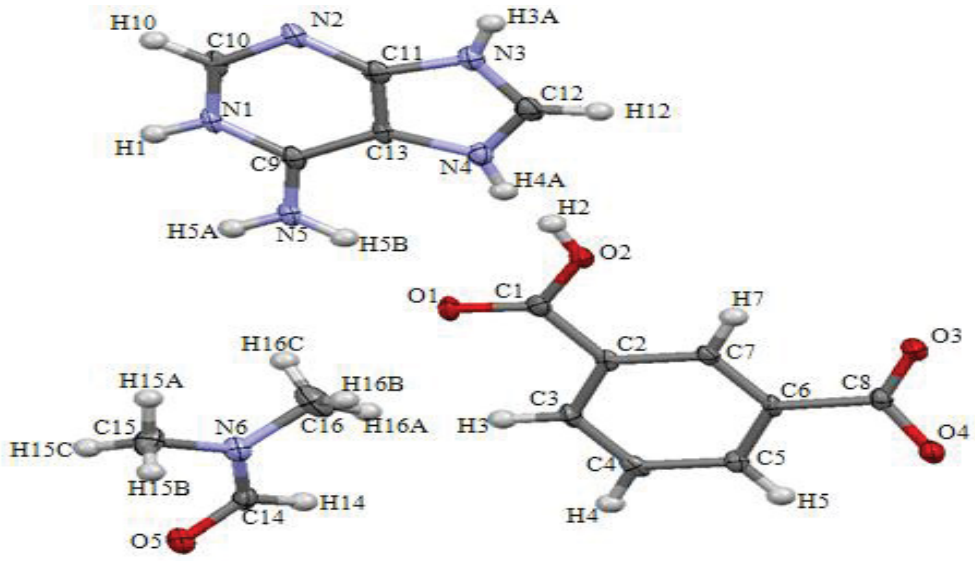

Figure 22: View of the asymmetric unit cell packing with atom numbering

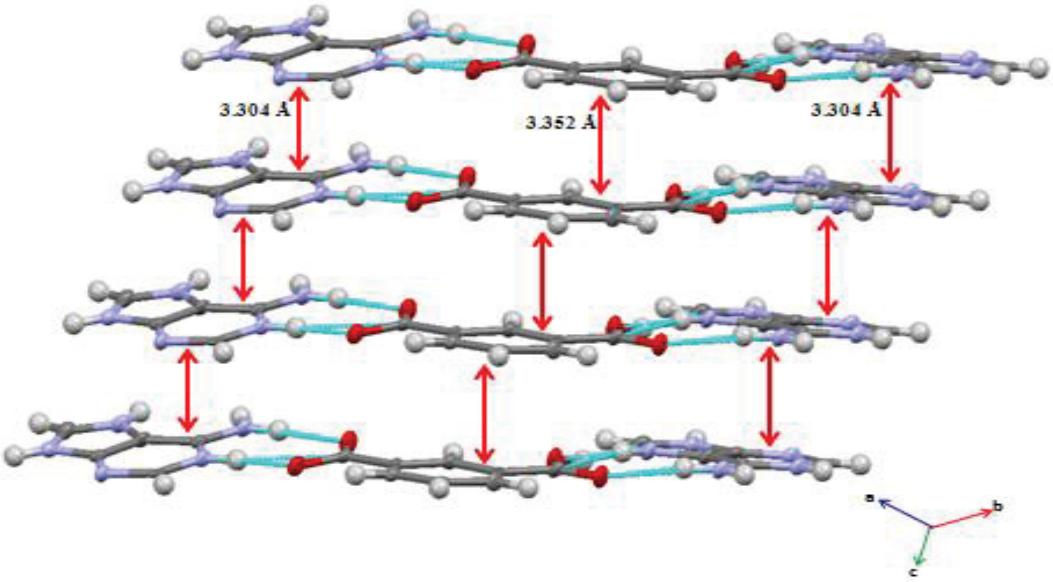

Figure 23: View of the π-stacking of chains. Distance between neighboring (parallel) adenine-adenine is 3.304 Å and isophthalic acid-isophthalic acid is 3.352 Å

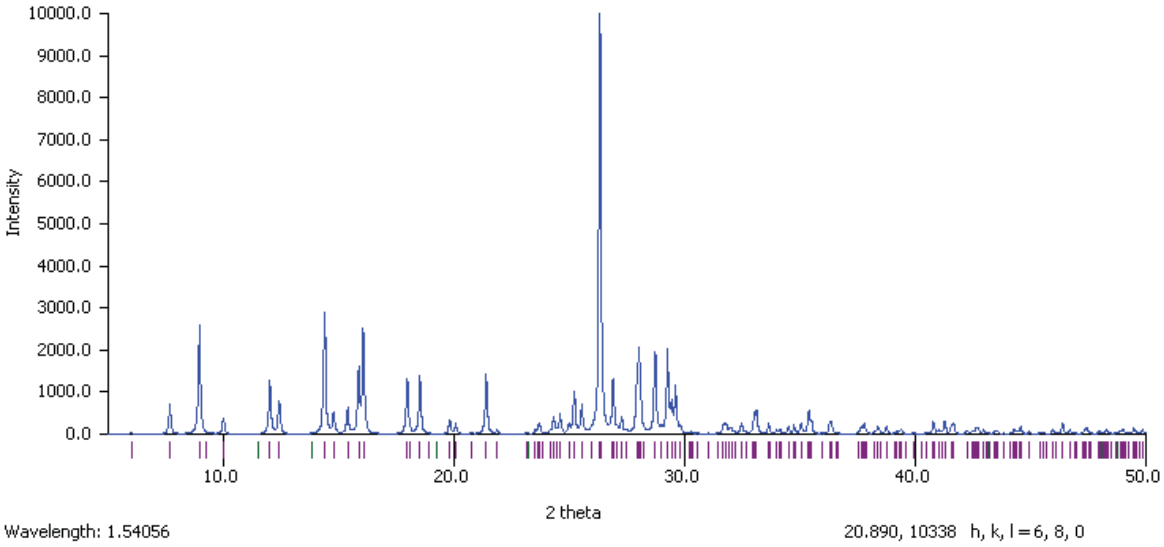

Figure 24: Simulated X-ray diffraction pattern of Adenin-1-ium isophthalate dimethylformamide, $[C_5H_{6.3}N_5]^+.[C_8H_{4.7}O_4]^-.C_3\ H_7\ NO$

III. Two Dimensional, $[Mg_4(IPA)_4(DMF)_6].2(DMF)$

The asymmetric unit of the above compound, $[Mg_4(IPA)_4(DMF)_6].2(DMF)$, consists of four molecules of isophthalic acid and six molecules of DMF coordinated to two different dimers of magnesium, and the unit cell that is crystallized in the monoclinic crystal system. The magnesium atoms are strongly bonded with the oxygen of two four isophthalic acid molecules and six DMF molecules along with a free DMF molecule packed in the asymmetric unit. The resulting structure gives rise to chains forming two-dimensional layer stacked over each other in ABAB fashion having a square grid along (100) direction (Fig. 26). The layers are stacked one over the above and can slide over each other to give rise to a supramolecular structure. Unit cell dimensions are as follows:

a = 17.8677(36) Å, b = 9.9918(19) Å, c = 18.2414(37) Å, β = 92.29(0)°, Cell volume: 3254.04(121) Å^3. Space group: $P1c1$ (no. 7).

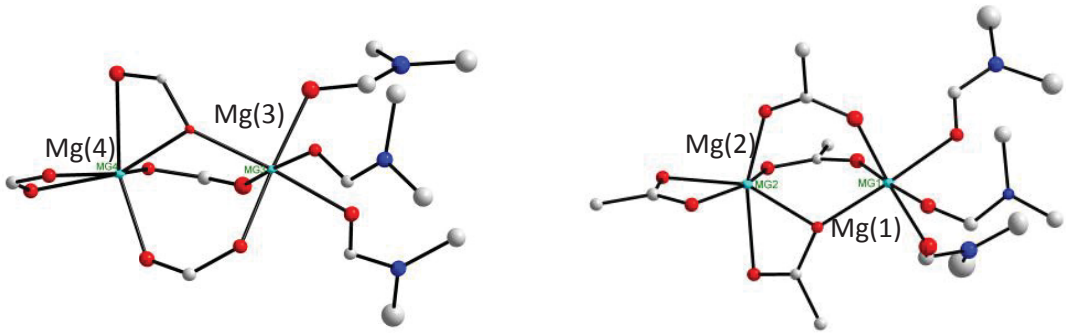

Figure 25: View of the Mg coordination and dimers as observed in the unit cell

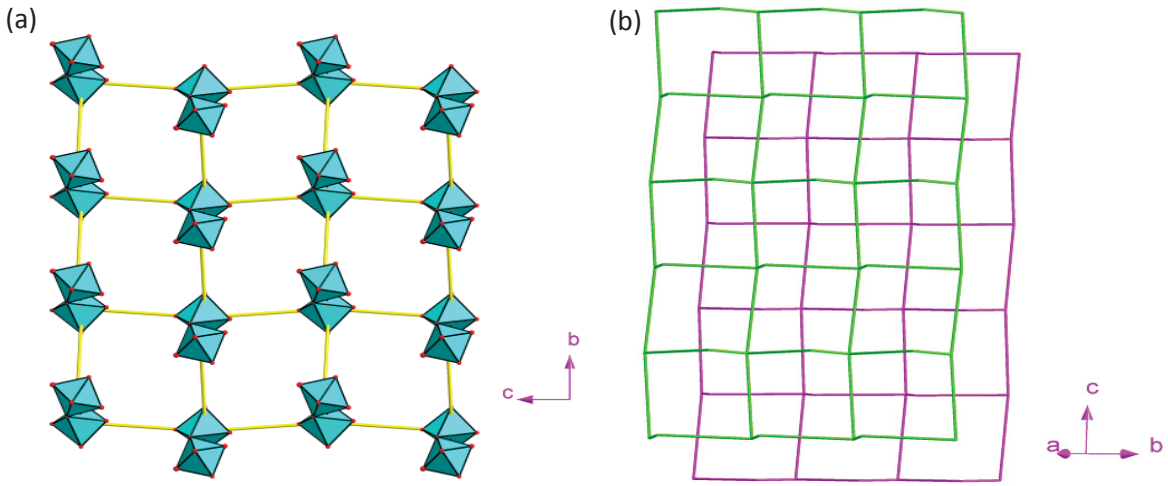

Figure 26: (a) View of the layer along [100] direction. Polyhedra represent the Mg dimers. (b) View of the two independent sliding layers along [110] direction for $[Mg_4(IPA)_4(DMF)_6].2(DMF)$ stacked in ABAB fashion

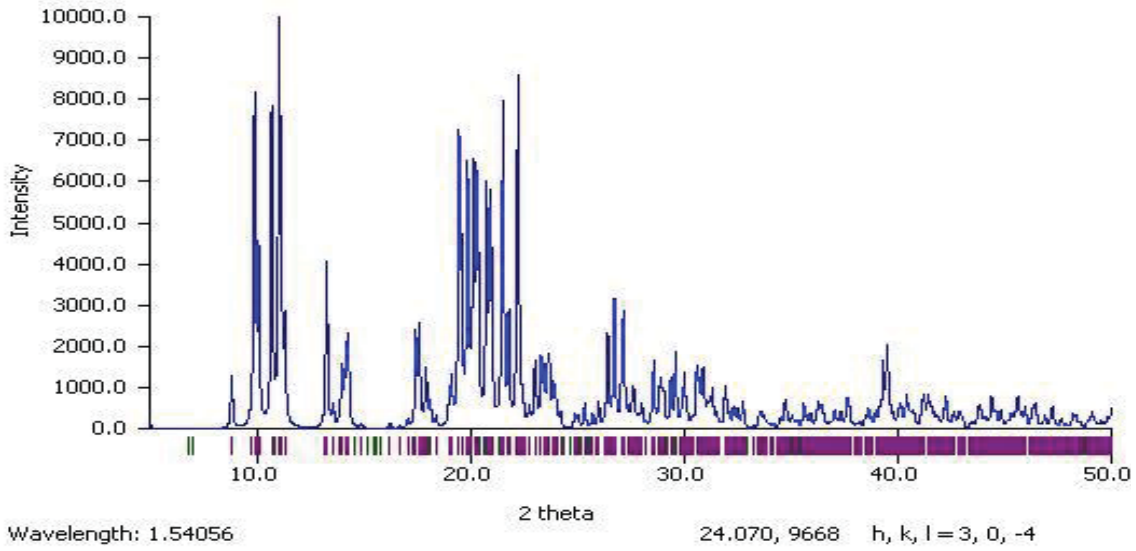

Figure 27: Simulated X-ray diffraction pattern of $[Mg_4(IPA)_4(DMF)_6].2(DMF)$ created from the single crystal XRD data

IV. Two Dimensional, $[Mg_4(IPA)_4(DMF)_6(CH_3OH)_2].(DMF)$

The asymmetric unit of the given compound, $[Mg_4(IPA)_4(DMF)_6(CH_3OH)_2].(DMF)$, consists of four molecules of isophthalic acid and six molecules of DMF coordinated to two different dimers of magnesium along with two molecules of methanol, and the unit cell that is crystallized in the monoclinic crystal system. The magnesium dimers are strongly bonded with the oxygen of two four isophthalic acid molecules and six DMF molecules, two methanol molecules along with a free DMF molecule packed in the asymmetric unit. The resulting structure gives rise to chains propagating in all directions giving rise to a two-dimensional supramolecular layered framework structure. Unit cell

dimensions are as follows: a = 12.617(2) Å, b = 16.259(3) Å, c = 15.673(3) Å, α = 90.00°, β = 90.00°, γ = 90.00°, Cell volume: 3215.03 (121) Å^3. Space group: $P2_1$ (no. 4).

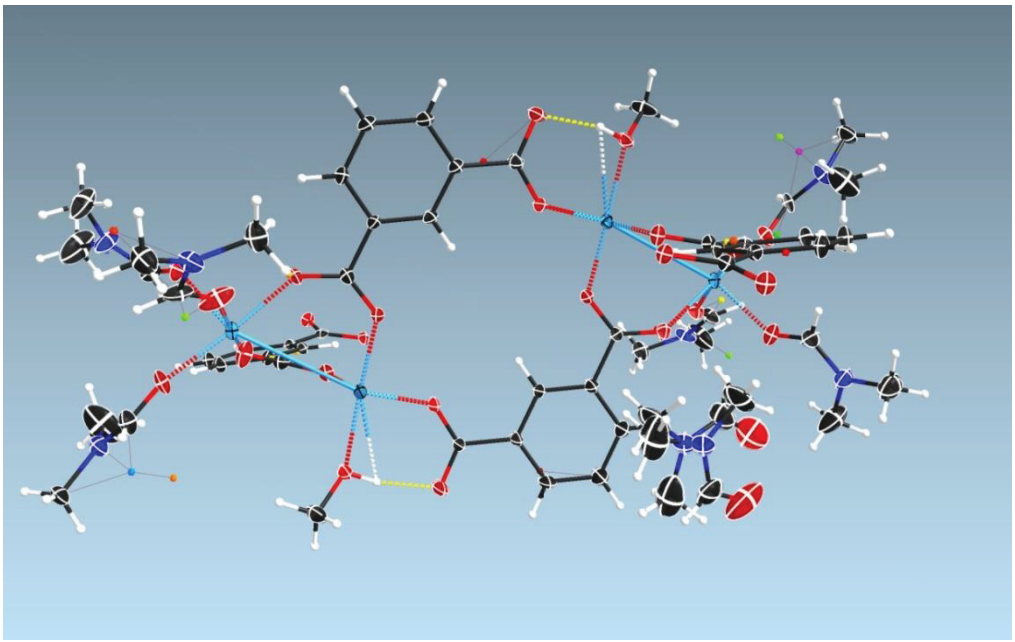

Figure 28: View of the asymmetric packing Unit cell packing

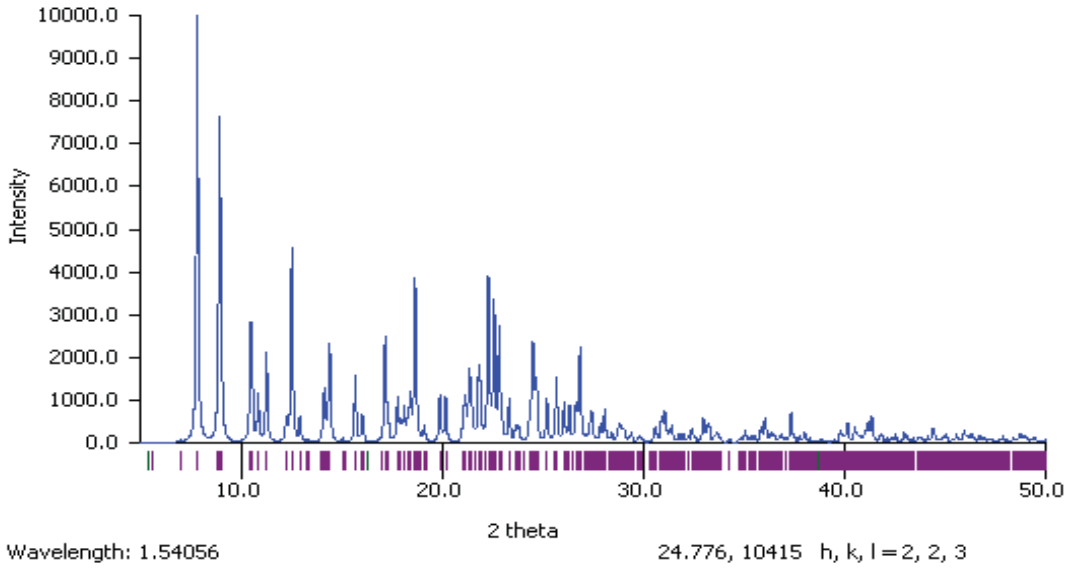

Figure 29: Simulated X-ray diffraction pattern of $[Mg_4(IPA)_4(DMF)_6(CH_3OH)_2].(DMF)$, created from the single crystal XRD data

V. Two Dimensional, $[Mg_2(IPA)_2(DMF)_3(C_2H_5OH)_2].(DMF)$

The asymmetric unit of the given compound, $[Mg_2(IPA)_2(DMF)_3(C_2H_5OH)_2].(DMF)$, consists of two molecules of isophthalic acid and three molecules of DMF coordinated to a magnesium dimer, along with two molecules of ethanol, and the unit cell that is crystallized in the monoclinic crystal system. The magnesium dimers are strongly bonded with the oxygen of two isophthalic acid molecules and three DMF molecules, two ethanol molecules along with a free DMF molecule packed in the interlamellar space. The resulting structure gives rise to a two-dimensional supramolecular layered framework structure. The layers are stacked in ABAB…fashion (Fig.31). Unit cell dimensions are as follows: a = 12.4082(14) Å, b = 16.3969(18) Å, c = 15.9188(17) Å, β = 90.61(0) °, Cell volume: 3238.59(62) $Å^3$. Space group: $P2_1/c$ (no. 14).

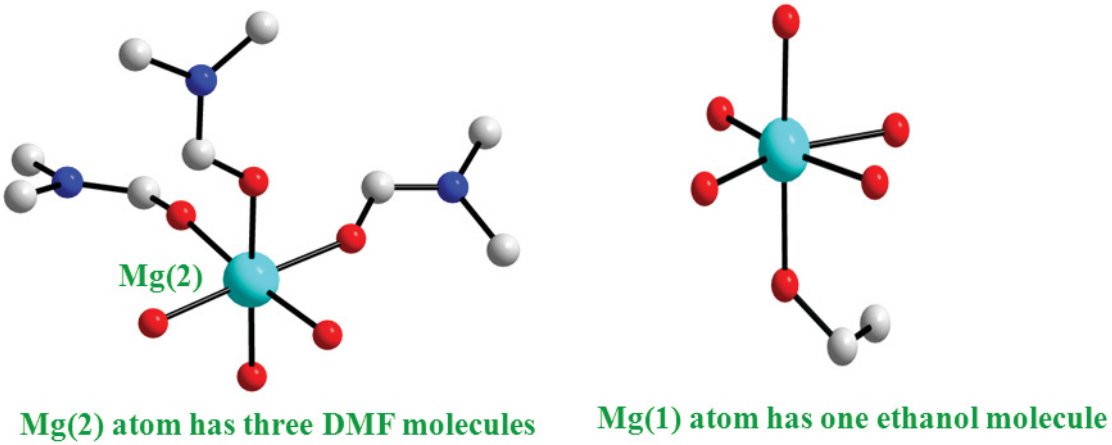

Figure 30: View of the constituents of the asymmetric unit and their linkages

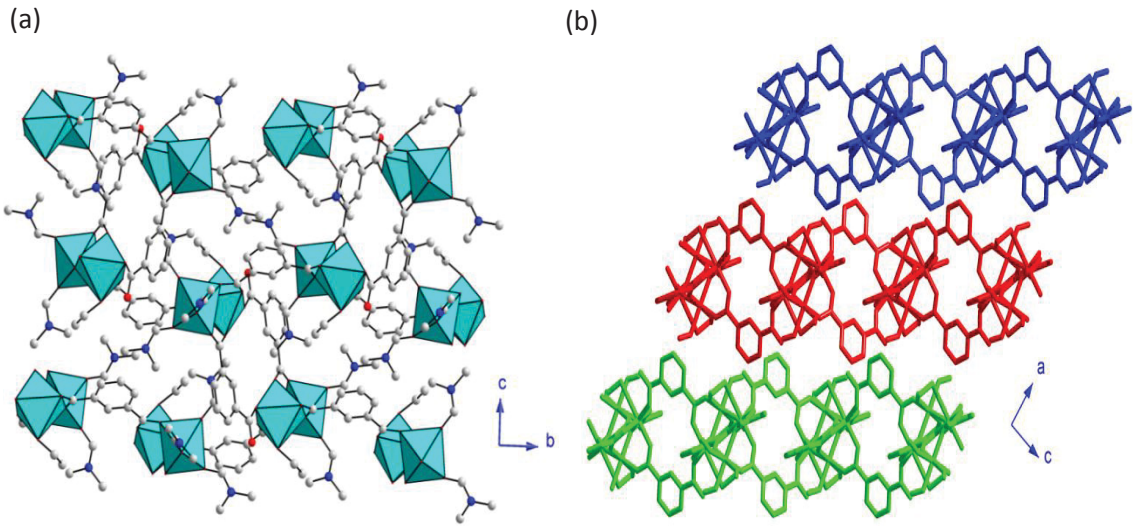

Figure 31: (a) View of the 2-D layer structure along [100] direction. Polyhedra represent the Mg dimers. (b) View of the layers for $[Mg_2(IPA)_2(DMF)_3(C_2H_5OH)_2].(DMF)$ stacked in ABAB fashion represented by different colors

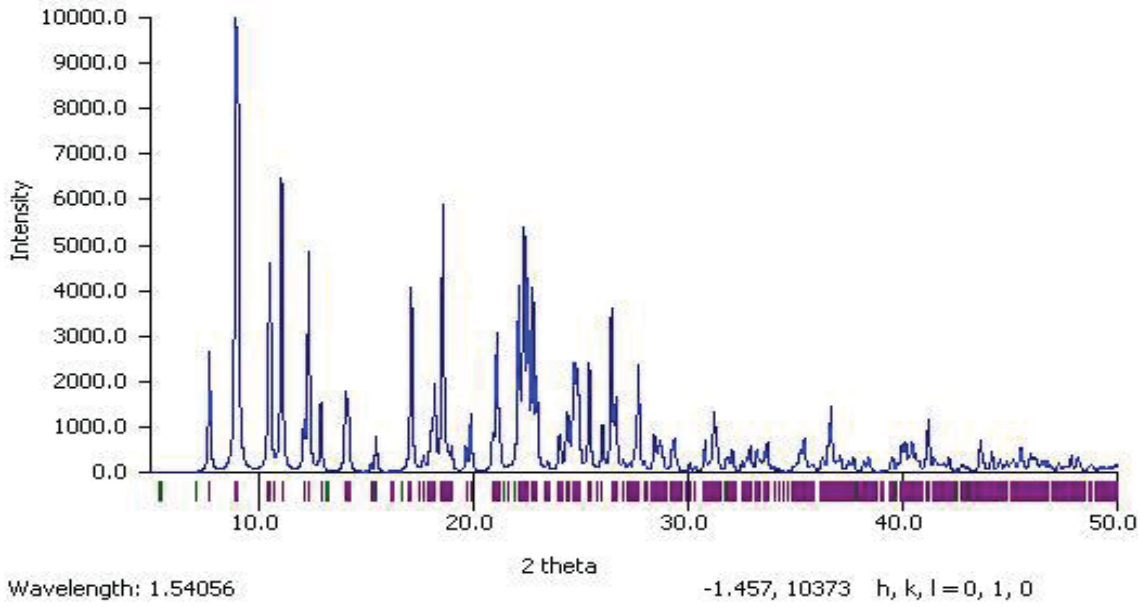

Figure 32: Simulated X-ray diffraction pattern of $[Mg_2(IPA)_2(DMF)_3(C_2H_5OH)_2].(DMF)$, created from the single crystal XRD data

VI. Three Dimensional, $[Mg_3(IPA)_4(DMF)(C_2H_5OH)].(DMF).2(Me_2N\text{-}H)$

The asymmetric unit, $[Mg_3(IPA)_4(DMF)(C_2H_5OH)].(DMF).2(Me_2N\text{-}H)$, consists of four molecules of isophthalic acid and one molecule of DMF coordinated to a magnesium trimer, along with two molecules of ethanol, and the unit cell that is crystallized in the orthorhombic crystal system. The trinuclear magnesium connected to isophthalic acid to give rise to the 3D structure (Fig. 34), are strongly bonded with the oxygen of four isophthalic acid molecules, one DMF molecule and two ethanol molecules. The pores are occupied by two DMF and two protonated dimethylamine molecules. The resulting structure gives rise to a three-dimensional supramolecular layered framework structure. The layers are stacked in ABAB…fashion (Fig. 34). Unit cell dimensions are as follows: a = 11.8808(4) Å, b = 16.0956(5) Å, c = 24.3167(7) Å, Cell volume: 4650.05(25) Å^3. Space group: $P2_12_12_1$ (no. 19).

The thermal decomposition profile for this compound was studied through thermo-gravimetric analysis (TGA). The data is given in Figure 62 (Appendix C). The gradual loss of weight in this case suggested the absence of desired pores in the structure which are generally observed in a high surface area / high porosity MOFs. MOFs with high porosity tend to show a sudden loss of weight for a narrow range of temperature increase during TGA analysis due to the rapid decomposition of structure.[26]

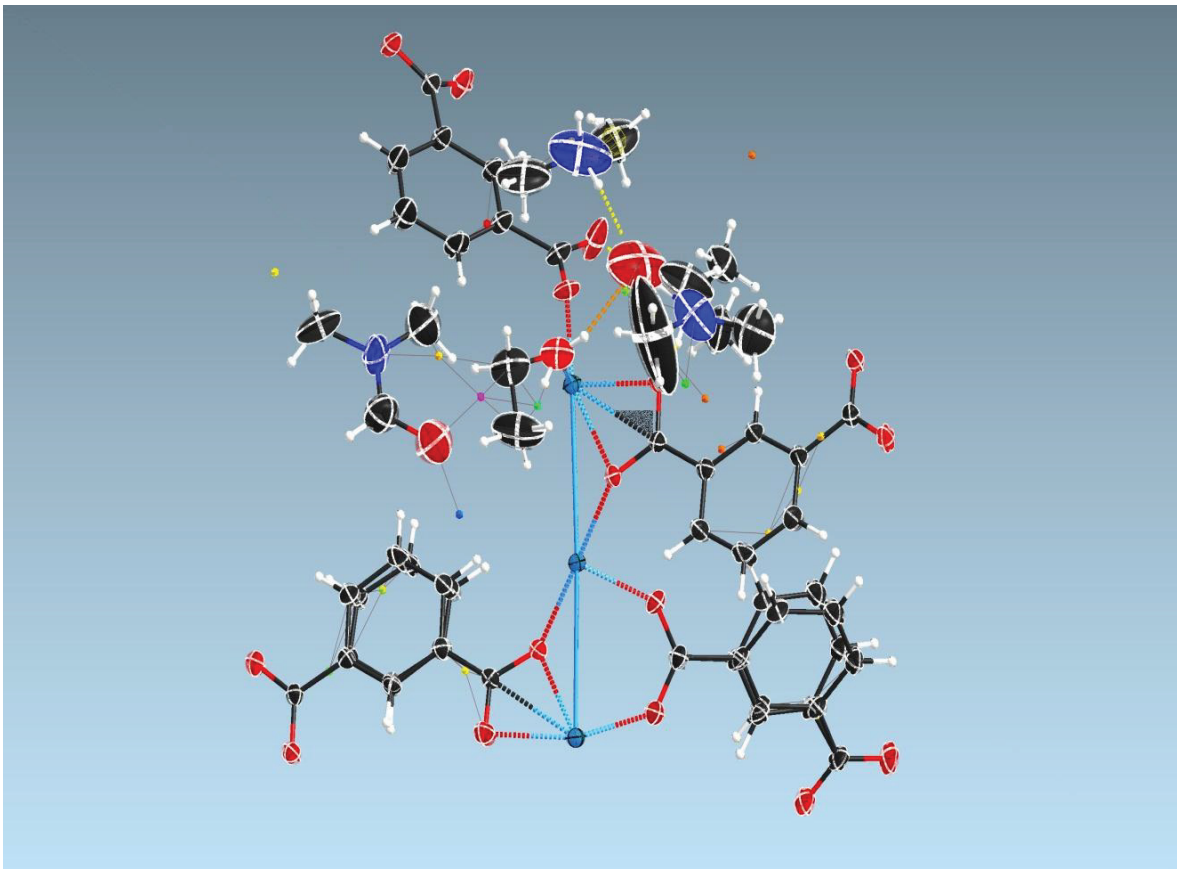

Figure 33: View of the asymmetric packing Unit cell packing of the compound $[Mg_3(IPA)_4(DMF)(C_2H_5OH)].(DMF).2(Me_2N\text{-}H)$

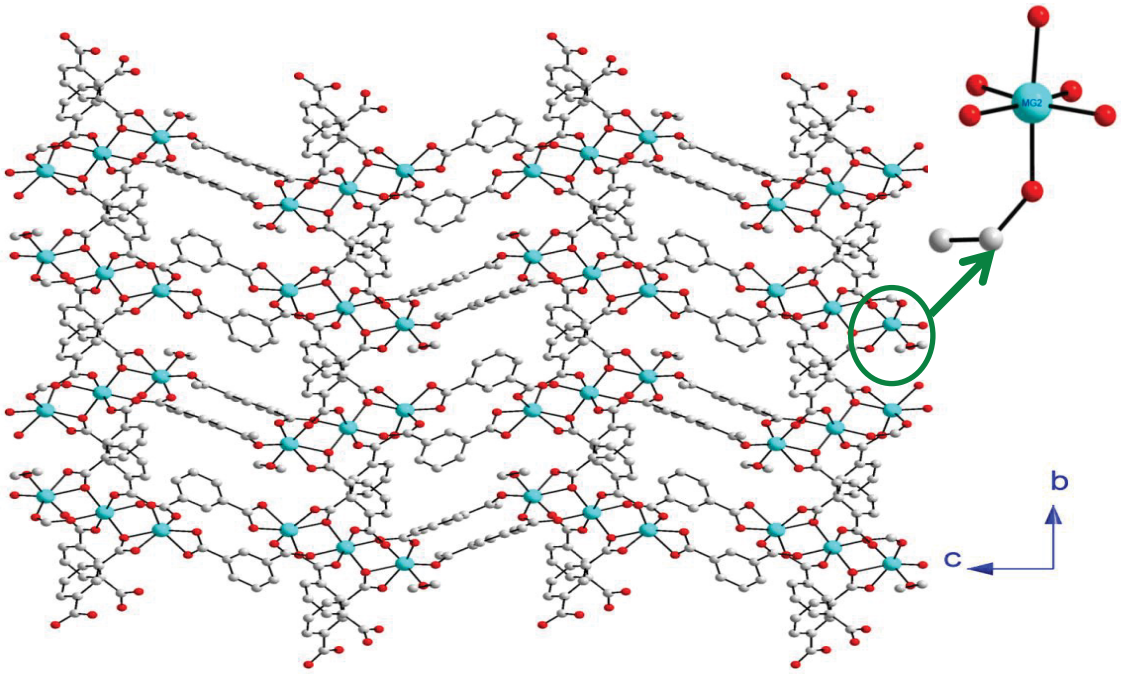

Figure 34: View of the 3-D structure. Magnesium trimers are clearly observed as blue atoms, which are connected to isophthalic acid to give 3-D structure

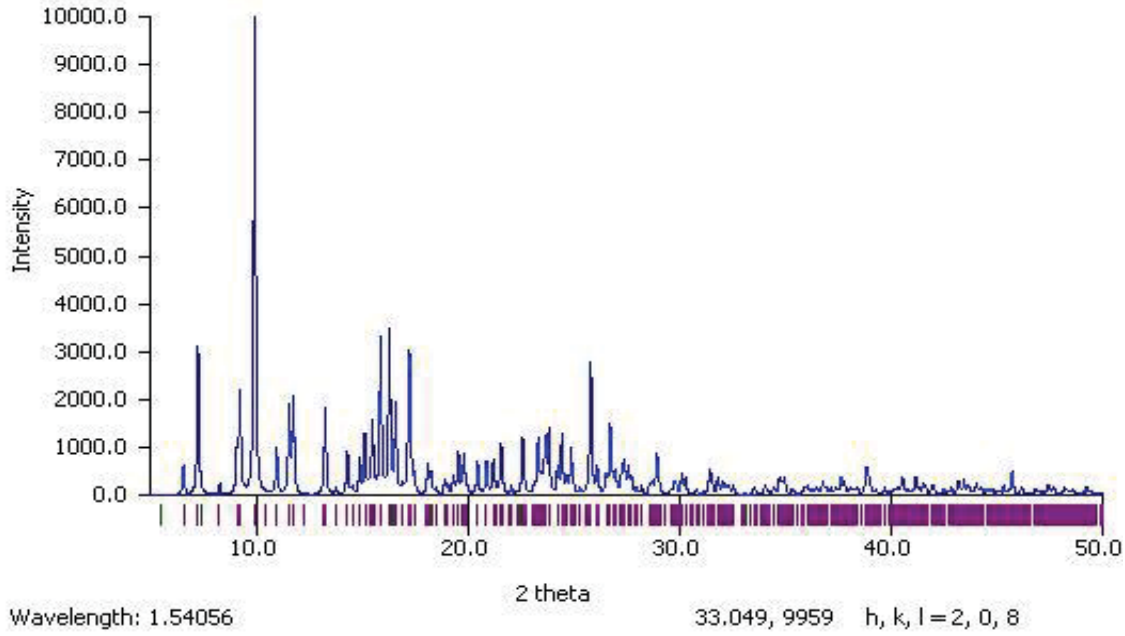

Figure 35: Simulated XRD pattern of $[Mg_3(IPA)_4(DMF)(C_2H_5OH)].(DMF).2(Me_2N\text{-}H)$, created from the single crystal XRD data

Reaction with trimesic acid (benzene-1,3,5-tricarboxylic acid): In our continued research to attain structures with higher dimensionality, the next set of reactions were performed using benzene-1,3,5-tricarboxylic acid as a rigid organic linker.

I. Three Dimensional, $[Mg_2(BTC)_2].(NH_4).(DMF)_2$

The asymmetric unit, $[Mg_2(BTC)_2].(NH_4).(DMF)_2$, consists of two molecules of trimesic acid and two magnesium centers, along with two molecules of DMF and one ammonium ion, and the unit cell is crystallized in the hexagonal crystal system. Each Mg is connected to three trimesic acid and two DMF to generate a 3D structure (Fig. 37). There is a presence of channels or porosity in the 3D structure which can be investigated further for possible gas adsorption characteristics (Fig. 38). The interlamellar spaces are occupied by two DMF and one ammonium ion. The resulting structure gives rise to a three-dimensional supramolecular layered framework structure. Unit cell dimensions are as follows: a = 16.619(5) Å, b = 16.619(5) Å, c = 14.097(4) Å, α = 90.00°, β = 90.00°, γ = 120.00°, Cell volume: V = 3371.8(17) Å^3. Space group: $P6_3/m$ (no. 176).

The single crystal structure was not fully solved and therefore the structural data is kept for a broad idea of the compound. The structure can be resolved further for future analysis.

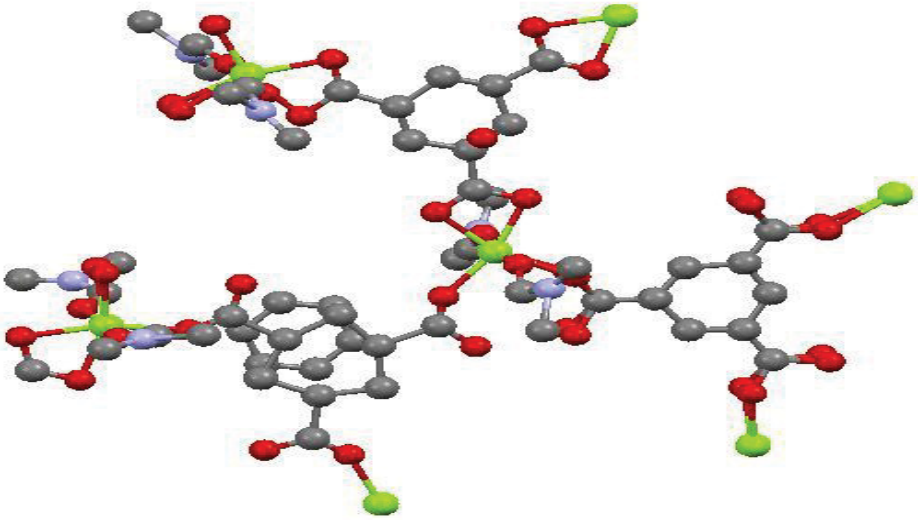

Figure 36: View of the asymmetric unit of $[Mg_2(BTC)_2].(NH_4).(DMF)_2$

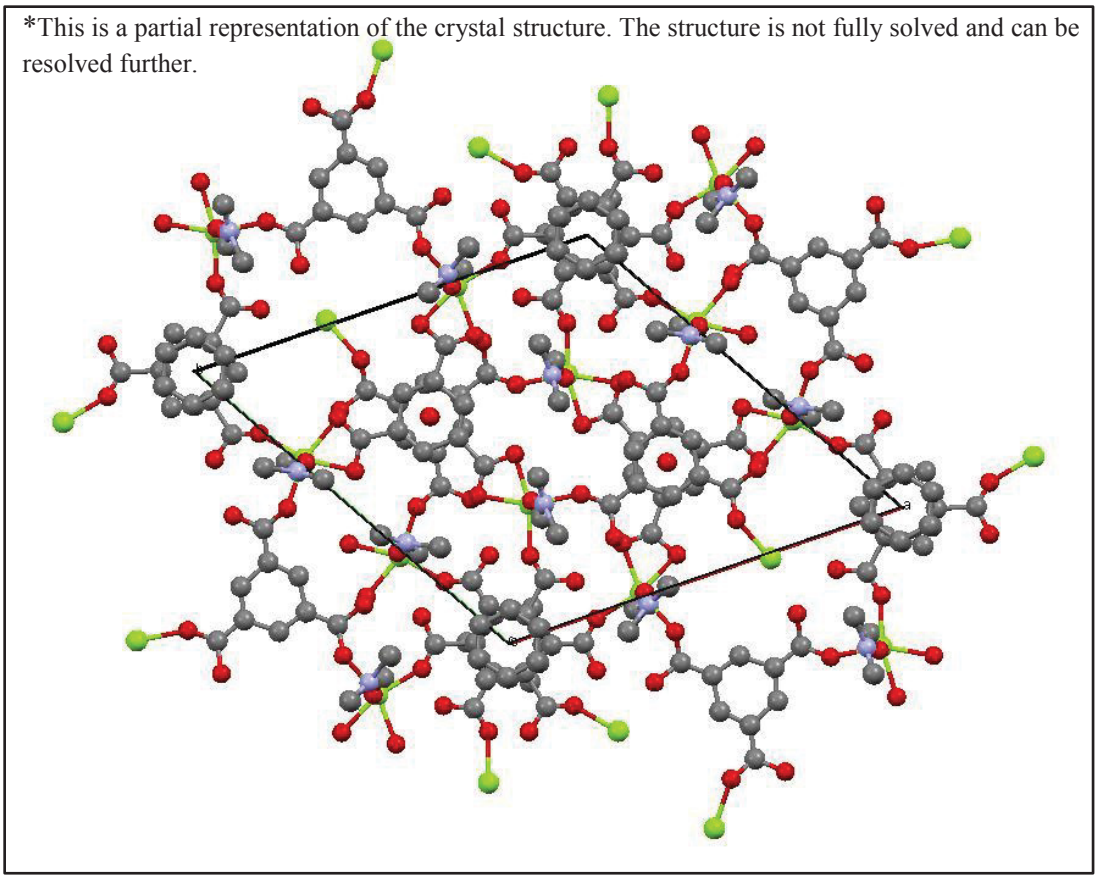

Figure 37: *View of the packing of $[Mg_2(BTC)_2].(NH_4).(DMF)_2$

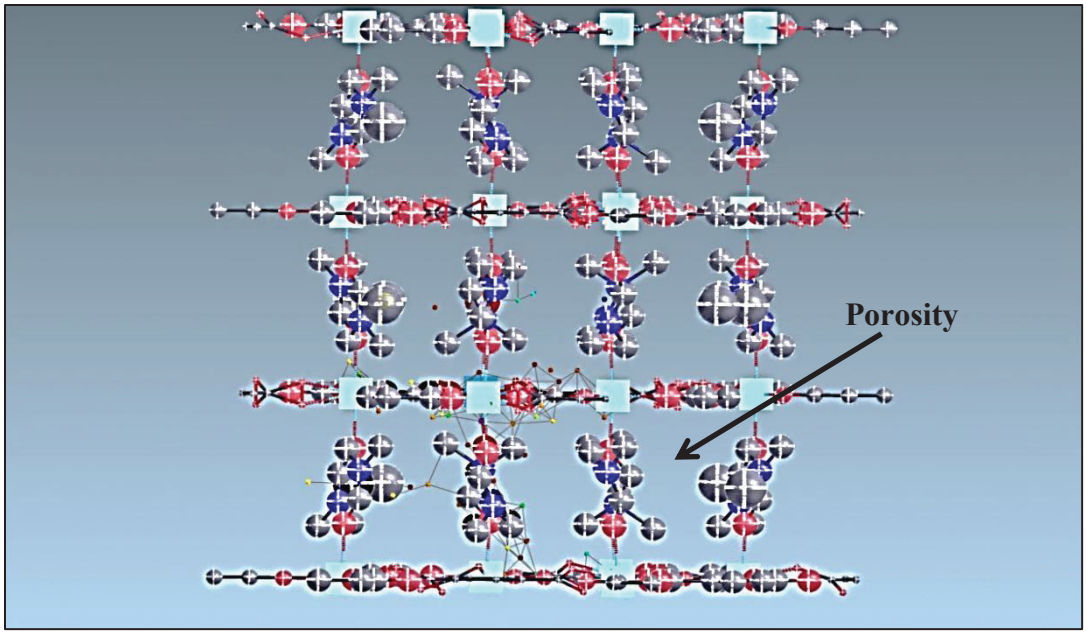

Figure 38: Alternate view of the packing of $[Mg_2(BTC)_2].(NH_4).(DMF)_2$ showing the channels or porosity. It's a partial representation of the crystal structure and is meant to display the suggested presence of porosity. The structure can be solved further

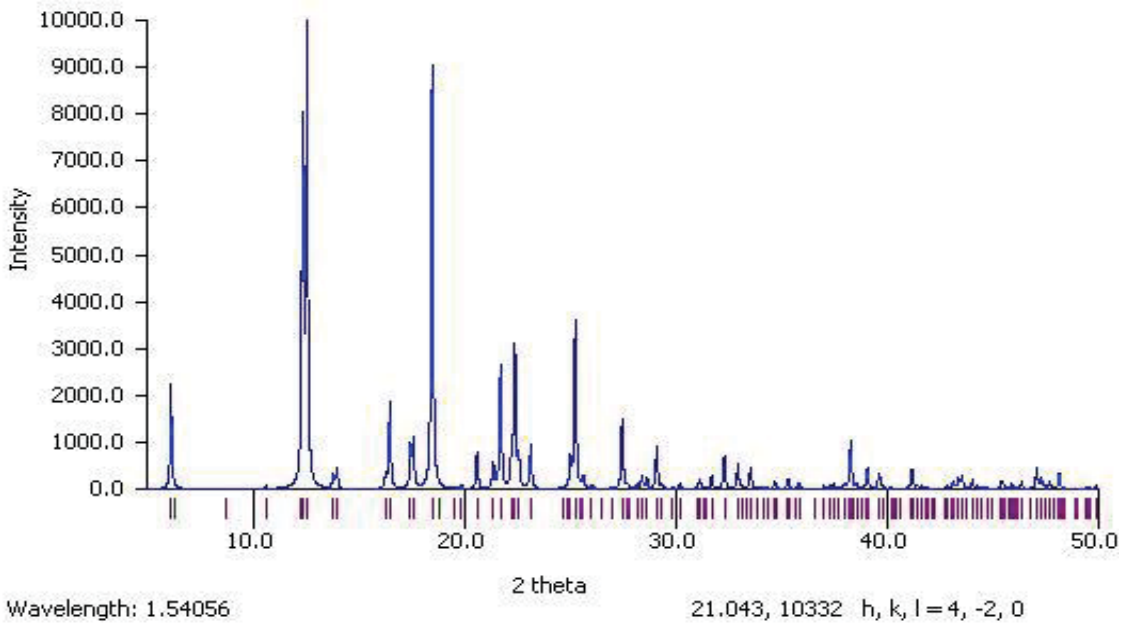

Figure 39: Simulated XRD pattern of $[Mg_2(BTC)_2].(NH_4).(DMF)_2$, created from the single crystal XRD data

Experimental Section:

Mg with 1,4- cyclohexanedicarboxylic acid (1,4-CHDA):

Using magnesium as the metal in focus and utilizing 1,4-cyclohexanedicarboxylic acid (1,4-CHDA) as the flexible organic linker, four new compounds were synthesized in glass vials by employing a variety of synthetic conditions.

I. Zero Dimensional, $[PIP\text{-}H_2][Mg(H_2O)_6].4.0Cl$

Solution A: 0.188 g 1,4-CHDA (1.09 mmol) is mixed with 5 mL acetonitrile (CH_3CN) at 70 °C.

Solution B: 0.28 g magnesium chloride $MgCl_2.6H_2O$ (1.37 mmol) is dissolved in 5 mL C_2H_5OH at room temperature.

The solutions (A and B) were then mixed together under constant stirring at room temperature. Thereafter, 0.05 g piperazine (0.58 mmol) was added to the above solution. The solution is then stirred at room temperature for about 30 minutes. The reaction mixture was then filtered and the filtrate developed crystals after keeping at room temperature for 7 days.

II. Zero Dimensional, $[Mg(H_2O)_6](trans\text{-}1,4\text{-}CHDA)].3H_2O$

Solution A: 0.188 g 1,4-CHDA (1.09 mmol) was mixed with 5 mL acetonitrile (CH_3CN) at 70 °C.

Solution B: 0.28 g magnesium Chloride $MgCl_2.6H_2O$ (1.37 mmol) was dissolved in 5 mL H_2O at room temperature.

The solutions (A and B) were then mixed together under constant stirring at room temp. Thereafter, 1 ml triethylamine (TEA) (7.17 mmol) is added to the above mixture. The solution was then stirred at room temperature for 30 minutes and then kept at room temperature for 16 days to obtain crystals.

III. Zero Dimensional, $[Mg(H_2O)_6][Mg(H_2O)_4(1,4\text{-}CHDA)_2].H_2O$

Solution A: 0.188 g (1.09 mmol) of 1,4-CHDA was dissolved in 5 mL C_2H_5OH.

Solution B: 0.282 g (1.38 mmol) of $MgCl_2.6H_2O$ was dissolved in 5 mL C_2H_5OH.

Both the solutions (A & B) were mixed together by stirring at room temperature and after complete mixing, 0.043 g (0.5 mmol) of piperazine was added and the whole mixture was mixed under stirring for 30 minutes. The vial was closed and kept at room temperature for a week to obtain crystals.

IV. Two Dimensional, $[Mg(1,4\text{-}CHDA\text{-}H)_2(H_2O)_2]$

Solution A: 0.188 g 1,4-CHDA (1.09 mmol) is mixed with 5 mL acetonitrile (CH_3CN) at 70 °C.

Solution B: 0.280 g magnesium chloride, $MgCl_2.6H_2O$ (1.37 mmol) is dissolved in 5 mL Ethanol (C_2H_5OH) at room temperature.

The solution (A and B) were then together under constant stirring at room temperature. Thereafter, 0.043 g piperazine (0.5 mmol) was added to the above mixture. The

solution was then stirred at 70 °C for 30 minutes (on a hot plate). It was then kept at room temperature for 24 hours and then filtered. The filtrate developed crystals after keeping for 7 days at room temperature.

Reaction of mg with isophtahlic acid (1,3-BDC or IPA): Six novel compounds were synthesized in glass vials by employing a variety of synthesis conditions.

I. Zero Dimensional, Dimethyl ammonium 3-carboxybenzoate, $[(CH_4)_2NH\text{-}H][IPA\text{-}H]$

The compound was synthesized under solvothermal conditions. In a typical synthesis, $Mg(NO_3)_2.6H_2O$ (0.064 g, 0.25 mmol) was dissolved in a 1:1 mixture of DMF (5.0 mL) and C_2H_5OH (5.0 mL). Then, alumina (Sorbent Technologies, Atlanta, GA) (0.051 g, 0.5 mmol), isophthalic acid (0.166 g, 1.0 mmol) and piperazine (0.043 g, 0.5 mmol) were added to the reaction mixture which was stirred for one hour before transferring the mixture into a glass vial. The final mixture was heated to 373 K for 48 hours. The vial was then slowly cooled to room temperature. Slow cooling of the reaction mixture yielded colorless plate-like crystals of the title compound as a minor product.[27]

II. Zero Dimensional, Adenin-1-ium isophthalate dimethylformamide, $[C_5H_{6.3}N_5]^+.[C_8H_{4.7}O_4]^-.C_3H_7NO$

The compound was synthesized under solvothermal conditions. In a typical synthesis, $Mg(NO_3)_2.6H_2O$ (0.128 g, 0.5 mmol) and adenine (Sigma-Aldrich (≥99%), 0.068 g, 0.5 mmol) were dissolved in DMF (10.0 mL). Then isophthalic acid (0.166 g, 0.5 mmol) was added to the reaction mixture. The mixture was stirred for 30 minutes before transferring the mixture into a 23 mL Teflon-lined stainless steel autoclave. The final mixture, with a composition of 1:1:1, was heated to 423 K (150 °C) for 96 hours (4 days). The autoclave was then slowly cooled to room temperature. Slow cooling of the reaction mixture yielded colorless plate-like crystals of the title compound as a minor product, along with some sand like precipitate of magnesium dihydrate diformate ($Mg(HCOO)_2.2H_2O$), (ICSD #151330).

III. Two Dimensional, $[Mg_4(IPA)_4(DMF)_6].2(DMF)$

The compound was synthesized under solvothermal conditions. In a typical synthesis, magnesium nitrate, $Mg(NO_3)_2.6H_2O$ (0.128 g, 0.5 mmol) and isophthalic acid (0.166 g, 1.0 mmol) were dissolved in DMF (10.0 mL) at room temperature. Then piperazine (0.086 g, 1.0 mmol) was added to the reaction mixture and stirred for one hour before transferring the mixture in to a 23 mL teflon-lined stainless steel autoclave. The final mixture was heated to 413 K (140 °C) for 72 hours. The autoclave

was then slowly cooled to room temperature yielding colorless crystals of the title compound as a minor product along with an unidentified white powder.

IV. Two Dimensional, $[Mg_4(IPA)_4(DMF)_6(CH_3OH)_2].(DMF)$

The compound was synthesized under solvothermal conditions, In a typical synthesis, $Mg(NO_3)_2.6H_2O$ (0.128 g, 0.5 mmol) and isophthalic acid (0.166 g, 0.5 mmol) were dissolved in a mixture of DMF (8.0 mL) and methanol CH_3OH (2.0 mL). Then, piperazine (0.043 g, 0.5 mmol) was added to the reaction mixture and stirred for one hour before transferring the mixture into a glass vial. The final mixture was heated to 373 K (100 °C) for 24 hours. The glass vial was then slowly cooled at room temperature yielding colorless to get colorless crystals.

V. Two Dimensional, $[Mg_2(IPA)_2(DMF)_3(C_2H_5OH)_2].(DMF)$

In solution A, 0.166 g (1.0 mmol) isophthalic acid was dissolved in 5 mL of DMF at room temperature. In solution B, 0.128 g (0.5 mmol) magnesium nitrate, $Mg(NO_3)_2.6H_2O$ was dissolved in 5 mL ethanol (C_2H_5OH) at room temperature. The solutions (A and B) were then mixed together under constant stirring at room temp. Thereafter, 0.043 g piperazine (0.5 mmol) was added to the above solution. The mixture was then stirred at room temperature for 30 minutes. It was then kept in a tightly capped glass vial at 373 K (100 °C) for 3 days to obtain colorless crystals of the title compound.

VI. Three Dimensional, $[Mg_3(IPA)_4(DMF)(C_2H_5OH)].(DMF).2(Me_2N\text{-}H)$

In Solution A, 0.166 g of isophthalic acid (1.0 mmol) was dissolved in 5 mL DMF. In solution B, 0.128 g magnesium nitrate (0.5 mmol) $Mg(NO_3)_2.6H_2O$ was dissolved in 5 mL ethanol (C_2H_5OH) at room temperature. The solutions (A and B) were then mixed together under constant stirring at room temperature. Thereafter, 0.086 g piperazine (1.0 mmol) was added to the above solution. The mixture was then stirred at room temp for 30 minutes. It was then kept in a tightly capped glass vial at 373 K (100 °C) for 3 days to obtain colorless crystals of the title compound.

VII. Three Dimensional, $[Mg_2(BTC)_2].(NH_4).(DMF)_2$

In solution A, the trimesic Acid (1,3,5-benzene tricarboxylic acid) (0.5 mmol) was dissolved in 5 mL of DMF at room temp. In the solution B, 0.064 g (0.25 mmol) magnesium nitrate, $Mg(NO_3)_2.6H_2O$ was dissolved in 5 mL methanol (C_2H_5OH) at room temperature. The solutions (A and B) were then mixed together under constant stirring at room temperature. Thereafter, 0.099 g (0.5mmol) 4,4'-trimethylene dipyridine (4,4'-TMDiPy) was added to the above solution. The mixture was then stirred at room temperature for 30 minutes. It was then kept in a tightly capped glass vial at 408 K (135 °C) for 1 day to obtain thin and hexagonal plate like colorless crystals of the title compound.

Conclusion:

The lab synthesis of the compound Mg-MOF-74 was performed and it was studied for N_2 and CO_2 adsorption isotherms and its BET surface area was calculated. The value was found to be lesser as compared to the published values.[20] Further, a series of reactions were performed with a systematic approach using the flexible organic linkers like 1,4-cyclohexanedicarboxylic acid (1,4-CHDA), 4,4'-trimethylene dipyridine (4,4'-TMDiPy) and piperazine, and rigid linkers like isophthalic acid (1,3-BDC or IPA), trimesic acid (1,3,5-benzene tricarboxylic Acid) and 4,4'-bipyridine (N-donor ligand), to synthesize various novel metal organic framework structures. 0D to 3D framework materials were successfully produced and some were characterized for various physical and chemical properties. One of the major challenges faced was the reproduction of the pure phase for subsequent characterization. Some of the compounds could not be reproduced in pure phase and therefore could not be characterized fully. All the compounds were successfully synthesized employing the solvothermal approach. While we achieved synthesis of some novel 3D framework compounds, they can be further investigated to develop materials with the desired porosity in the basic structure. These compounds can be studied to grow within an aluminum alumina matrix or alumina platform so as to increase the overall applicability of these newly developed compounds.

References

1) Banerjee, D.; Finkelstein, J.; Smirnov, A.; Forster, P. M.; Borkowski, L.A.; Teat, S.J.; Parise, J.B. "Synthesis and Structural Characterization of Magnesium Based Coordination Networks in Different Solvents." pubs.acs.org/crystal, Revised: April 17, **2011**.

2) Bao, Z.Z.; Yu, L.; Ren, Q.; Lu, X.; Deng, S. "Adsorption of CO_2 and CH_4 on a Magnesium Based Metal Organic Framework." Z. Bao et al., *Journal of Colloid and Interface Science*, 353 (**2011**) 549–556.

3) Dietzel, P.D.C.; Besikiotis, V.; Blom, R. "Application of Metal–Organic Frameworks with Coordinatively Unsaturated Metal Sites in Storage and Separation of Methane and Carbon Dioxide" *J. Mater. Chem*., **2009**, 19, 7362–7370.

4) Rood, J.A.; Noll, B.C.; Henderson, K. W. "Synthesis, Structural Characterization, Gas Sorption and Guest-Exchange Studies of the Lightweight, Porous Metal-Organic Framework-$[Mg_3(O_2CH)_6]$." *Inorganic Chemistry*, Vol. 45, No. 14, **2006**.

5) Mallick, A.; Saha, S.; Pachfule, P.; Roy, S.; Banerjee, R. "Selective CO_2 and H_2 Adsorption in a Chiral Magnesium-Based Metal Organic Framework (Mg-MOF) with Open Metal Sites." *J. Mater. Chem*., **2010**, 20, 9073–9080.

6) Davies, R.P.; Less, R.J.; Lickiss, P.D.; White, A.J.P. "Framework Materials Assembled from Magnesium Carboxylate Building Units." *Dalton Trans.*, **2007**, 2528–2535.

7) Mallick, A.; Saha, S.; Pachfule, P.; Roy, S.; Banerjee, R. "Structure and Gas Sorption Behavior of a New Three Dimensional Porous Magnesium Formate." pubs.acs.org/IC Published on Web 12/30/**2010**.

8) Glover, T.G.; Peterson, G.W.; Schindler, B.J.; Britt, D.; Yaghi, O.M. “MOF-74 Building Unit has a Direct Impact on Toxic Gas Adsorption.” T.G. Gloveretal./ChemicalEngineeringScience66 (**2011**)163–170.

9) Senkovska, I.; Kaskel, S. “Solvent-Induced Pore-Size Adjustment in the Metal-Organic Framework $[Mg_3(ndc)_3(dmf)_4]$ (ndc = naphthalenedicarboxylate).” *Eur. J. Inorg. Chem.*, **2006**, 4564–4569.

10) R. Herm, Z.; Swisher, J.A.; Smit, B.; Krishna, R.; Long, J.R. “Metal Organic Frameworks as Adsorbents for Hydrogen Purification and Precombustion Carbon Dioxide Capture.” *J. Am. Chem. Soc.*, **2011**, 133, 5664–5667.

11) Liu, B.; Smit, B. “Comparative Molecular Simulation Study of CO_2/N_2 and CH_4/N_2 Separation in Zeolites and Metal-Organic Frameworks.” *Langmuir*, **2009**, 25(10),5918–5926.

12) Ma, S.; Zhou, H.-C. “A Metal-Organic Framework with Entatic Metal Centers Exhibiting High Gas Adsorption Affinity.” *J. Am. Chem. Soc.,* **2006**, 128, 11734-11735.

13) Ma, S. “Gas Adsorption Applications of Porous Metal–Organic Frameworks.” **2009** IUPAC, *Pure and Applied Chemistry,* 81, 2235–2251.

14) Dietzel, P.D.C.; Blom, R.; Fjellvåg, H. “Base-Induced Formation of Two Magnesium Metal-Organic Framework Compounds with a Bifunctional Tetratopic Ligand.” *Eur. J. Inorg. Chem.,* **2008**, 3624–3632.

15) Devic, T.; David, O,; Valls, M.; Marrot, J.; Couty, F.; Ferey, G. “An Illustration of the Limit of the Metal Organic Framework’s Isoreticular Principle Using a

Semirigid Tritopic Linker Obtained by “Click” Chemistry.” *J. Am. Chem. Soc.*, **2007**, 129, 12614-12615.

16) Eddaoudi, M.; Moler, D.B.; Li, H.; Chen, B.; Reineke, T.M.; O'Keeffe, M.; Yaghi, O.M. *Accounts of Chemical Research* , **2001**, 34, 319.

17) Schröder, F.; Esken, D.; Cokoja, M.; Van den Berg, M.W.E.; Lebedev, O.I.; Tendeloo, G.van.; Walaszek, B.; Buntkowsky, G.; Limbach, H.H.; Chaudret, B.; Fischer, R.A. *J. Am. Chem. Soc.,* 130 (**2008**) 6119.

18) Furukawa, H.; Cordova, K.E.; O’Keeffe, M.; Yaghi, O.M. “The Chemistry and Applications of Metal-Organic Frameworks.” *Science*, 30 August **2013,** Vol 341.

19) Tella, A.C.; Aaron, I.Y. “Syntheses And Applications Of Metal-organic Frameworks Materials : A Review.” *Acta Chim. Pharm. Indica*, 2(2), **2012**, 75-81.

20) Yang, D.-A.; Cho, H.-Y.; Kim, J.; Yang, S.-T.; Ahn, W.-S. “CO_2 Capture and Conversion Using Mg-MOF-74 Prepared by a Sonochemical Method.” *Energy & Environmental Science*; **2012**, 5, 6465.

21) Calderone, P.J.; Banerjee, D.; Santulli, A.C.; Wong, S.S.; Parise, J.B. “Synthesis, Characterization, And Luminescence Properties Of Magnesium Coordination Networks Using A Thiophene-Based Linker.” *Inorganica Chimica Acta*, **2011**, 378, 109–114.

22) Saha, D.; Maity, T.; Das, S.; Koner, S. “A Magnesium-Based Multifunctional Metal–Organic Framework: Synthesis, Thermally Induced Structural Variation, Selective Gas Adsorption, Photoluminescence and Heterogeneous Catalytic Study.” RSC publishing; *Dalton Trans.,* **2013**, 42, 13912.

23) Lucas, K. “Magnesium Sulfonyldibenzoates: Synthesis, Structure, Phase Transformation and Microscopic Studies.” Youngstown State University, MS Thesis, **2013**.

24) Mutinda, S.I. “Hydrothermal Synthesis of Shape/Size-Controlled Cerium-Based Oxides.” Youngstown State University, MS Thesis, **2013**.

25) Fiquet, G.; Guyot, F.; Kunz, M.; Matas, J.; Andrault, D.; Hanfland, M. “Structural Refinements of Magnesite at Very High Pressure.” *American Mineralogist*, Volume 87, pages 1261–1265, **2002.**

26) Gu, J.-M.; Kim, S.-J.; Kim, Y.; Huh, S. “Structural Isomerism of an Anionic Nanoporous In-MOF with Interpenetrated Diamond-Like Topology.” *CrystEngComm*, The Royal Society of Chemistry, **2012**.

27) Siddiqui, T.; Rao, V.K.; Zeller, M.; Lovelace-Cameron, S.R. “Dimethylammonium 3-carboxybenzoate.” Structure Reports, *Acta Crystallographica Section E,* **2012**, E68, o1778.

28) Birkbeck College, University of London, Copyright 1997-99. Crystallographic Space Group Diagrams and Tables. Retrieved December 04, **2013** from: http://img.chem.ucl.ac.uk/sgp/mainmenu.htm.

Appendix A

PXRD Data

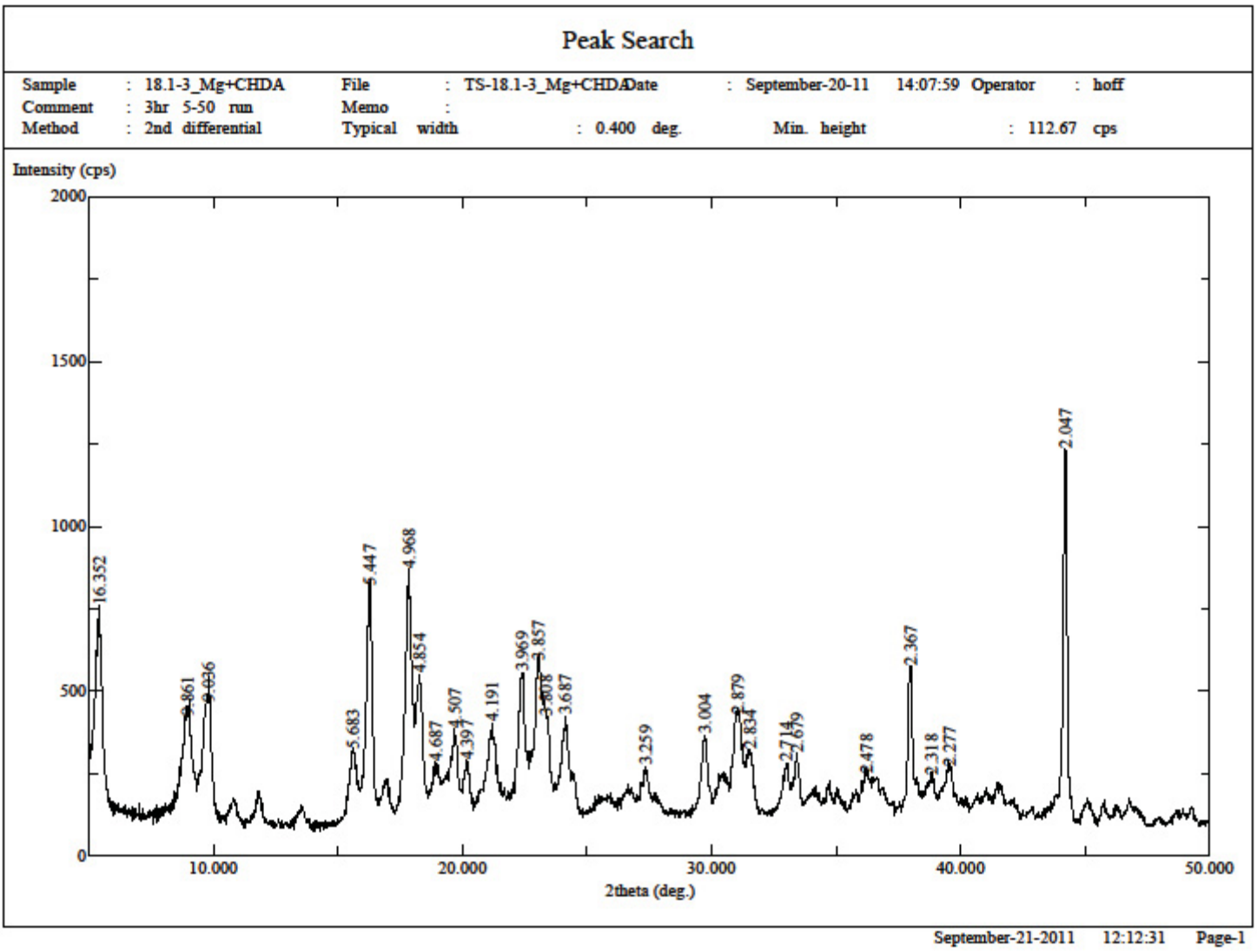

Figure 40: Powder X-ray diffraction data for Mg-MOF-74 (lab sample – 09/20/2011)

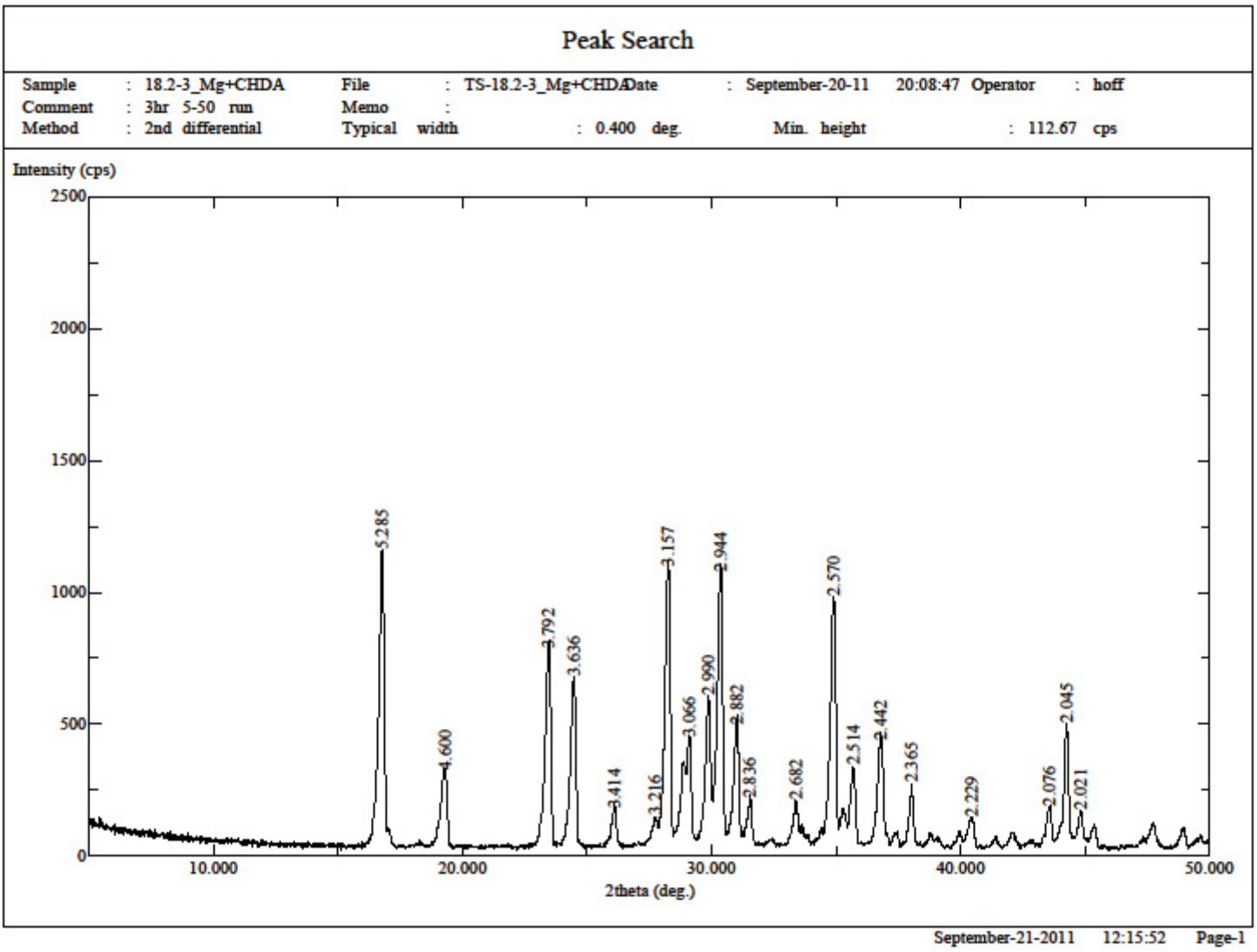

Figure 41: Powder X-ray diffraction data for Mg-MOF-74 (lab sample – 09/20/2011)

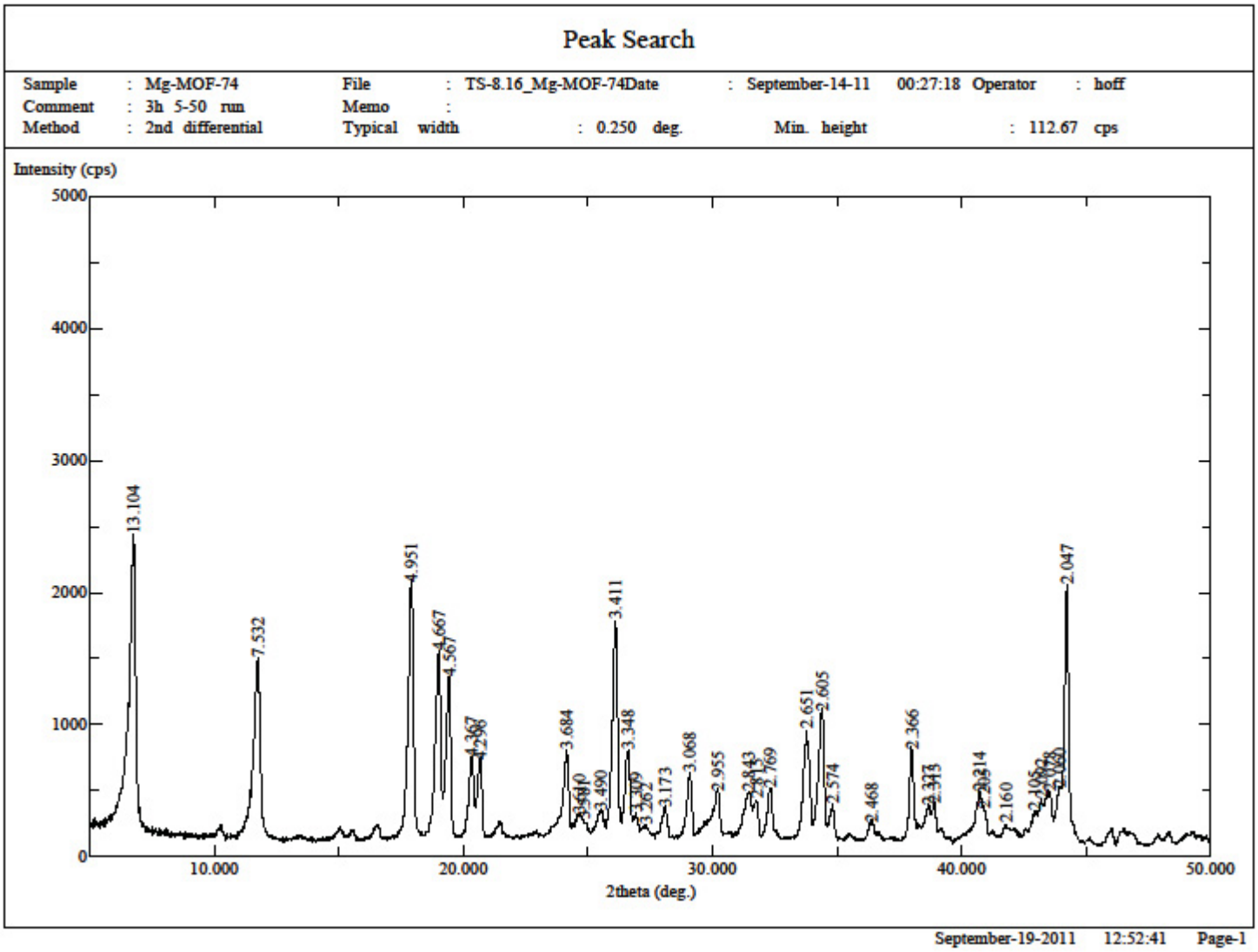

Figure 42: Powder X-ray diffraction data for Mg-MOF-74 (lab sample – 09/14/2011)

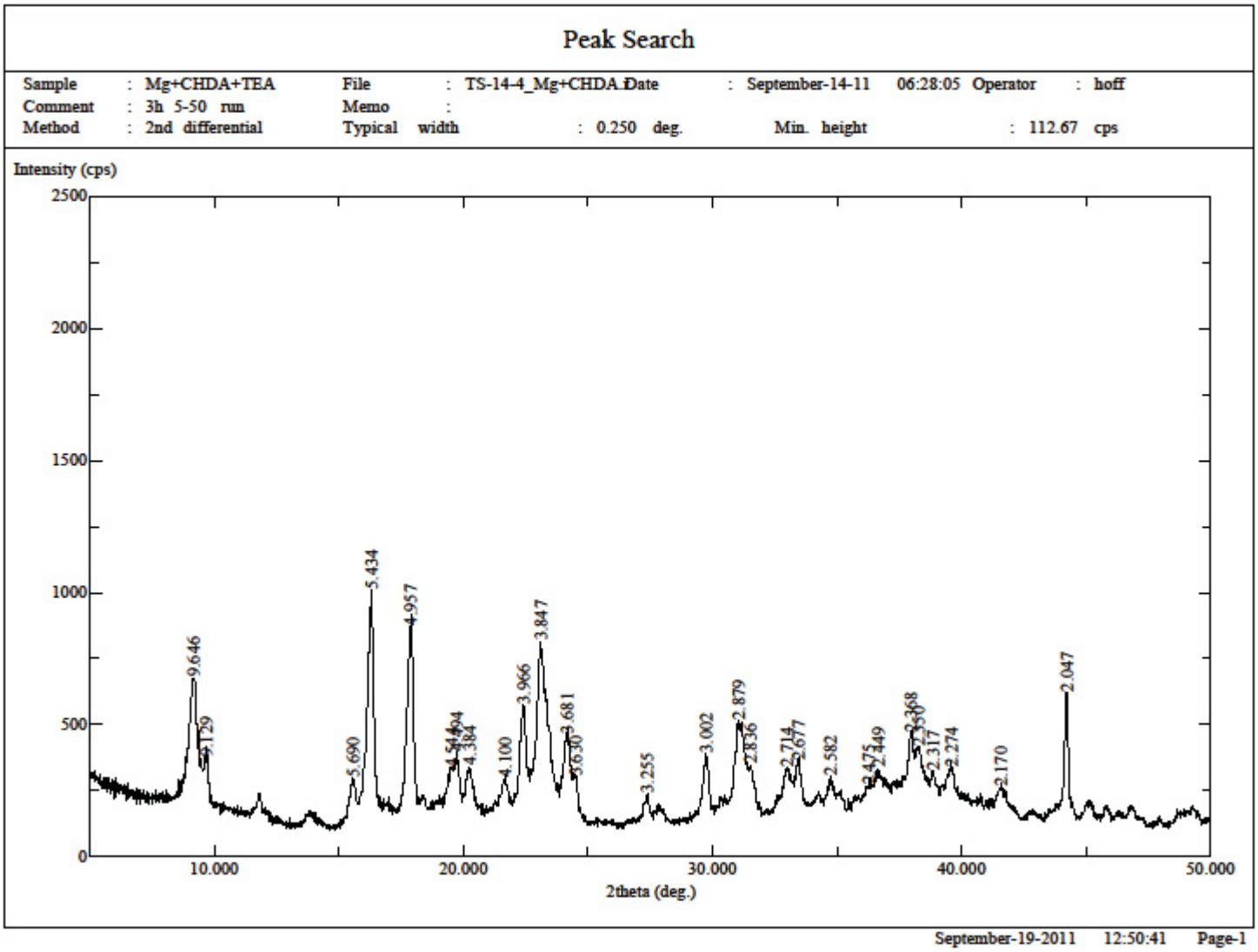

Figure 43: Powder X-ray diffraction data for Mg-MOF-74 (lab sample – 09/14/2011)

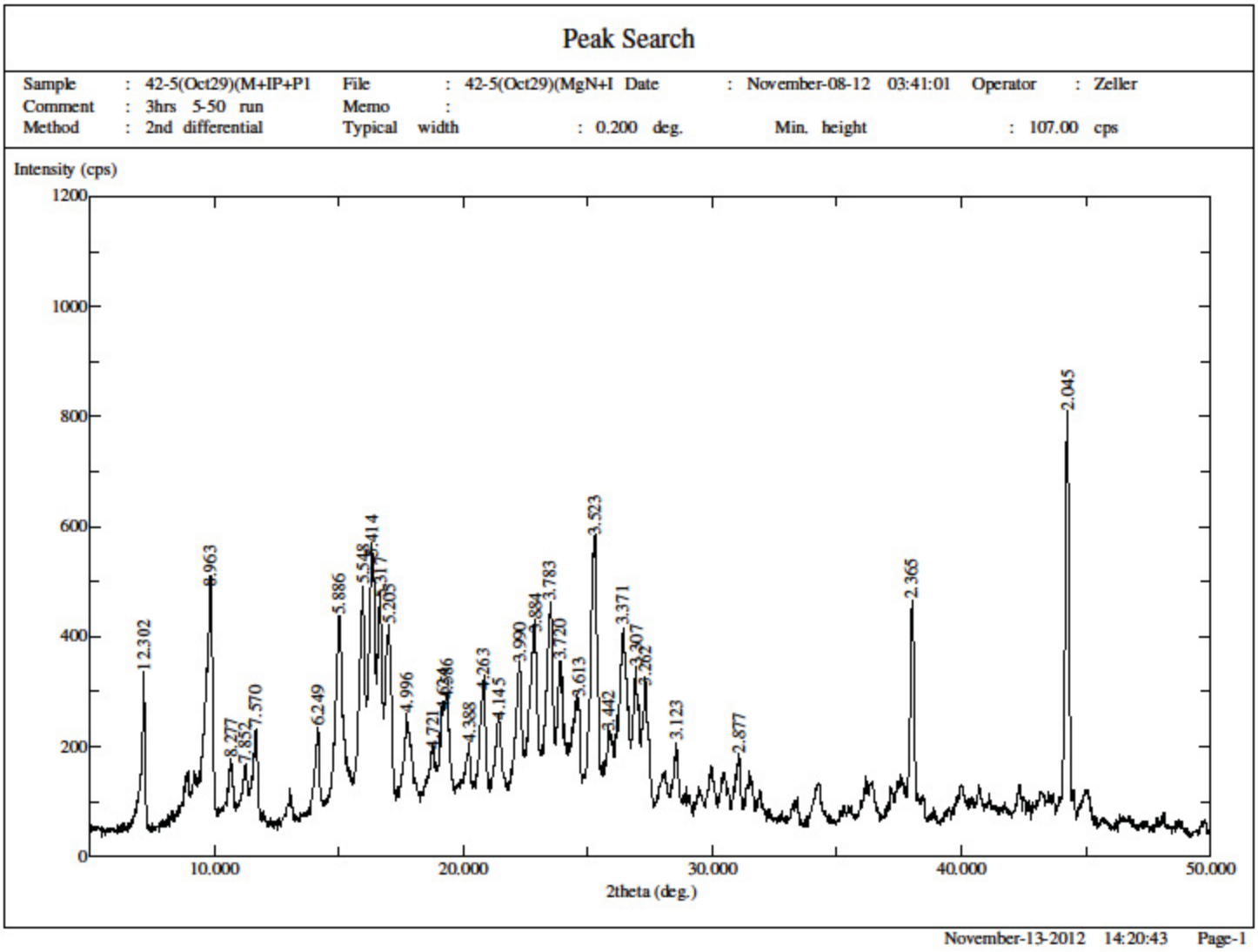

Figure 44: Powder X-ray diffraction data for Mg based MOF using isophthalic acid and piperazine (lab sample – 11/08/2012)

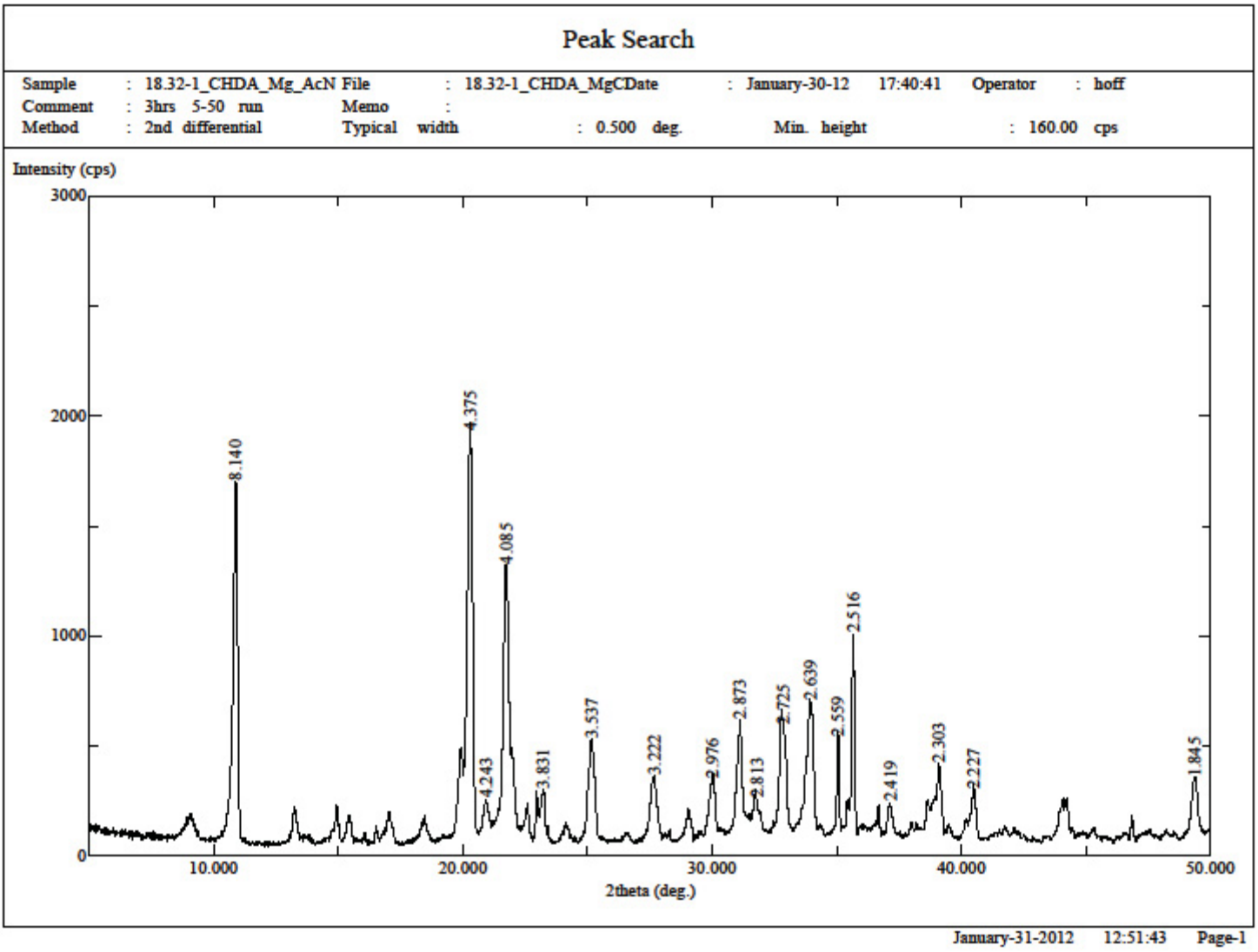

Figure 45: Powder X-ray diffraction data for Mg based MOF (lab sample – 01/30/2012)

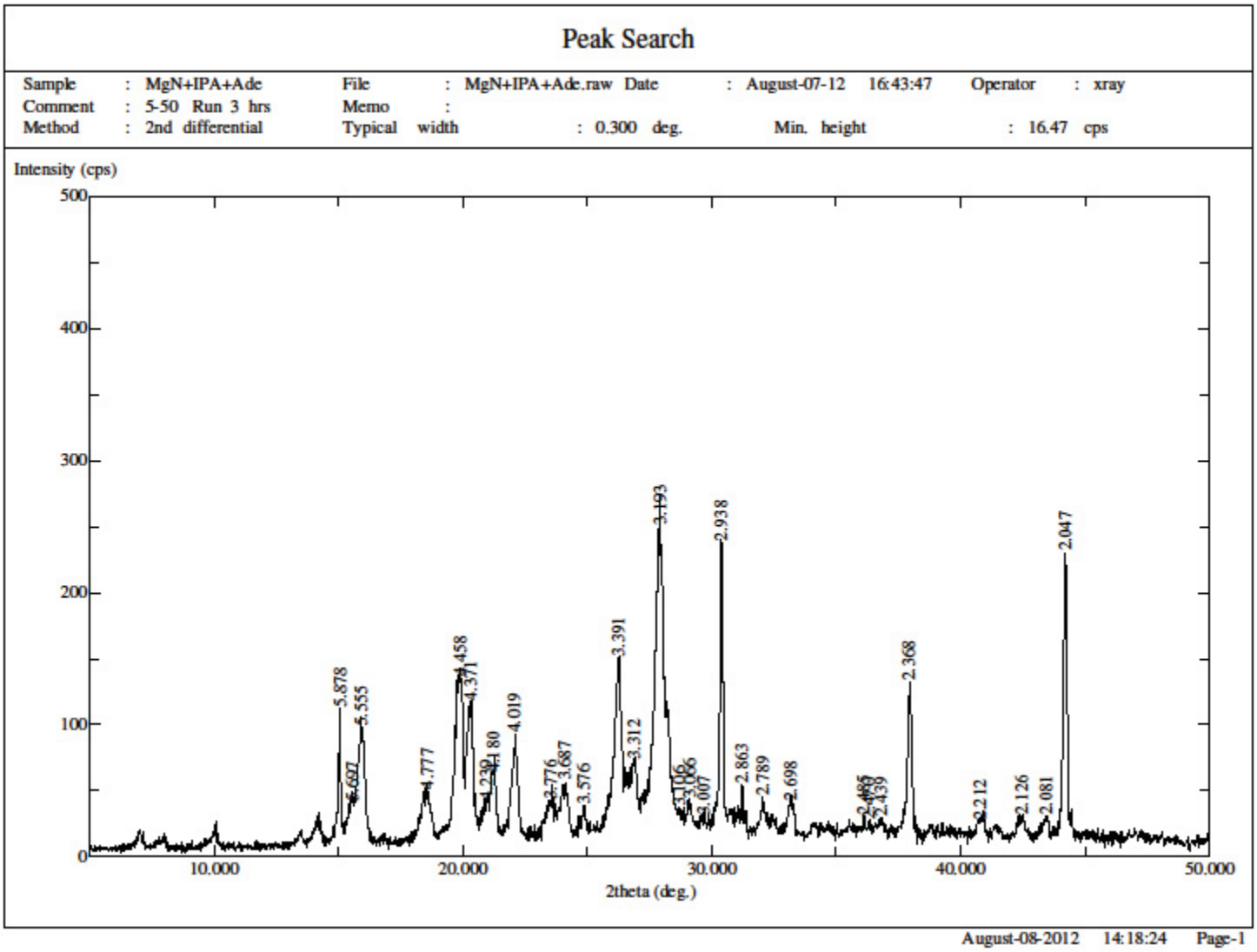

Figure 46: Powder X-ray diffraction data for Mg based MOF using isophthalic acid and adenine (lab sample – 08/07/2012)

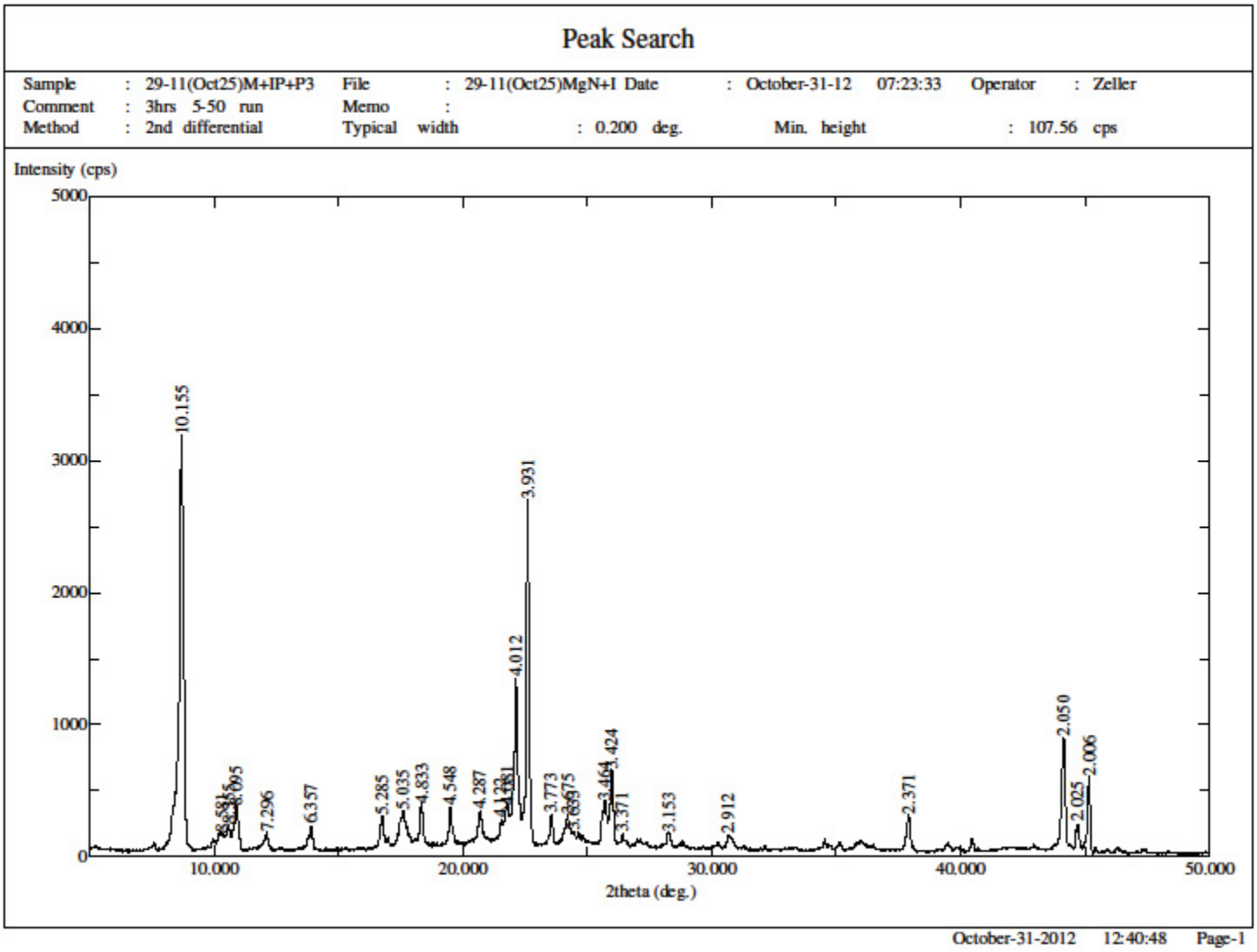

Figure 47: Powder X-ray diffraction data for Mg based MOF (lab sample – 10/31/2012)

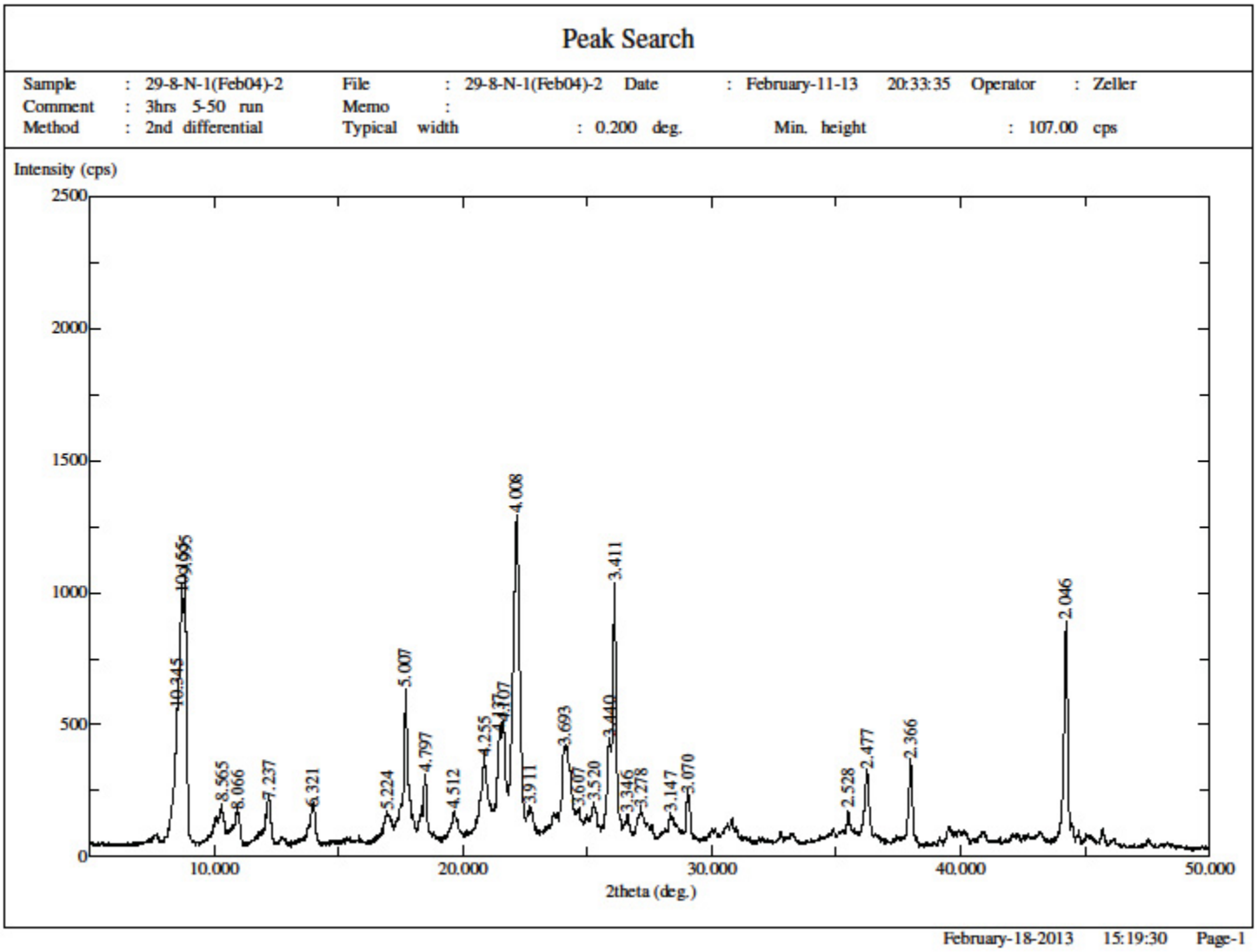

Figure 48: Powder X-ray diffraction data for Mg based MOF (lab sample – 02/11/2013)

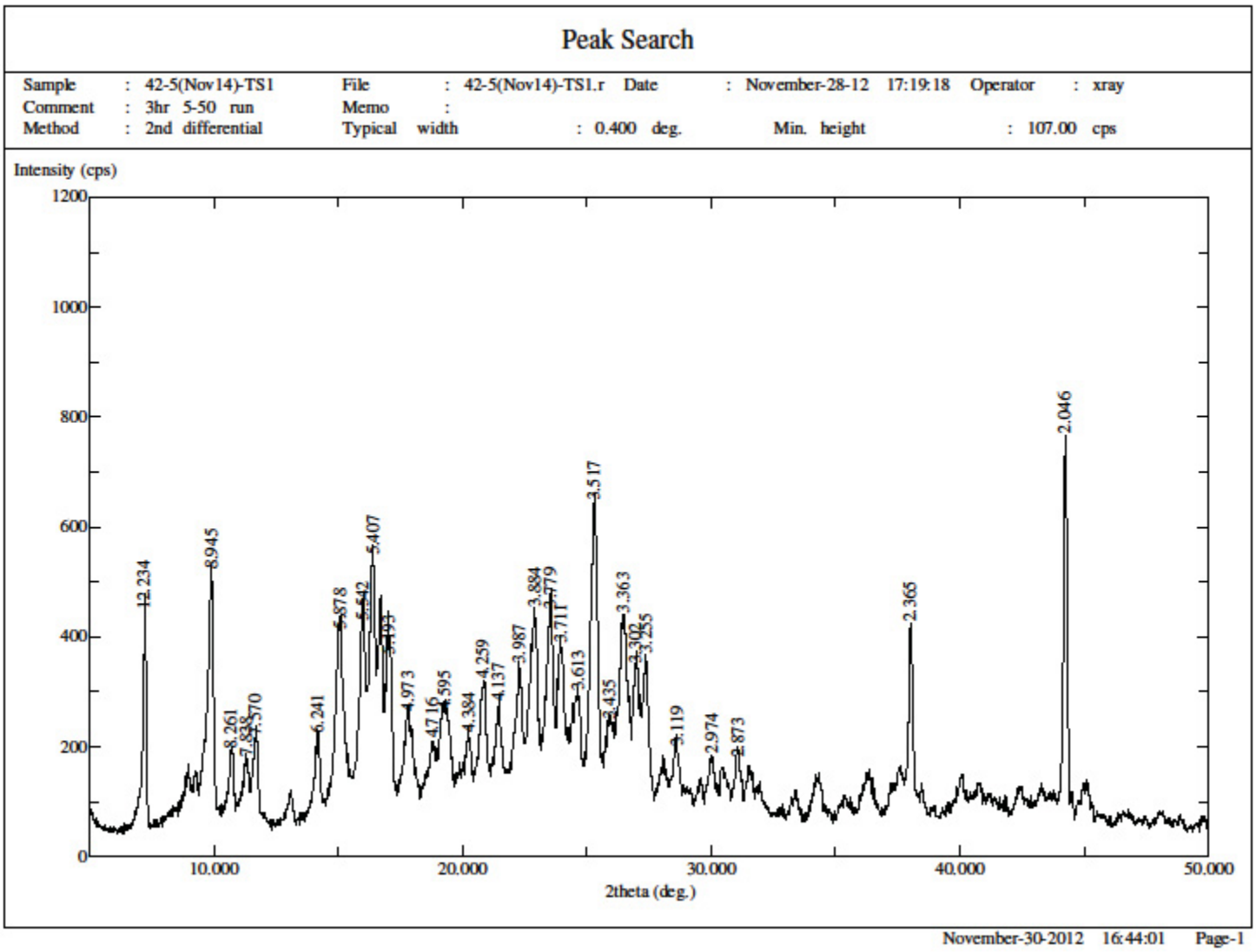

Figure 49: Powder X-ray diffraction data for Mg based MOF (lab sample – 11/28/2012)

Appendix B

TEM Images of lab synthesized Mg-MOF-74

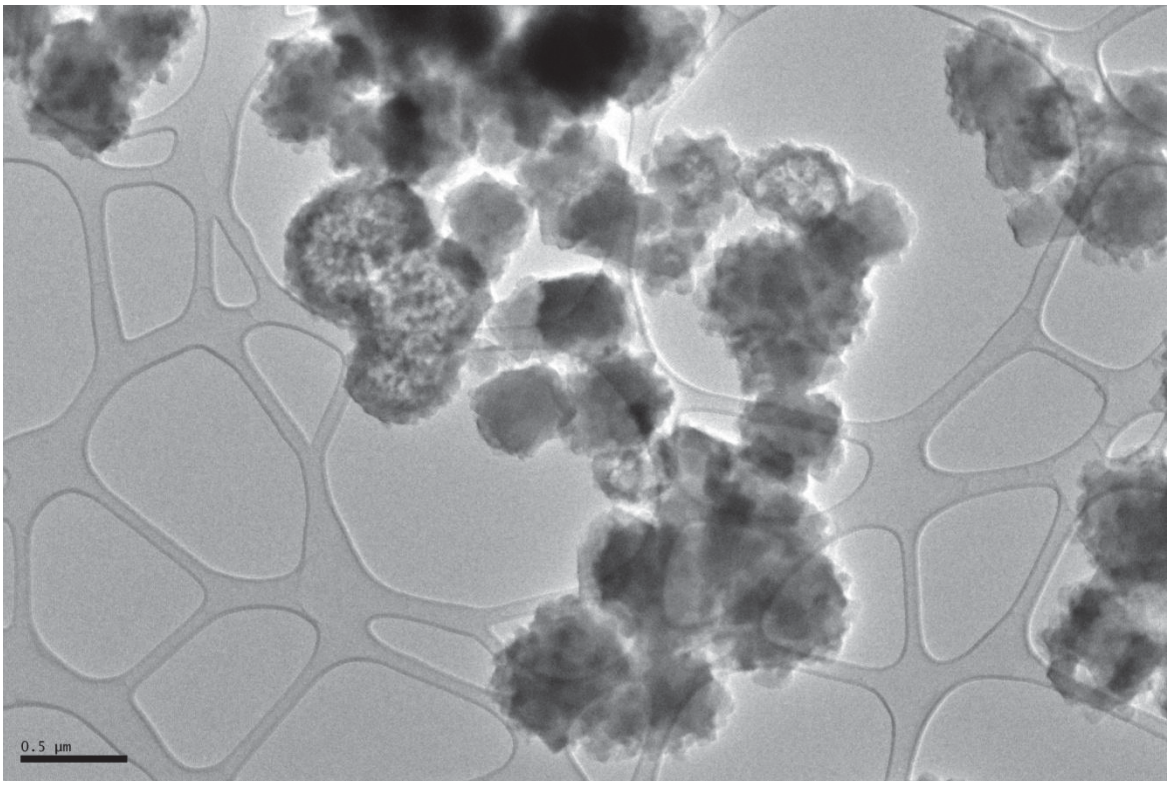

Figure 50: Mg-MOF-74 (lab sample) - Magnification 5K

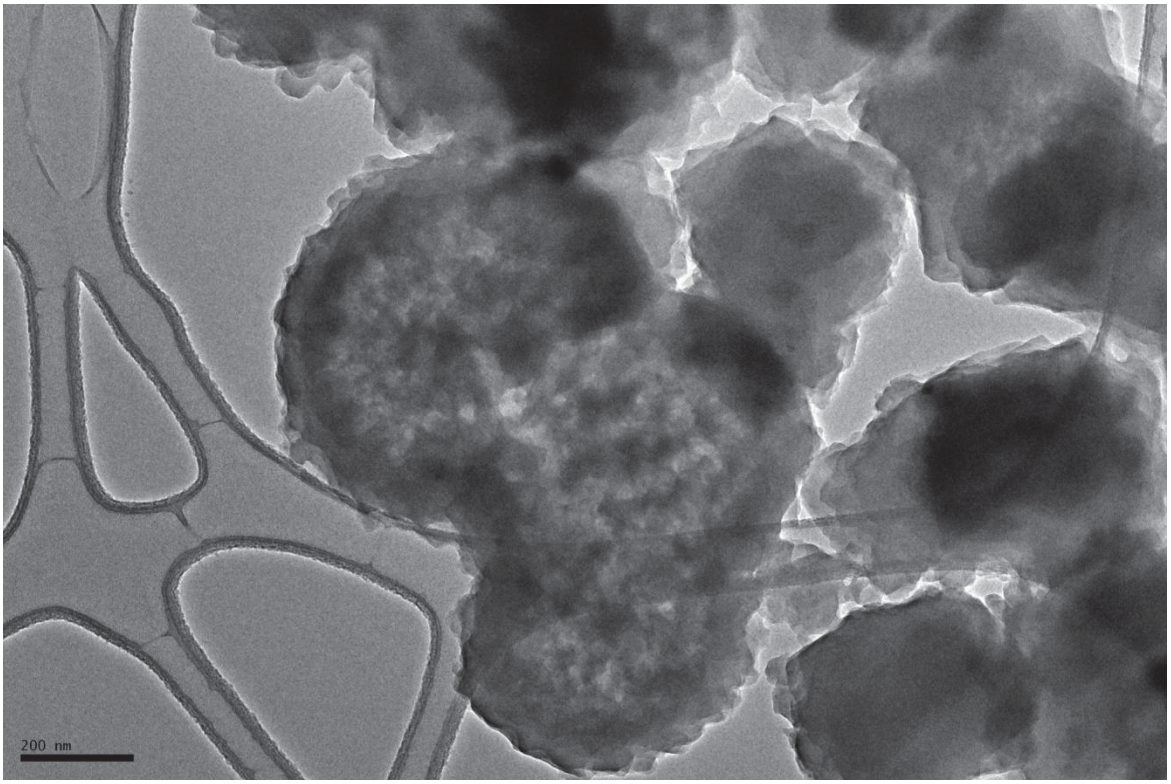

Figure 51: Mg-MOF-74 (lab sample) - Magnification 12K

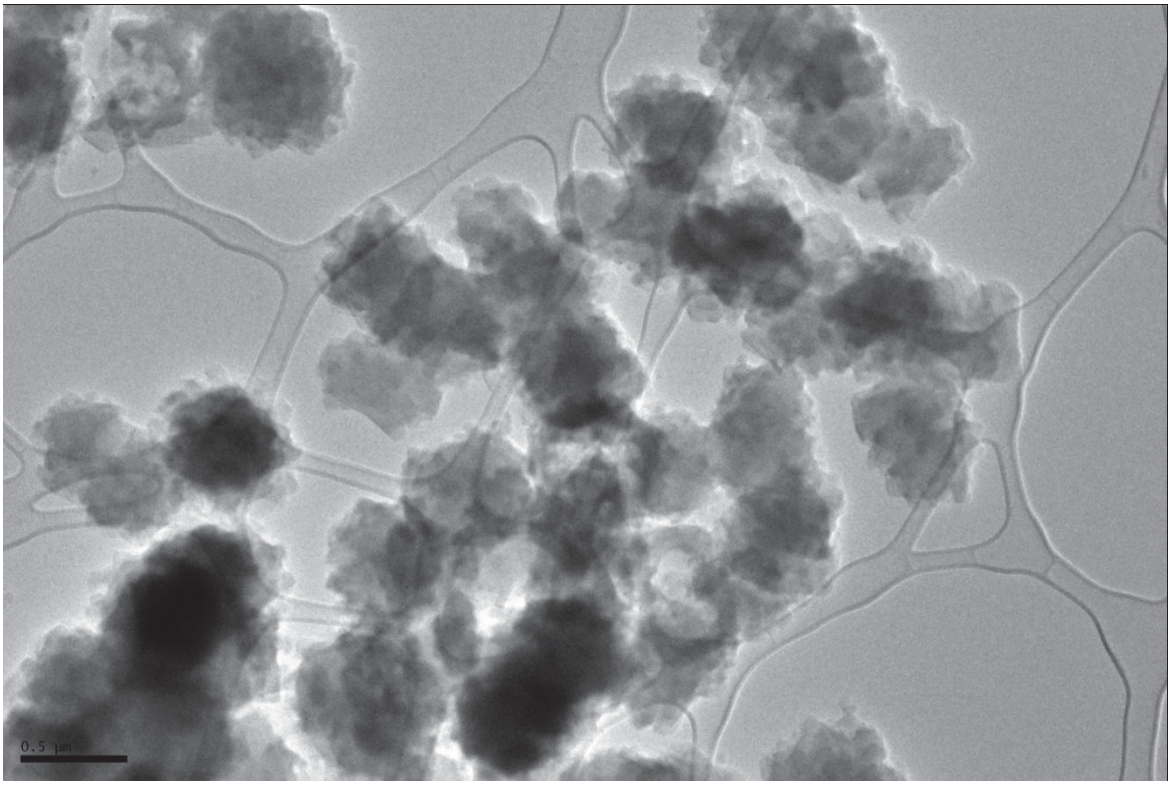

Figure 52: Mg-MOF-74 (lab sample) - Magnification 5K

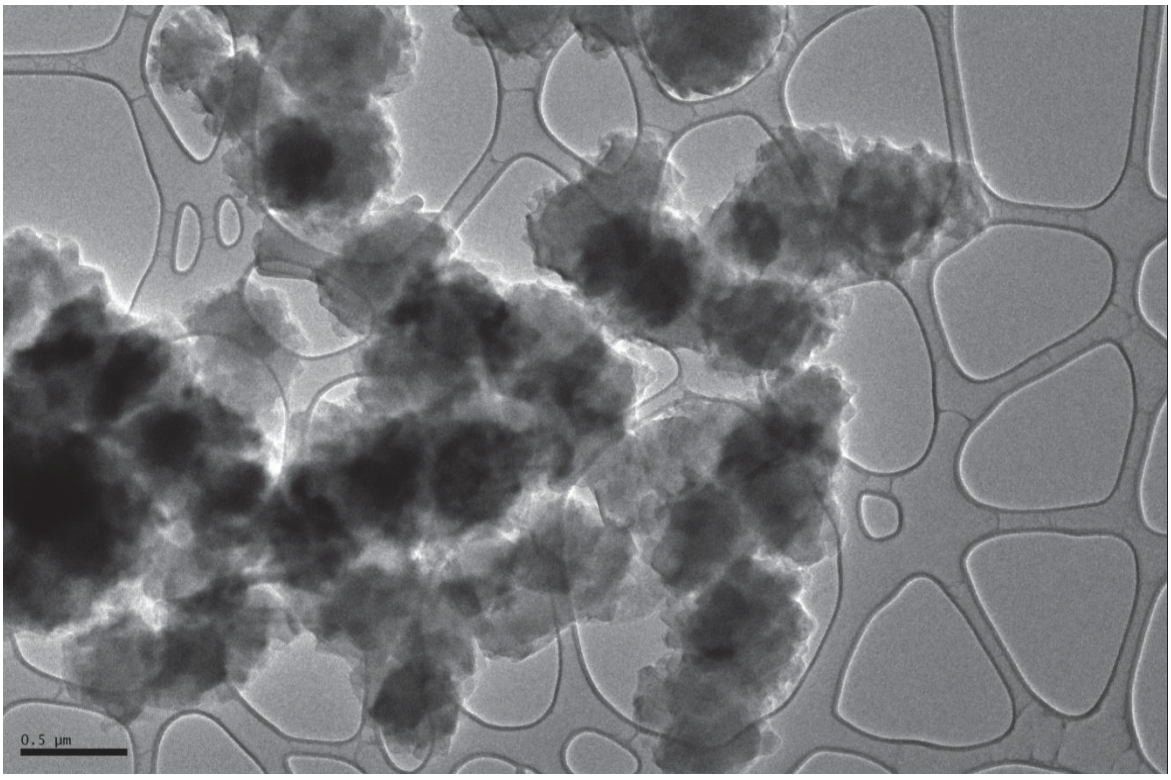

Figure 53: Mg-MOF-74 (lab sample) - Magnification 5K

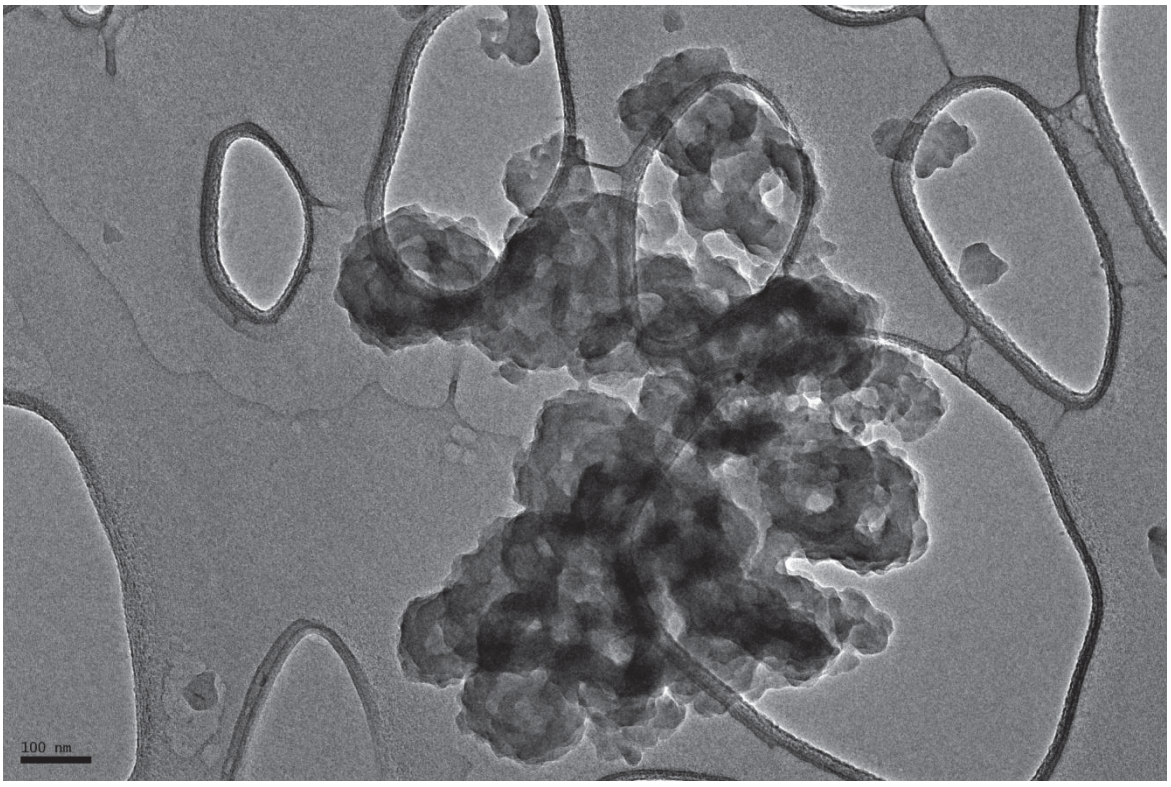

Figure 14: Mg-MOF-74 (lab sample) - Magnification 15K

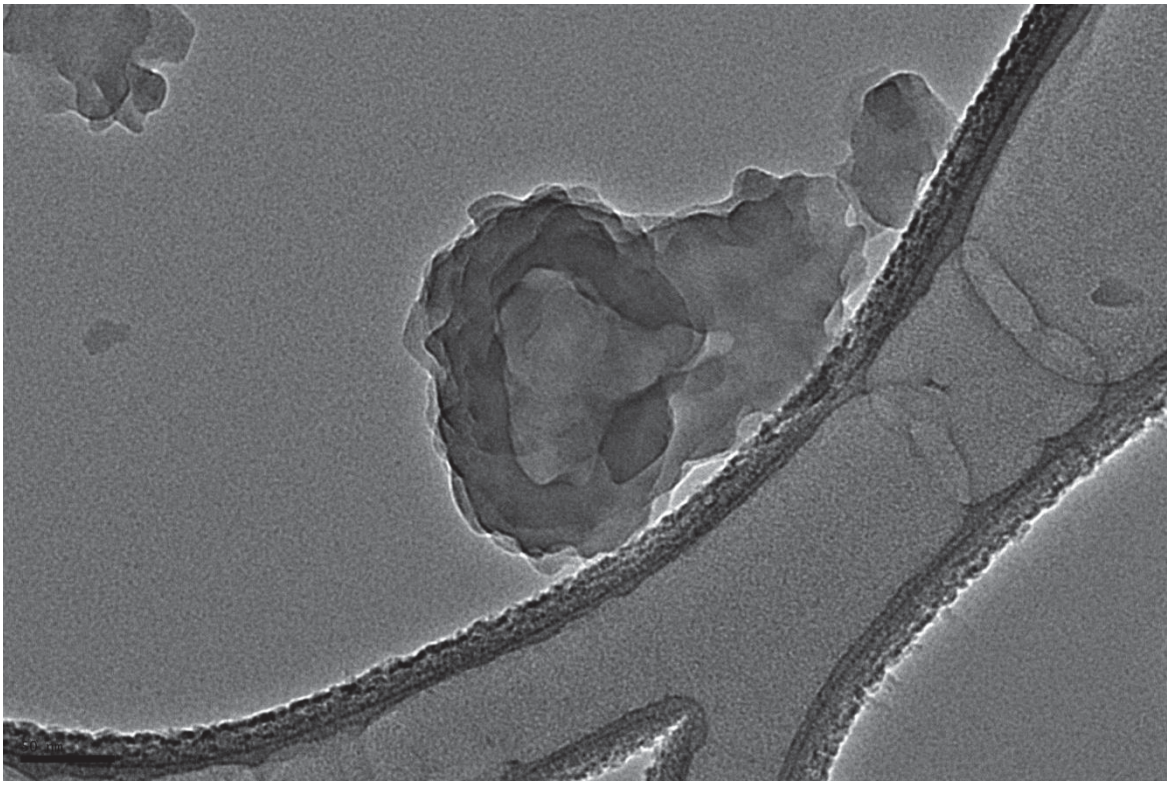

Figure 55: Mg-MOF-74 (lab sample) - Magnification 40K

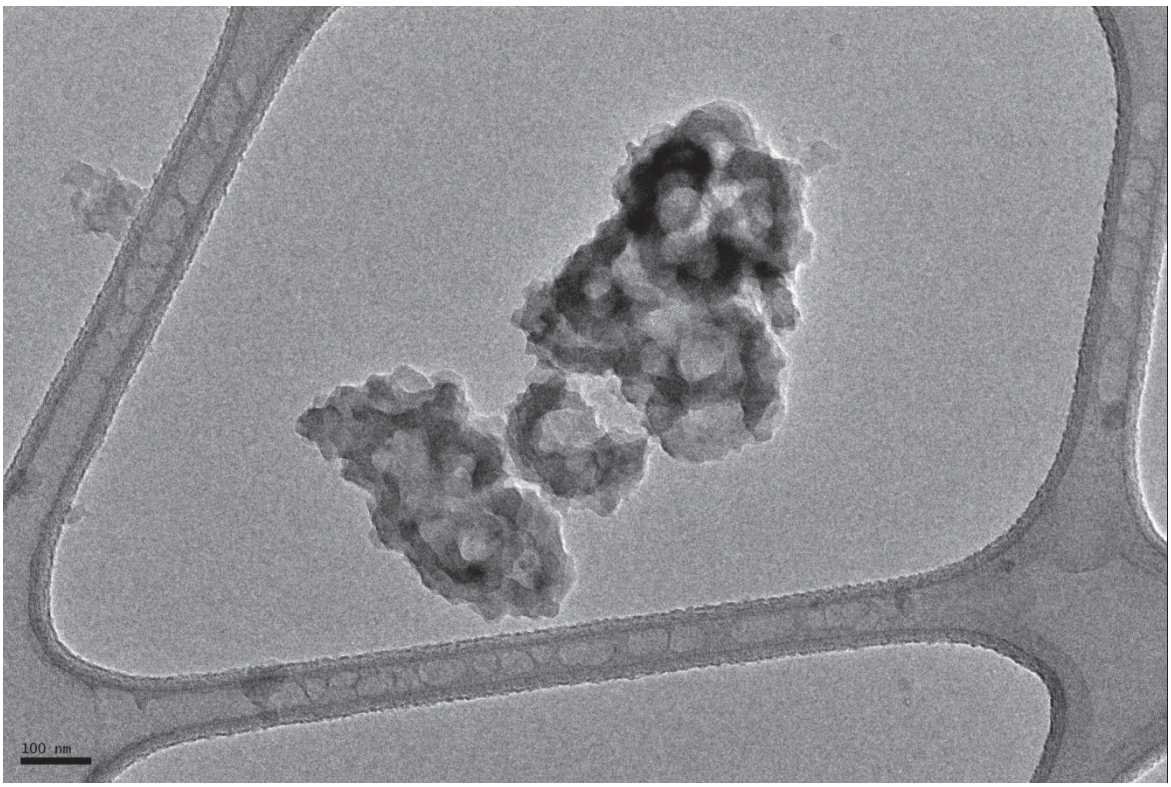

Figure 56: Mg-MOF-74 (lab sample) - Magnification 15K

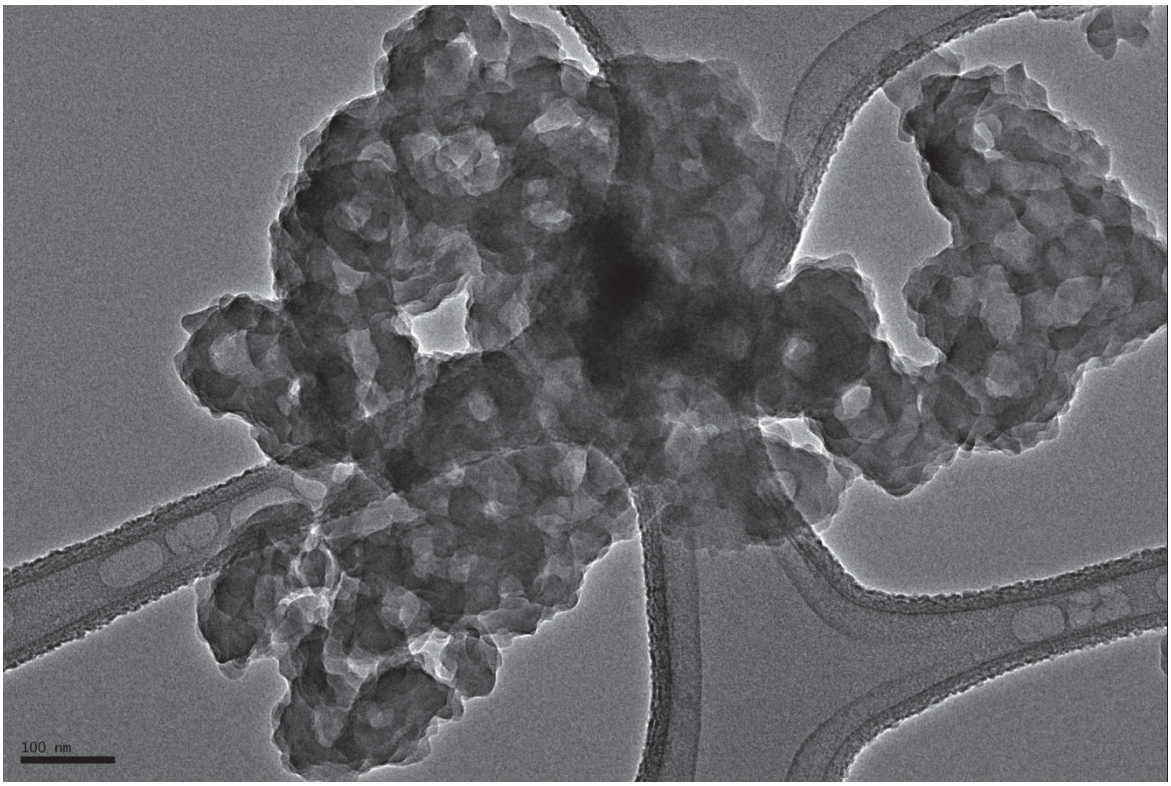

Figure 57: Mg-MOF-74 (lab sample) - Magnification 20K

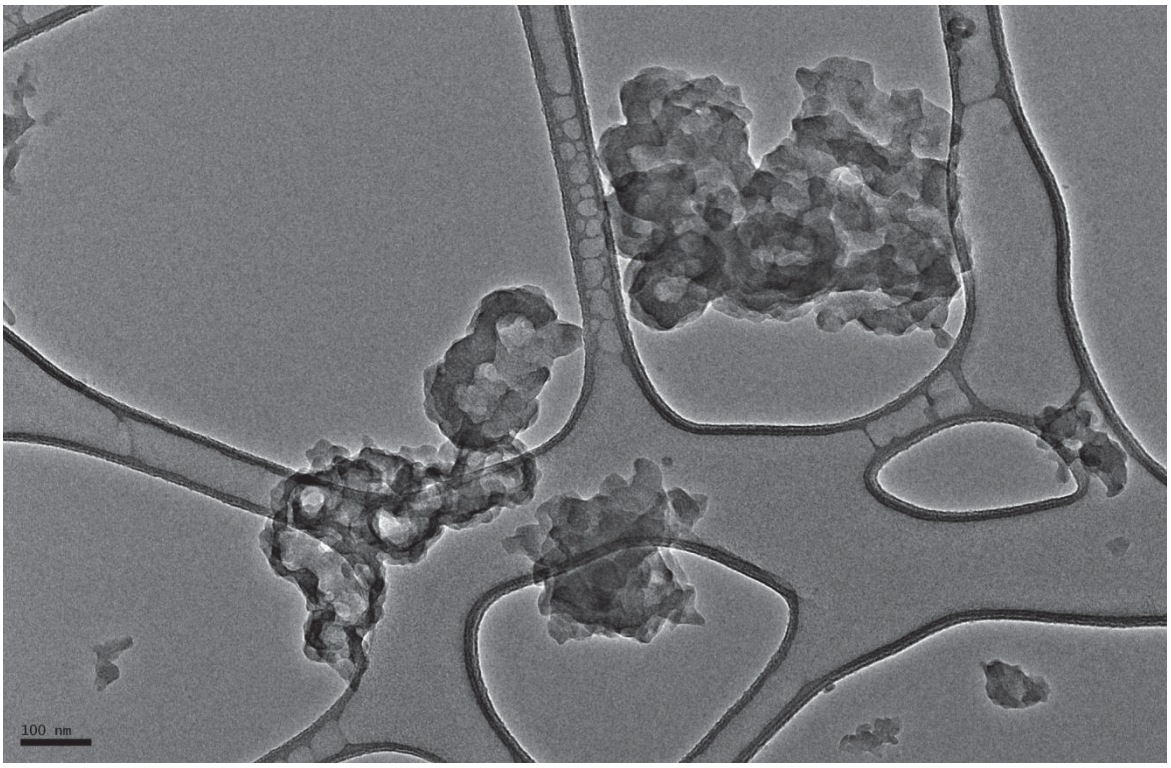

Figure 58: Mg-MOF-74 (lab sample) - Magnification 15K

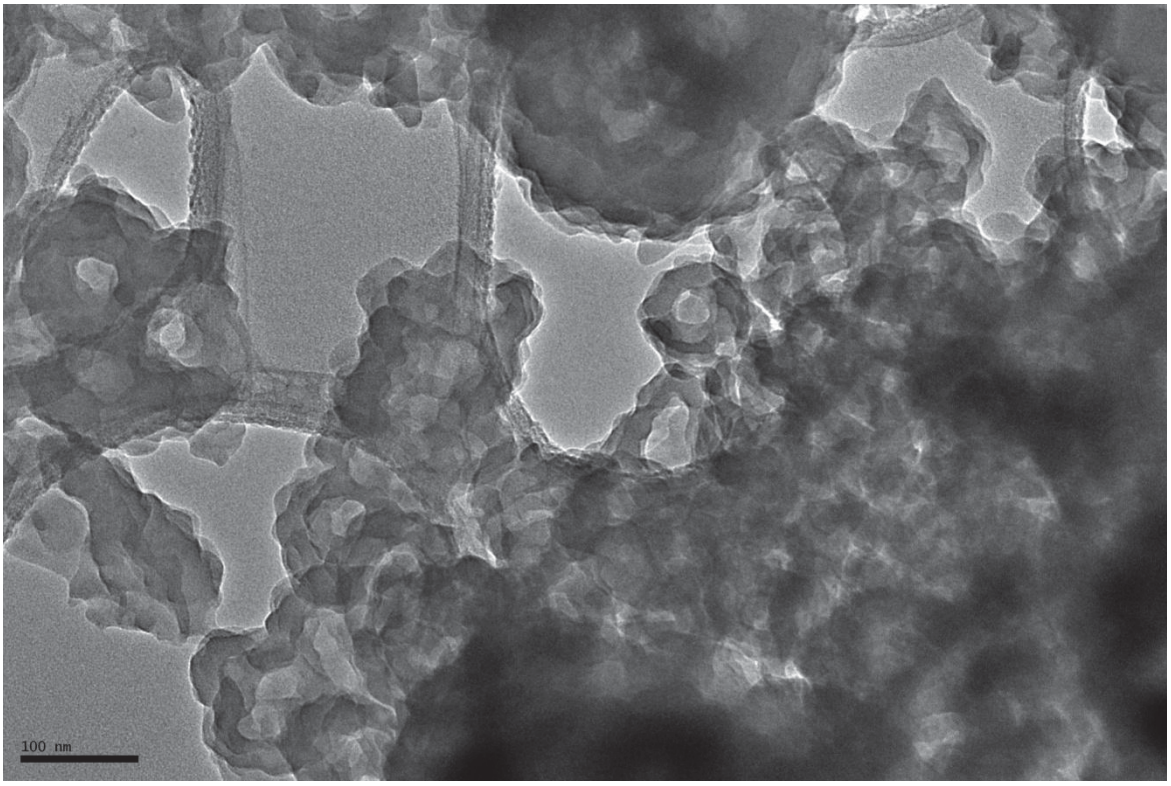

Figure 59: Mg-MOF-74 (lab sample) - Magnification 25K

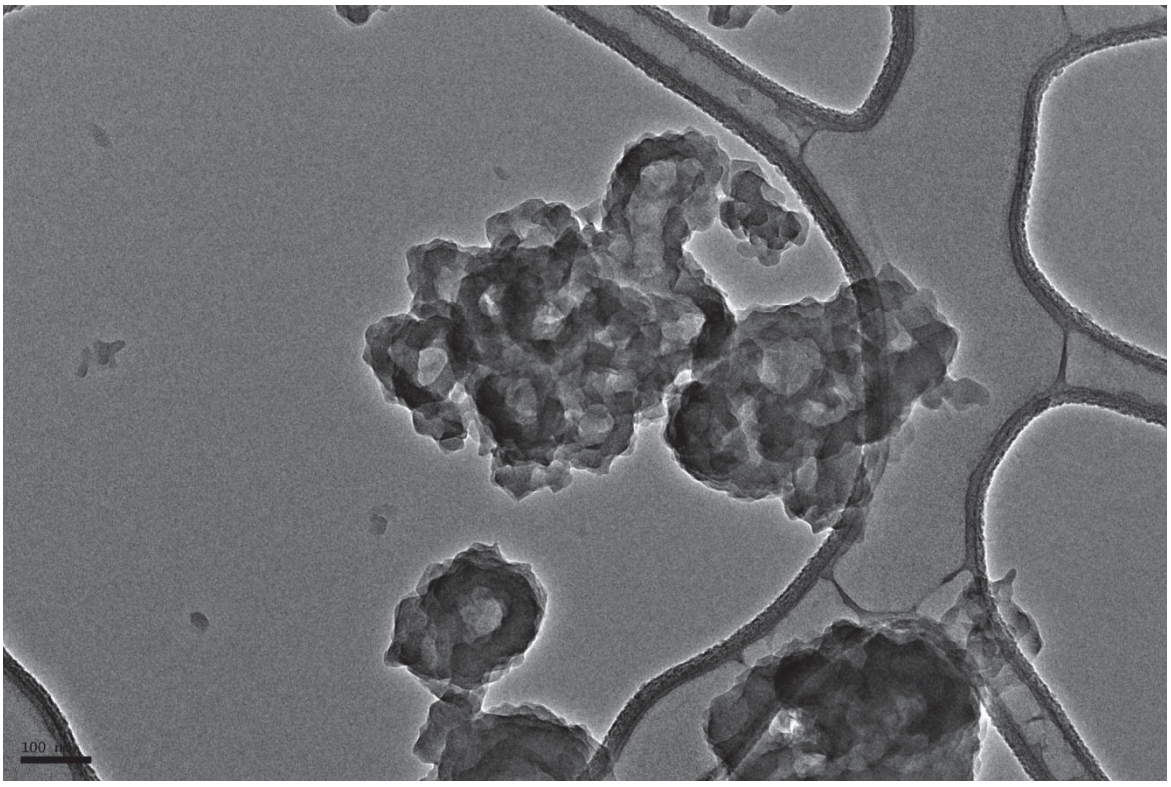

Figure 60: Mg-MOF-74 (lab sample) - Magnification 15K

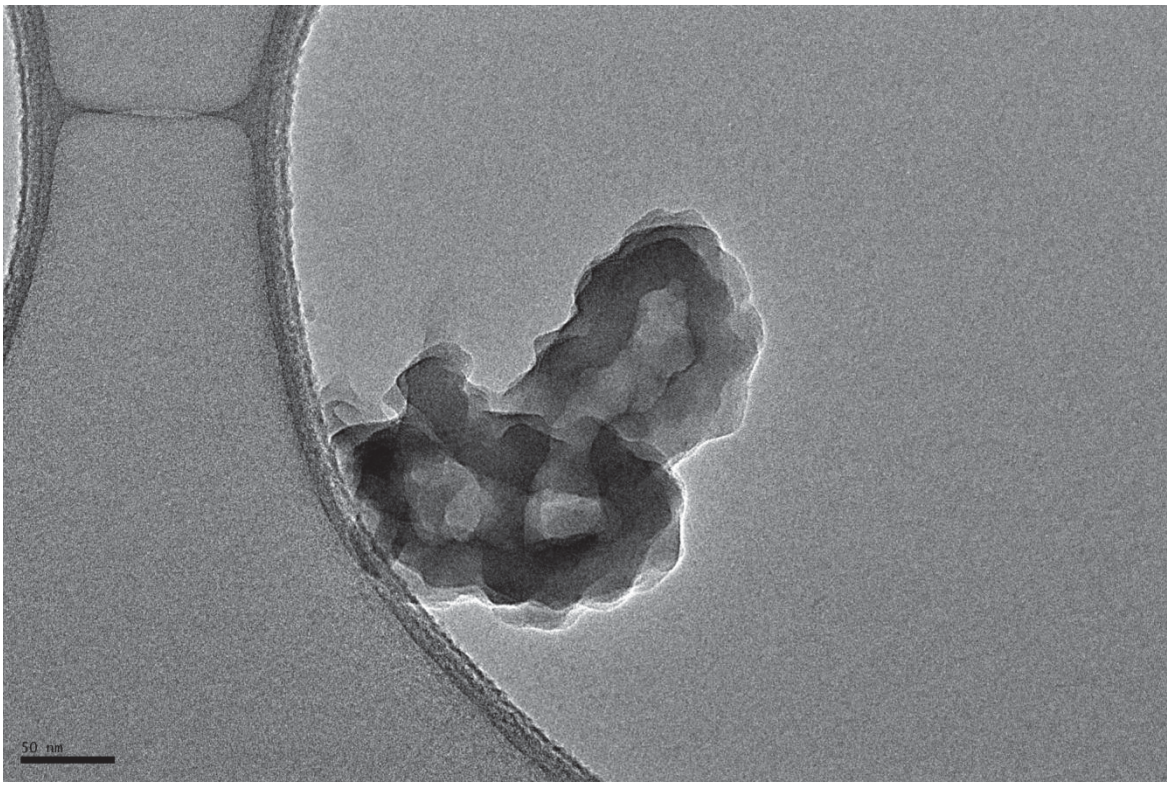

Figure 61: Mg-MOF-74 (lab sample) - Magnification 40K

Appendix C

TGA profiles

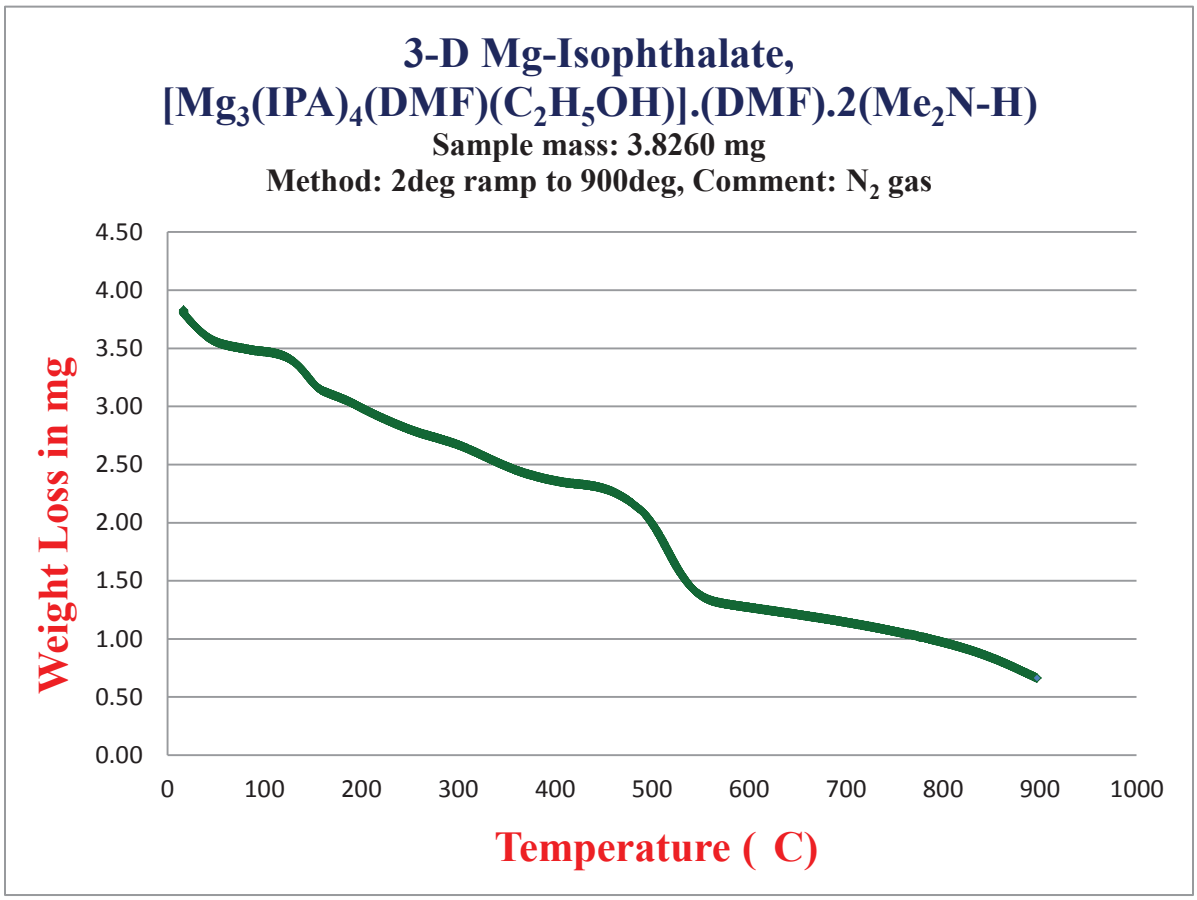

Figure 62: TGA profile data for $[Mg_3(IPA)_4(DMF)(C_2H_5OH)].(DMF).2(Me_2N\text{-}H)$

Appendix D

NETL Gas adsorption data

YSU Lab Sample:

	N_2 isotherm at -196 °C (77 K)	CO_2 isotherm at 30 °C (303 K)
Sample	BET Area (m^2/g)	Amount adsorbed at 760 torr (cc/g)
Mg-MOF-74	15.83	18.31

SAMPLE ID:	Mg-MOF-74
SAMPLE WEIGHT (g):	0.1709
N2 77 K	

P/Po	P (torr)	Vol. adsorbed (cc)	Vol. adsorbed (cc/g)
0.104584	79.48384	0.602068	3.523
0.152376	115.80576	0.669512	3.918
0.203268	154.48368	0.724068	4.237
0.251073	190.81548	0.799647	4.679
0.303148	230.39248	0.852988	4.991

BET Surface Area (m^2/g) 15.83 m^2/g

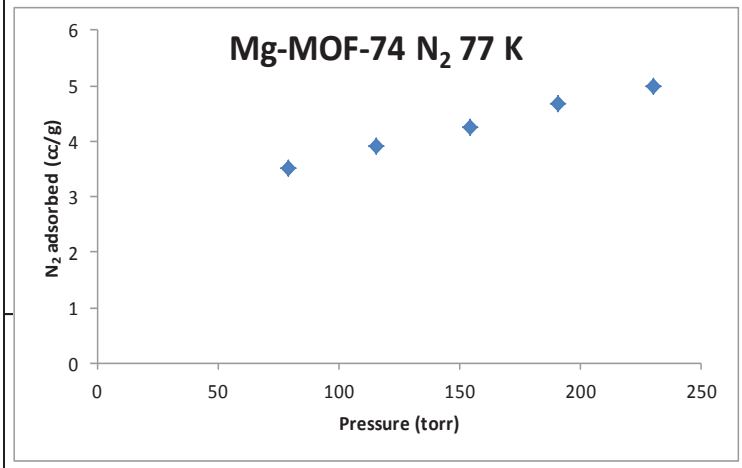

SAMPLE WEIGHT: 0.171
P/Po TOLERANCE: 1
EQUILIBRATION TIME: 3
ANALYSIS TIME: 87.8667 MINUTES
GAS TYPE: Nitrogen
CROSS-SECTIONAL AREA: 16.2
MOLECULAR WEIGHT: 28.013
NONIDEALITY CORR FACTOR: 6.58e-5
ENDRUN: Thu May 19 15:32:20 2011
DATE: Thu May 19 15:32:20 2011
PC SOFTWARE VERSION: 1.50
STATEFLAGS: 3
SAMPLE DESC: 100 C, 1.5 hr
AMBIENT TEMPERATURE: 296.715
ANALYSIS TEMPERATURE: 77.3
LAST Po: 758.437
OPERATOR: KK
OUT GAS TEMP: 100.000000
OUT GAS TIME: 1.500000

Figure 63: NETL Nitrogen (N_2) gas adsorption data obtained for a sample of Mg-MOF-74 (lab sample)

LAB SAMPLE:	Mg-MOF-74
SAMPLE WEIGHT (g):	0.1709
TEMP	**303 K**

Langmuir-Freundlich Fit Parameters

y = m1*(m2*m0^(1/m3))/(1+m2*m0^(1/m3))		
	Value	**Error**
m1 (Q_m)	13.39825	1.39523
m2 (B)	0.00043	0.00002
m3 (t)	0.98221	0.02059
Chisq	0.00022	
R	0.99989	

P/Po	P (torr)	Vol. adsorbed (cc)	Vol. adsorbed (cc/g)	CO_2 adsorbed (wt. %)		
				Experimental	Calculated	Difference
0.000999327	0.759	0.00339981	0.020	0.004	0.004	-0.0004
0.00512641	3.896	0.0321303	0.188	0.037	0.023	0.0140
0.0100245	7.619	0.0651997	0.382	0.075	0.045	0.0296
0.0522478	39.708	0.205316	1.201	0.236	0.240	-0.0042
0.0981357	74.583	0.382695	2.239	0.440	0.449	-0.0092
0.201565	153.189	0.79309	4.641	0.912	0.902	0.0099
0.298345	226.742	1.13511	6.642	1.305	1.301	0.0035
0.398391	302.777	1.4697	8.600	1.689	1.690	-0.0012
0.498711	379.020	1.79647	10.512	2.065	2.058	0.0068
0.599374	455.524	2.11205	12.358	2.428	2.406	0.0219
0.698372	530.763	2.36139	13.817	2.714	2.728	-0.0141
0.799245	607.426	2.66732	15.607	3.066	3.039	0.0269
0.898709	683.019	2.90263	16.984	3.336	3.329	0.0077
0.994125	755.535	3.13024	18.316	3.598	3.592	0.0057

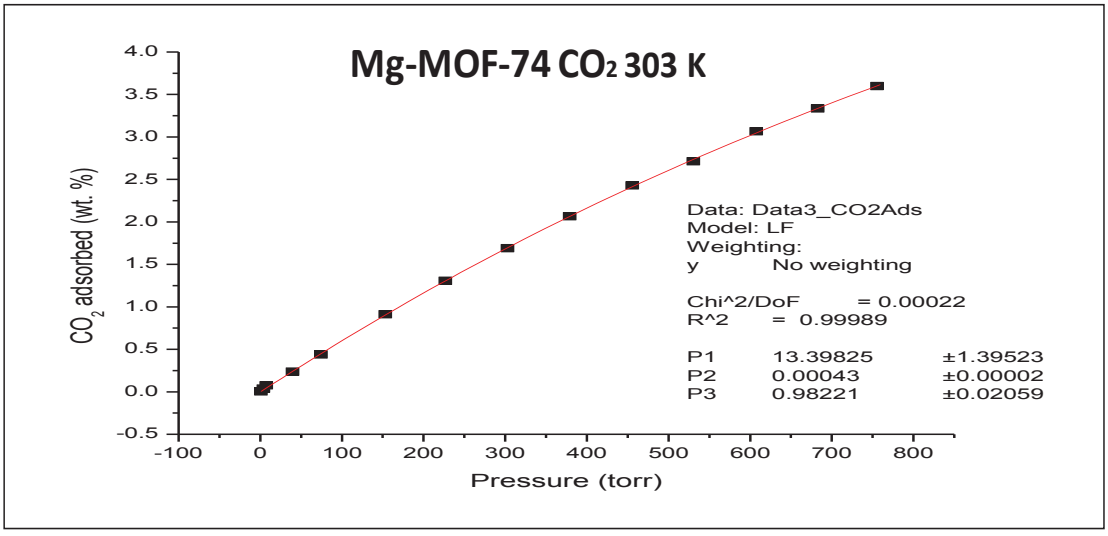

Figure 64: NETL Carbon dioxide (CO_2) gas adsorption data obtained for a sample of Mg-MOF-74 (lab sample)